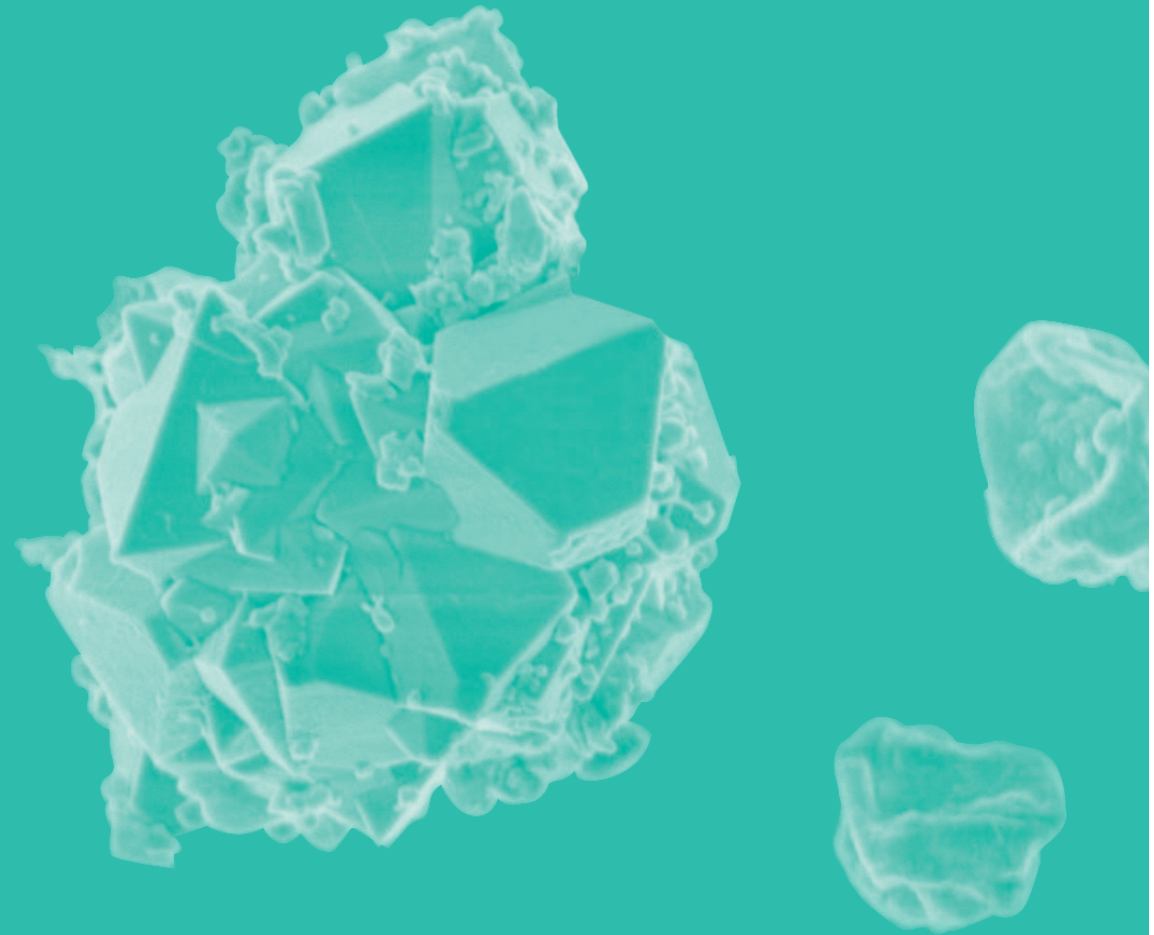


# EXPANDING THE BIOSCORODITE PROCESS FOR AS(III) WASTEWATER REMEDIATION



SILVIA VEGA HERNANDEZ

EXPANDING THE BIOSCORODITE PROCESS FOR AS(III) WASTEWATER REMEDIATION

SILVIA VEGA HERNANDEZ

## Propositions

1. Biologically induced crystallization is the primary mechanism for the precipitation of scorodite. (this thesis)
2. Pyrite as an alternative iron source for the biological precipitation of low-leaching scorodite further decreases the cost of the bioscorodite process. (this thesis)
3. The irrational collective behavior in time of crisis worsens an already adverse situation.
4. In a modern world where documents are prone to be read online, printing a PhD thesis implies a high environmental cost.
5. Peer review of scientific articles should be a completely double-blind process.
6. Building resilience is the only way of exploiting the unknown inner-strength to face challenges in life.

Propositions belonging to the thesis entitled  
“Expanding the bioscorodite process for As(III) wastewater remediation”

Silvia Patricia Vega Hernandez

Wageningen, 1<sup>st</sup> of September, 2020

**EXPANDING THE BIOSCORODITE  
PROCESS FOR AS(III)  
WASTEWATER REMEDIATION**

**SILVIA VEGA HERNANDEZ**

## **THESIS COMMITTEE**

### **Promotor:**

Prof. Dr CJN Buisman  
Professor of Environmental Technology  
Wageningen University & Research

### **Co-promotor:**

Dr J Weijma  
Assistant professor of Environmental Technology  
Wageningen University & Research

### **Other members:**

Prof. Dr A.J.M Stams, Wageningen University & Research  
Dr. A. Ghahreman, Queen's University, Ontario, Canada  
Dr T. Behrends, Utrecht University  
Dr P. Gonzalez Contreras, Paques B.V., Balk

This research was conducted under the auspices of the Graduate School for Socio-Economic and Natural Sciences of the Environment (SENSE).

# **EXPANDING THE BIOSCORODITE PROCESS FOR AS(III) WASTEWATER REMEDIATION**

**SILVIA VEGA HERNANDEZ**

Thesis

submitted in fulfilment of the requirements for the degree of doctor  
at Wageningen University  
by the authority of the Rector Magnificus,  
Prof. Dr A.P.J. Mol,  
in the presence of the  
Thesis Committee appointed by the Academic Board  
to be defended in public  
on Tuesday 1 September 2020  
at 11 a.m. in the Aula.

**Silvia Vega Hernandez**

Expanding the bioscorodite process for As(III) wastewater remediation  
172 pages.

PhD thesis, Wageningen University, Wageningen, the Netherlands (2020)  
With references, with summary in English

DOI-link: <https://doi.org/10.18174/528087>

ISBN: 978-94-6395-480-8

To Iris and Benilde

“The brain is a world consisting  
of a number of unexplored  
continents and great stretches  
of unknown territory”

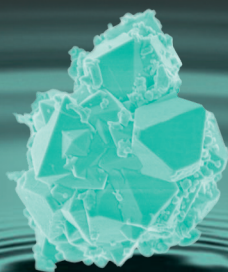
-Santiago Ramón y Cajal-



## TABLE OF CONTENTS

<b>Chapter 1</b>	General Introduction	9
<b>Chapter 2</b>	Proof of principle: biological scorodite precipitation through the catalyzed As(III) oxidation by granular activated carbon (GAC).	31
<b>Chapter 3</b>	Evaluating the effect of GAC in the biological crystallization of scorodite	53
<b>Chapter 4</b>	Scale-up of the Bioscorodite crystallization for the continuous treatment of diluted As(III) streams	77
<b>Chapter 5</b>	Exploring alternative iron sources for the microbial growth in the biomineralization of scorodite	109
<b>Chapter 6</b>	General Discussion	135
	Summary	155
	Acknowledgements	161
	About the author	167

# CHAPTER 1



# GENERAL INTRODUCTION

### 1. GENERAL INTRODUCTION

Arsenic (As) is a ubiquitous natural element in the earth's crust [1] but also present in sea water and in the human body [2]. Humans are exposed to arsenic through water, air, soil and food. The contamination of groundwater is considered the most serious threat and direct route for chronic exposure [3-6] as it is also an important source of drinking water and irrigation water in several countries and a direct path to the human body. Both natural interactions with sediment and minerals as well as industrial activities (i.e. agriculture, mining, coal/oil combustions) are the main sources by which arsenic gets into the groundwater and is mobilized through biogeochemical reactions [7]. This is of particular concern in countries such as India, Bangladesh, China, Vietnam, Mexico, Argentina, and Chile, where arsenic concentrations in groundwater exceed the advised limit of the World Health Organization (WHO) ( $0.01 \text{ mg L}^{-1}$ ) [8-10] and particularly in regions of Asia with levels of arsenic in water above  $0.05 \text{ mg L}^{-1}\text{As}$  [11, 12]. Currently, over 200 million people worldwide are severely affected and still at risk of exposure to high As concentrations in drinking water [13]. The poisoning by arsenic due to long-term exposure has been reported in endemic areas where the concentration rises by natural processes [14, 15] or because of mining and agricultural activities [16-19]. Bangladesh and India are regarded as the most affected countries of massive arsenic poisoning of a population in history [20-22].

Arsenic is an undesirable product in many industrial processes for the extraction of valuable metals. Penalties imposed for this impurity in the concentrates and effluent discharged can be high causing significant economic implications to a project or operation [19]. In operational terms, it is also problem of concern due to the technical limitations of smelters. The problems caused by the overproduction of arsenic in metallurgical processes has largely intensified due to the trend towards the exploitation of low-grade ore, by which higher efforts in terms of treatment methods and waste management are required. To address arsenic contamination, effluents from metallurgical processing must be treated for safe disposal. Therefore, technologies allowing the selective oxidation of the most toxic form, arsenite ( $\text{As(III)}$ ) and the fixation of this element are essential, in this way long term safe storage is possible. The overall aim of my thesis is to develop and optimize technologies for the selective oxidation of  $\text{As(III)}$  and the long-term immobilization of this highly toxic element.

#### 1.1. NATURAL SOURCES OF ARSENIC

The global distribution of arsenic is determined by the influence of mining, geothermal

activity and the combustion of coal with high content of this element, making it a worldwide economic, social and environmental problem. Although arsenic release is often related to both geogenic and anthropogenic sources, the input from the latter can be highly relevant for toxicity effects in water sources. Arsenic is found in more than 300 minerals in nature as arsenates (60%), sulfides and sulfosalts (20%) and oxides (10%) and in less proportion as arsenites, arsenides, and metal alloys. Arsenic is a major constituent of a variety of sulfide and oxide minerals such as realgar ( $\text{As}_4\text{S}_4$ ), orpiment ( $\text{As}_2\text{S}_3$ ), arsenopyrite ( $\text{FeAsS}$ ), arsenolite ( $\text{As}_2\text{O}_3$ ), and scorodite ( $\text{FeAsO}_4 \cdot 2\text{H}_2\text{O}$ ) [23]. Despite its occurrence in a variety of natural sources, As in the environment is primarily found coprecipitated with Fe hydroxides ( $\text{Fe}(\text{OH})_3$ ) and in sulfide minerals, which are also commonly associated with other metals of commercial value (i.e. Cu, Au, Co) [24, 25]. Arsenopyrite and arsenic-bearing pyrite (known as arsenian pyrite,  $(\text{Fe}(\text{S},\text{As})_2)$ ) represent the most abundant As minerals [26], other primary minerals include enargite ( $\text{Cu}_3\text{AsS}_4$ ) cobaltite ( $\text{CoAsS}$ ) tennantite ( $\text{Cu}(\text{Fe},\text{Zn})_{12}\text{As}_4\text{S}_{13}$ ), proustite ( $\text{Ag}_3\text{AsS}_3$ ) and olivenite ( $\text{Cu}_2\text{OHAsO}_4$ ) [7].

The chemistry of arsenic closely follows that of sulfur, which explains its high occurrence in sulfide minerals and the replacement of sulfur by arsenic in the crystal structure of iron minerals such as pyrite [27, 28]. From an environmental point of view, this association is of significance since many of the redox reactions involving these minerals will determine its role as important sources or sinks of arsenic in nature [15, 28, 29].

**Table 1.1** Arsenic concentrations in sulfides and oxides groups  
(adapted from Smedley and Kinniburgh [26]).

Mineral group	As concentration (mg/kg)
<b>Sulfides</b>	
Arsenopyrite	46% by mass
Pyrite	100–77000
Pyrrhotite	5–100
Marcasite	20–126000
Galena	5–10000
Sphalerite	5–17000
Chalcopyrite	10–5000
<b>Oxides</b>	
Hematite	≤160
Fe oxides	≤2000
Fe III oxyhydroxide	≤76000
Magnetite	2.7–41
Ilmenite	<1

## CHAPTER 1

Arsenic-containing compounds can be found in natural waters and biological systems in different oxidation states and chemical forms (Table 1.2). Redox potential (Eh) and pH are the most important environmental parameters controlling As speciation [30]. In aqueous solutions arsenic forms As(III) and As(V) oxyanions [26, 31]. Thus, under oxidizing conditions in a pH range between 4-10, arsenate species prevail ( $\text{AsO}_4^{3-}$ ,  $\text{HAsO}_4^{2-}$ ,  $\text{H}_2\text{AsO}_4^-$  and  $\text{H}_3\text{AsO}_4^0$ ) [32]. Under reducing conditions at a pH below 9.2, arsenious acid,  $\text{H}_3\text{AsO}_3^0$  dominates in solution [26].

There is significant concern to As(III) due to its' high toxicity, stability and mobility in environment [31, 33]. The toxicity, mobility, and fate of arsenic in the environment is determined by a number of factors, including the speciation, mineralogy and biological processes [34]. Being a metalloid, arsenic can stably occur in different oxidation states: -III (arsine), 0 (arsenic), +III (arsenite) and +V (arsenate). However, in aqueous solutions it is mainly found in the inorganic form as the oxyanions arsenite and arsenate. Arsenic can readily interact with a variety of elements forming covalent bonding, although in nature it primarily bounds to oxygen and sulfur thereby generating a diversity of soluble species and minerals [35]. Furthermore, due to their amphoteric property, some of the arsenic species are soluble in a wide range of pH [36].

**Table 1.2.** Predominant arsenic compounds in water sources.

(Adapted from Mandal [37]).

Compound	Abbreviation	Formula
<b>Inorganic compounds</b>		
Arsenous acid (arsenite)	As(III)	$\text{As}(\text{OH})_3$
Arsenic acid (arsenate)	As(V)	$\text{AsO}(\text{OH})_3$
<b>Organic compounds</b>		
Monomethylarsonic acid	MMA(V)	$\text{CH}_3\text{AsO}(\text{OH})_2$
Dimethylarsinic acid	DMA(V)	$(\text{CH}_3)_2\text{AsO}(\text{OH})$
Arsenobetaine	AsB	$(\text{CH}_3)_3\text{As}^+\text{CH}_2\text{COOH}$
Arsenocholine	AsCho	$(\text{CH}_3)_3\text{As}^+\text{CH}_2\text{CH}_2\text{OH}$

### 1.2. ANTHROPOGENIC SOURCES OF ARSENIC

In the early 1990s global producers of arsenic raw materials (commonly  $\text{As}_2\text{O}_3$  or As metal of technical grade) were France, Sweden, the Soviet Union, followed in minor volume by Mexico, Chili, Canada and other countries [38]. Currently, China and Russia are reported as main countries still manufacturing As [39]. Historically, arsenic was

utilized as a pesticide in agriculture. Arsenic trioxide was also used as a key ingredient for the manufacture of the wood preservative chromated copper arsenate (CCA) [40]. Until 1975, approximately 90% of the arsenic was consumed for the treatment of wood with CCA and pesticides in countries like the U.S. However, over the last 20 years arsenic use in agriculture has largely declined since the use of organic arsenical pesticides was phased out in 2003 due to U.S. EPA regulations [41]. The usage of arsenic still remains for the production of semiconductors [42] furthermore, in small markets like Russia, arsenical products (e.g.  $\text{As}_2\text{O}_3$ , arsenic acid) are commercialized with a limited price of 2-3\$ $\text{kg}^{-1}$  up to 50 \$ $\text{Kg}^{-1}$  for the manufacture of optic fibers [38].

Currently, mining and smelting of arsenic-bearing ores contributes significantly to environmental arsenic contamination from the emission during operation to the storage of arsenic in the tailing and rock wastes [43]; these activities account for 75% of the global arsenic pollution in water sources [44, 45]. Environmental legislation has been put in place in order to limit the production, consumption and the discharge of arsenic for process streams or waste effluents. Strict regulations are implemented to protect the consumption in drinking water, but the regulation can exceed up to 500 times the value established for safe drinking water (Table 1.3).

Arsenic is detrimental from the economic point of view, affecting the quality of exported metal concentrates. This is reflected in the penalties imposed by large custom smelters (e.g. China and Japan) to treat copper concentrates with a content above 0.2% arsenic [46] as well as, in the guidelines and regulations developed in several countries to limit arsenic discharge in industrial effluents (Table 1.3). Additionally, it results in health problems to operators and environmental pollution due to the release of volatile arsenic compounds (e.g.  $\text{As}_2\text{O}_3$ ,  $\text{As}_4\text{O}_6$ ) [47]. Due to its low price, the recycling of arsenic from end-of-life arsenic-containing products is of non-economic interest. Thus, the major aim of arsenic management in the final stage is stabilization and subsequent disposal.

### 1.3. ARSENIC BIOTRANSFORMATION AND DETOXIFICATION

Inorganic and organic As are the predominant compounds in water sources (Table 1.2), with the former being most toxic and prevalent. The toxic effect of arsenic has been directly related to its mobility in water and body fluids. Accordingly, it follows (from the high to the lower toxicity): arsines > inorganic arsenites > organic trivalent compounds (arsenooxides) > inorganic arsenates > organic pentavalent compounds > arsonium compounds > elemental arsenic [2, 54]. Thus, inorganic arsenic has been listed as “group I” carcinogen by the International Agency for Research on Cancer (IARC) [55]

**Table 1.3.** Authorized arsenic discharge in industrial effluents.

Country	Arsenic concentration (mgL <sup>-1</sup> )	Regulation title-code
Chile	0.5	D.S. 90/2000, 2008 [48]
China	0.5	Integrated wastewater discharge standards (GB26132-2010) [49]
Canada	0.5	Metal and Diamond Mine Effluent Regulations [50]
Brazil	0.5	CONAMA Directive 357/2005 [51]
Mexico	0.5	NOM-002-ECOL-1996 [52]
United States of America	0.692	EPA Nonferrous Metals Manufacturing (NFMM) Effluent Guidelines and Standards (40 CFR Part 421)
Australia	0.1	National water quality management strategy (NHMRC-AWRC) [53]
Zambia	1	The local administration (trade effluent) regulations

and by US Environmental Protection Agency (US EPA) meaning As is a known carcinogen and a cause of skin, lung and urinary bladder cancer in humans [56]. After ingestion, arsenic is quickly metabolized mainly in the liver. Biotransformation of arsenic follows the reduction of As(V) to As(III) and the consequent addition of a methyl group. This process results in the formation of monomethylarsonic acid (MMA) and dimethylarsinic acid (DMA) which are readily excreted in the urine [5, 56]. MMA and DMA are less toxic compounds, so the methylation process acts as a detoxification process.

Microbes have developed several other mechanisms to detoxify As, including oxidation, reduction, biosorption and biomethylation [57-60]. Microbial arsenic transformation occurs in a wide range of habitats at different environmental conditions. Likewise, As-oxyanions can be used either as an electron acceptor for anaerobic respiration by dissimilatory As(V)-reducing prokaryotes or as electron donor, in the oxidation of arsenite by As(III)-oxidizing heterotrophic (HAOs) or chemolithotrophic (CAOs) microbes [58, 61, 62]. Microbial As(III) oxidation can impact the mobility and the fate of arsenic in the aqueous environment. Furthermore, it can be a detoxification strategy or energy conservation as in the case of heterotrophic [58] or chemolithotrophic As(III)-oxidizers that use As(III) as electron donor to obtain energy and fixate CO<sub>2</sub> [63]. Oxidation of As(III) by acidophiles is often coupled to the cycling of other elements such as carbon, nitrogen iron and sulfur [58, 64]. In extreme environments such as mine waters this is of high importance due the low diversity of microbes known to grow in such acid solutions, rich in soluble As(III) [65-67].

#### 1.4. METHODS AND STRATEGIES FOR ARSENIC TREATMENT BY BIOTRANSFORMATION AND DETOXIFICATION

The speciation of arsenic and its concentration in polluted waters are main factors determining the appropriate technique for removal. A number of measures for the treatment of arsenic contaminated streams are in practice, involving among others the addition of chemicals, activated carbon, reverse osmosis, and adsorption on nanomaterials. It is needed to remove arsenic from water systems and especially from metallurgical streams in order to comply with environmental regulations. Besides effluents, the generation and stability of the obtained arsenic residue is controlled by environmental regulations. Currently, the toxicity leaching procedure (TCLP) of U.S.EPA is the standard method performed in several countries to evaluate the potential mobility of arsenic in the obtained waste [68]. The TCLP method simulates landfill conditions and involves the leaching of the solids in a buffered acetic acid solution (pH 5). In order to be classified as non-hazardous, the concentration of arsenic in the leachate (20 hours) must be below  $5 \text{ mg}\cdot\text{L}^{-1} \text{ As}$ .

Many of the problems regarding the mobilization of arsenic arise from the immobilization, i.e. the sludge generated and the short/long-term impact of this arsenic waste when disposed. At present most of the use of arsenic ceased but these industrial remnants together with the continuous generation of arsenic waste from metallurgical industry, represent a big challenge. Commonly, large effluents containing arsenic ( $\geq 500 \text{ mg L}^{-1}$ ) are the output of mineral processing such as arsenopyrite ( $\text{FeAsS}$ ), enargite, ( $\text{Cu}_3\text{AsS}_4$ ), tennantite ( $(\text{Cu,Fe})_{12}\text{As}_4\text{S}_{13}$ ), orpiment ( $\text{As}_2\text{S}_3$ ) and cobaltite ( $\text{CoAsS}$ ) [69]. These effluents differ widely in pH, level of other components such as iron and other metals and in the speciation of arsenic, which in many cases can hinder the treatment [70, 71].

Most of the available technologies (i.e. precipitation, ion exchange, coagulation, adsorption) are efficiently applied for arsenic removal in the oxidized form, As(V) [72-75]. Of these, sorption technologies such as ion exchange, use of activated alumina, commercial carbons or iron precipitation, have been used or currently practiced to remove As(III) [75-77], work well in small systems for low concentrations ( $\mu\text{g}\cdot\text{L}^{-1}$ ) and when arsenic is the only contaminant in solution. However, the main drawback lies in the cost of the selective resin, maintenance/regeneration in the case of ion exchange; and the generation of a second waste stream containing As(III), from the recycling adsorbents, that will require further treatment [75]. In the sections below, the current status of a number of reported technologies for arsenic removal are described.

## CHAPTER 1

### 1.4.1. ARSENIC OXIDATION

Arsenite (As(III)) is 60 times more toxic and mobile than arsenate (As(V)) and is commonly released in weak acid process waters produced by mineral processing [37]. Thus, in order to optimize the removal of arsenic and stability of the precipitates, the first step is to oxidize As(III). Available studies on As(III)-oxidation in acid streams (pH<1.5) are limited. In the presence of oxygen or air, As(III) conversion is not too slow, which can be overcome by the application of stronger oxidants such as hydrogen peroxide, ozone, chlorine, manganese and exposure to UV [47, 78]. The main characteristics of the chemical oxidants is shown in Table 1.4. To date, hydrogen peroxide has been considered as an attractive oxidant, used in industry by Codelco's subsidiary Ecometales to treat As concentrates. However, one of the main disadvantages besides the high cost of the oxidant is its instability as it decomposes in contact with solids [47].

Recently, advanced oxidation became an attractive option due to the fast kinetics. Catalyst systems such as Fenton (Fe(II)/H<sub>2</sub>O<sub>2</sub>), Fenton-like ((Fe(III)/H<sub>2</sub>O<sub>2</sub>), photocatalytic processes (i.e. UV/TiO<sub>2</sub> UV/Fenton(-like)) are based on the production of hydroxyl radicals (OH•) as strong oxidant for As(III) in wastewaters at acidic conditions [79]. Also the SO<sub>2</sub>/O<sub>2</sub> mixture has been used as powerful oxidant of Fe(II) and As(III) in acid solution. The mechanism works effectively in excess of pure O<sub>2</sub> (rather than air) and differs from the above mentioned methods in the formation of oxy-sulfur intermediate species, where the presence of Fe(III) is essential to initiate the catalyzed mechanism of oxidation [80, 81]. The process of arsenic detoxification and mobility in natural environments at milder conditions is known to be controlled microbially [66, 82]. However, in acid streams, biological oxidation of As(III) has been scarcely reported for thermophilic microbes of the genus *Sulfolobus* [59] and *Acidianus* [60, 83].

### 1.4.2. ACTIVATED CARBON FOR ARSENIC OXIDATION

Carbonaceous materials such as activated carbon are porous materials of high surface area and functionalities that make it a versatile material for its application as adsorbents, catalyst and catalyst support [85]. The high degree of porosity of activated carbon as well as the variety of surface functional groups (which include carboxyl, carbonyl, phenol, hydroxyl quinone, lactone) composed of oxygen, hydrogen, sulfur and nitrogen, determine the adsorptive or catalytic behavior of this material [86]. Hence, by the pretreatment of carbon (either in gas or in aqueous phase) it is possible to tailor oxygen surface complexes in relation to the catalytic properties of activated carbon.

**Table 1.4.** Advantages and disadvantages of the main conventional methods used for the treatment of acid wastewater (adapted from [47, 71, 78, 84]).

Oxidant	Advantages	Disadvantages
Air	<ul style="list-style-type: none"> <li>Relatively simple, low cost</li> </ul>	<ul style="list-style-type: none"> <li>Slow process.</li> <li>Low oxidation rate.</li> </ul>
Chlorine	<ul style="list-style-type: none"> <li>rapid arsenic oxidation</li> <li>low relative cost (0.20\$/lb)</li> </ul>	<ul style="list-style-type: none"> <li>Rates dependent of high pH</li> <li>Generation of harmful by products</li> <li>Membrane fouling</li> </ul>
Permanganate	<ul style="list-style-type: none"> <li>Rapid arsenic oxidation.</li> <li>Unreactive with membranes</li> <li>No formation of disinfection by-products.</li> </ul>	<ul style="list-style-type: none"> <li>High relative cost (1.35\$/lb).</li> <li>Formation of MnO<sub>2</sub> particulates.</li> <li>Difficult to handle.</li> <li>An additional oxidant may be required for secondary reaction.</li> </ul>
Ozone	<ul style="list-style-type: none"> <li>No chemical storage or handling required.</li> <li>No chemical by-products left in water.</li> </ul>	<ul style="list-style-type: none"> <li>Short half-life</li> <li>Rates dependent of high pH</li> <li>High production cost.</li> <li>Effectiveness decreased by presence of organic carbon or sulfides</li> </ul>
Hydrogen peroxide	<ul style="list-style-type: none"> <li>Rapid arsenic oxidation</li> </ul>	<ul style="list-style-type: none"> <li>Expensive</li> <li>Dependent on initial As(III) concentrations.</li> <li>Needed in excess to achieve 90% of conversion</li> <li>Decompose in the presence of solids.</li> </ul>
UV Radiation	<ul style="list-style-type: none"> <li>high oxidation rate</li> </ul>	<ul style="list-style-type: none"> <li>Alone is ineffective for As(III) oxidation</li> <li>High energy consumption</li> <li>Long reaction time</li> <li>Yield can be affected by turbidity.</li> </ul>

The use of activated carbon as cheap adsorbent for arsenic has been widely reported in the literature [75, 87, 88]. Adsorption capacities for As(III) and especially As(V) depend upon carbon characteristics (mesoporous or microporous) and range between 0.5-25 mg As g<sup>-1</sup> carbon at pH>2.3 [75, 76, 87]. The surface charge of the carbon is determined by pH. Acid pre-treatment with HNO<sub>3</sub> or H<sub>2</sub>SO<sub>4</sub> is the most employed technique to introduce negatively charged acidic functional groups (e.g. carboxylic, quinones, hydroquinones) on the surface of activated carbon, which in turns favor the catalytic performance of this material [86, 89].

Additionally its application as catalyst was also reported some decades ago. The mechanism behind the catalytic activity has been correlated to the formation of hydrogen peroxide in the presence of O<sub>2</sub> which takes place by contacting carbon materials in relatively acid solutions [86, 90, 91]; however, little is known about the application of activated carbon in hydrometallurgy for the treatment of As(III)-rich solution.

A patented process is applied in industry by Barrick Gold corporation to treat arsenic in

## CHAPTER 1

metallurgical streams at pH <2.5 [92]. The central technological claim of the patented process is that <95% of arsenite oxidation is achieved in the presence of oxygen and activated carbon at a minimum ratio (g L<sup>-1</sup>) catalyst: As of 10. The obtained As(V)-containing solution is then separated from the catalyst and mixed with a Fe(III) solution to produce ferric arsenate, Scorodite [92]. In the presence of activated carbon, the formation of hydrogen peroxide takes place by the reduction of oxygen (Equation 1) which is favored by oxygen surface groups [47, 86, 93]. The approach of catalyzed oxidation of As(III) by granular activated carbon (GAC) might be of advantage in terms of operational cost and performance considering the relatively low market price of GAC (\$ 0.75 kg<sup>-1</sup>) [94].



$C_{\text{red}}^*$  stands for reduced functional groups on the carbon surface

### 1.4.3. BIOHYDROMETALLURGICAL PROCESSING

Biomining processes, through bioleaching of As-bearing minerals, bio-oxidation, and bio-precipitation have been successfully applied to treat low-grade ores and acid waste streams such as mine tailings [95-98]. Chemolithoautotrophic microbes play a crucial role in the biogeochemical cycle of arsenic by using minerals and other inorganic compounds as energy source [99], thereby influencing the speciation and mobility of arsenic. Arsenic oxidation has been reported for acidophilic bacteria (i.e. *Acidithiobacillus thiooxidans*, *A. caldus*, *Leptospirillum ferriphilum*) and strains of *Thiomonas sp.* at milder temperature conditions and a range of pH (2.2-5) and at concentration as high as 20 gL<sup>-1</sup> As [67, 100-103]. At thermoacidophilic conditions As(III) biooxidation has been scarcely reported [59, 104]. So far, *Sulfolobus metallicus* (formerly *Sulfolobus acidocaldarius strain BC*) and *Acidianus brierleyi* have been described to oxidize As(III) [59, 60, 105, 106]. Many of the reported acidophilic species have shown remarkably resistance to arsenic species [99, 107] and the ability to promote As(III) oxidation. The latter might occur either through the metabolism of ferrous iron, an important growth source for most acidophiles abundant in mining areas or by direct arsenic metabolism associated to the expression of arsenite oxidase genes. Amongst thermoacidophilic archaea, encoding genes for arsenite oxidase subunits have been described for some member of Sulfolobales such as *Sulfolobus tokodaii* and recently in *Acidianus copahuensis*. Nevertheless, until now no genomic evidence of arsenite oxidation has been reported for the archaeon *Sulfolobus acidocaldarius BC* (renamed *Sulfolobus metallicus*) [59] and *Acidianus brierleyi* [105], being suggested as a detoxification mechanism.

#### 1.4.4. IMMOBILIZATION TECHNOLOGIES

All the removal technologies for As result in the generation of arsenic-rich wastes (either in the solid form or bound to a sorbent). Technologies for arsenic stabilization have been researched extensively since the 1980s. Lime neutralization to precipitate calcium arsenate and calcium arsenite was common practice for arsenic disposal. Neutralization with lime is a simple and relatively economic option, but the formed precipitates showed to be unstable as they decompose in contact with atmospheric  $\text{CO}_2$ , resulting in the release of arsenic (up to  $4400 \text{ mg As L}^{-1}$ ) [1, 69] in solution. Smelters in Chile (Codelco's Chuquicamata and Noranda's Altonorte plant) and China (Fanyuang Nonferrous metals Co.) continue producing calcium arsenic residues that are stored in hazardous landfills [108]. Other approaches demonstrated the adsorption and co-precipitation with ferrihydrite (FH) [1, 109-111]. This technology was considered as the best available technology based on USEPA leaching tests. However, as in the case of lime neutralization, solids characteristics such as the high Fe:As molar ratio ( $>3$ ), large sludge volume and the thermodynamic instability are of disadvantage for an aimed long-term disposal.

Most common practice in industry mainly involves the co-precipitation of ferric arsenate compounds [112]. The (co-)precipitation with ferric iron is one of the most attractive options due to the full widespread availability of this element in concentrates, due to the economic advantage and the effective arsenic removal [113]. Furthermore, materials for disposal should strive for crystalline phases in order to improve stability under environmental conditions [36]. Robust literature review has shown that ferric arsenate, especially crystalline scorodite represents the most appropriate carrier for long-term arsenic fixation in metallurgical processes due to its low solubility, high stability (in a wide range of conditions) and compactness [47, 114, 115].

Scorodite ( $\text{FeAsO}_4 \cdot 2\text{H}_2\text{O}$ ) is a naturally occurring mineral formed in oxidized zones of arsenic bearing ore deposits [116]. Removal of As (V) as scorodite has advantages compared to other technologies, due to the low iron requirement (molar Fe:As ratio close to 1) and high arsenic content (30% of arsenic) [116] of the solids and high density which allow better filterability [72]. There are two options of industrial relevance for the synthesis of scorodite; the first one is the autoclave or "hydrothermal scorodite process" that involves arsenic precipitation at high pressure and temperature (above  $150^\circ\text{C}$ ) [117-119]. While crystalline scorodite can be produced in autoclaves, the drawback of method for application at industrial scale is the high capital costs associated with the necessary equipment. In turn, atmospheric scorodite precipitation ( $<100^\circ\text{C}$ ), based on the controlled supersaturation of the solution [116] can be accomplished by the addition

## CHAPTER 1

of solids as seed and has been extensively researched [116, 120, 121] and is practiced at industrial level in Chile (EcoMetales Ltd.) and Japan (Dowa Metals and Mining Co. Ltd.) [119].

Due to the similarities with chemical (natural) mineral, the biologically precipitated scorodite is considered a more stable crystal on the long term in a wider range of pH (Gonzalez-Contreras, 2012). Although is not yet recognized as one of the best arsenic removal technologies it has been demonstrated to be a cost-efficient solution for the treatment of diluted As(V) solutions ( $\leq 3 \text{ g L}^{-1}$ ). Furthermore, it offers a more sustainable and safe process for arsenic fixation due to the elevated mineral stability, low arsenic solubility, lower iron consumption and high compactness [122, 123] compared to other arsenic carriers mentioned above. Scorodite needs the As to be in the As(V) oxidation state. As(III) need to be oxidized first in order to form scorodite. Mediated by (hyper) thermoacidophilic chemolithotrophic microorganisms, in the scorodite crystallization route, the arsenic (As(III)) present is indirectly oxidized using biologically oxidized iron (Fe(III)) and thus sequester them into scorodite [122]. Besides the biological oxidation of As(III) by *Acidianus brierleyi*, biogenic scorodite formation from As(III) solutions has been also reported by Okibe and co-workers [105, 106, 124].

It is crucial that the produced arsenic-containing precipitate is environmentally stable. It should be kinetically and/or thermodynamically resistant to the transformation into other phases that could lead to remobilization of arsenic. The stability of arsenic compounds on the long term depends on a number of factors such as particle characteristics, the size distribution, the effect of bacterial activity and conditions of the disposal site [1].

### 1.5. THESIS OBJECTIVE AND OUTLINE

The overall objective of my thesis is to explore the treatment of As(III)-bearing solutions through the biological oxidation and precipitation in a single unit process and to expand the range of application of the bioscorodite concept.

In Chapter 2, I investigated the possibilities of biological and chemical As(III) oxidation at low pH and high temperature by a thermoacidophilic iron-oxidizing mixed culture and, chemically, by the addition carbon catalyst. In Chapters 3-5, I focused on different ways to optimize the scorodite precipitation process. The first approach involved the control of the solution saturation via biological Fe(II) bio-oxidation towards formation of settleable stable crystals (Chapter 3) followed by the scale-up to continuous reactor systems (Chapter 4). Finally, I tested the effects of treatment of As(III) solutions in the presence of other Fe(II) sources (Chapter 5).

The conversion of As(III) solely by the mixed culture was poor and detrimental for cell growth, most likely due to the absence of an energy source. Conversely, in addition of Fe(II)<sup>+</sup>, the conversion of As(III) took place in solution at an average rate of 0.03 g L<sup>-1</sup> d<sup>-1</sup> giving some evidence for the microbial contribution to As(III) oxidation through the concomitant oxidation of Fe. However, the oxidizing activity of the mixed culture was hampered after day 9 which was overcome by the addition of granular activated carbon as catalyst. In **Chapter 2**, the proof of scorodite precipitation by biological Fe(II) oxidation coupled to the catalyzed oxidation of As(III) by granular activated carbon at thermoacidophilic conditions was demonstrated. Compared to the crystals produced in the Bioscorodite process of As(V) solutions, the size of the obtained precipitates was approximately 10 times lower as a result of the predominance of nucleation. To improve the formation of crystalline particles based on the concept of saturation control without a neutralization step, the optimization and characterization of the scorodite precipitates in different media with and without catalyst was studied (**Chapter 3**). Because the mechanism of precipitation occurring in these biological systems is presumably driven by the saturation control of the solution, we observed that the effect of the catalyst concentration in the biological process was of relevance to control this parameter. Thus by balancing the chemical As(III) oxidation with the Fe(II) oxidation of the mixed culture allowed controlled precipitation of scorodite. After the right balance of catalyst in the biological process for the precipitation of bigger particles was found, **Chapter 4** focuses on the feasibility of scaling up the process in an airlift reactor for the continuous oxidation and production of (bio)scorodite. This gave us insight into the possible applicability of the process to higher volumes of simulated streams and the long term stability of the crystals produced. Additionally, the composition of the thermoacidophilic iron oxidizing microbial community adapted to As(III) solutions was analyzed. **Chapter 5** presents the use of the alternative Fe(II) source pyrite which is a common sulphide mineral associated with arsenic. The bio-oxidation of pyrite was coupled to the uninterrupted removal of arsenic and was 4 times higher in biological experiments than in chemical experiments.

The general discussion in **Chapter 6** integrates the experimental results of my thesis with the current literature to evaluate the advances and future perspectives of biological oxidation and precipitation of the highly toxic arsenic.

## CHAPTER 1

### REFERENCES

1. Riveros, P., J. Dutrizac, and P. Spencer, *Arsenic disposal practices in the metallurgical industry*. Canadian Metallurgical Quarterly, 2001. **40**(4): p. 395-420.
2. Mandal, B.K. and K.T. Suzuki, *Arsenic round the world: a review*. Talanta, 2002. **58**(1): p. 201-235.
3. Hopenhayn-Rich, C., et al., *Chronic arsenic exposure and risk of infant mortality in two areas of Chile*. Environmental Health Perspectives, 2000. **108**(7): p. 667-673.
4. Anawar, H.M., et al., *Arsenic poisoning in groundwater: Health risk and geochemical sources in Bangladesh*. Environment International, 2002. **27**(7): p. 597-604.
5. Hopenhayn, C., *Arsenic in Drinking Water: Impact on Human Health*. Elements, 2006. **2**(2): p. 103-107.
6. Saha, R., et al., *Geogenic Arsenic and Microbial Contamination in Drinking Water Sources: Exposure Risks to the Coastal Population in Bangladesh*. Frontiers in Environmental Science, 2019. **7**(57).
7. Herath, I., et al., *Natural Arsenic in Global Groundwaters: Distribution and Geochemical Triggers for Mobilization*. Current Pollution Reports, 2016. **2**(1): p. 68-89.
8. World Health Organization, W., *Guidelines for Drinking-water Quality: 4th edition, incorporating the 1st addendum*. 2017: p. 631.
9. Nordstrom, D.K., *Worldwide Occurrences of Arsenic in Ground Water*. Science, 2002. **296**(5576): p. 2143.
10. WHO, *Arsenic in drinking-water: Background document for development of WHO guidelines for drinking-water quality*. 2011, World Health Organization: Geneva. p. 24.
11. Uppal, J.S., Q. Zheng, and X.C. Le, *Arsenic in drinking water—recent examples and updates from Southeast Asia*. Current Opinion in Environmental Science & Health, 2019. **7**: p. 126-135.
12. Mukherjee, A., et al., *Arsenic contamination in groundwater: a global perspective with emphasis on the Asian scenario*. Journal of health, population, and nutrition, 2006. **24**(2): p. 142-163.
13. Kumar, R., et al., *Emerging technologies for arsenic removal from drinking water in rural and peri-urban areas: Methods, experience from, and options for Latin America*. Science of The Total Environment, 2019. **694**: p. 133427.
14. Li, C., et al., *Geothermal spring causes arsenic contamination in river waters of the southern Tibetan Plateau, China*. Environmental Earth Sciences, 2014. **71**(9): p. 4143-4148.
15. Webster, J.G. and D.K. Nordstrom, *Geothermal Arsenic*, in *Arsenic in Ground Water: Geochemistry and Occurrence*, A.H. Welch and K.G. Stollenwerk, Editors. 2003, Springer US: Boston, MA. p. 101-125.
16. Huang, Y., et al., *Arsenic contamination of groundwater and agricultural soil irrigated with the groundwater in Mekong Delta, Vietnam*. Environmental Earth Sciences, 2016. **75**(9): p. 757.
17. Razo, I., et al., *Arsenic and Heavy Metal Pollution of Soil, Water and Sediments in a Semi-Arid Climate Mining Area in Mexico*. Water, Air, and Soil Pollution, 2004. **152**(1): p. 129-152.
18. Bech, J., et al., *Arsenic and heavy metal contamination of soil and vegetation around a copper mine in Northern Peru*. Science of The Total Environment, 1997. **203**(1): p. 83-91.

19. Cortina, J., Litter, M., Gibert, O., Valderrama, C., Sancha, A., Garrido, S., Ciminelli, V., *Latin American experiences in arsenic removal from drinking water and mining effluents*. CRC Press Taylor, 2016: p. p. 391-416.
20. Ahmad, S.A., M.H. Khan, and M. Haque, *Arsenic contamination in groundwater in Bangladesh: implications and challenges for healthcare policy*. Risk management and healthcare policy, 2018. **11**: p. 251-261.
21. Nickson, R., et al., *Arsenic poisoning of Bangladesh groundwater*. Nature, 1998. **395**(6700): p. 338-338.
22. Smith, A.H., E.O. Lingas, and M. Rahman, *Contamination of drinking-water by arsenic in Bangladesh: a public health emergency*. Bulletin of the World Health Organization, 2000. **78**(9): p. 1093-1103.
23. Drahota, P., et al., *Mobility and attenuation of arsenic in sulfide-rich mining wastes from the Czech Republic*. Science of The Total Environment, 2016. **557-558**: p. 192-203.
24. Violante, A., et al., *Coprecipitation of Arsenate with Metal Oxides. 2. Nature, Mineralogy, and Reactivity of Iron(III) Precipitates*. Environmental Science & Technology, 2007. **41**(24): p. 8275-8280.
25. Wang, Y.-Y., L.-Y. Chai, and W.-C. Yang, *Arsenic Distribution and Pollution Characteristics*, in *Arsenic Pollution Control in Nonferrous Metallurgy*, L.-Y. Chai, Editor. 2019, Springer Singapore: Singapore. p. 1-15.
26. Smedley, P.L. and D.G. Kinniburgh, *A review of the source, behaviour and distribution of arsenic in natural waters*. Applied Geochemistry, 2002. **17**(5): p. 517-568.
27. O'Day, P.A., et al., *The influence of sulfur and iron on dissolved arsenic concentrations in the shallow subsurface under changing redox conditions*. Proceedings of the National Academy of Sciences of the United States of America, 2004. **101**(38): p. 13703.
28. Bowell, R.J., et al., *The Environmental Geochemistry of Arsenic — An Overview —*. Reviews in Mineralogy and Geochemistry, 2014. **79**(1): p. 1-16.
29. Kolker, A., et al., *Mode of occurrence of arsenic in four US coals*. Fuel Processing Technology, 2000. **63**(2): p. 167-178.
30. Ferguson, J.F. and J. Gavis, *A review of the arsenic cycle in natural waters*. Water Research, 1972. **6**(11): p. 1259-1274.
31. Cullen, W.R. and K.J. Reimer, *Arsenic speciation in the environment*. Chemical Reviews, 1989. **89**(4): p. 713-764.
32. Drahota, P., et al., *Mineralogical and geochemical controls of arsenic speciation and mobility under different redox conditions in soil, sediment and water at the Mokrsko-West gold deposit, Czech Republic*. Science of The Total Environment, 2009. **407**(10): p. 3372-3384.
33. Macur, R.E., et al., *Bacterial Populations Associated with the Oxidation and Reduction of Arsenic in an Unsaturated Soil*. Environmental Science & Technology, 2004. **38**(1): p. 104-111.
34. Bowell, R.J. and D. Craw, *The management of arsenic in the mining industry*. Reviews in Mineralogy and Geochemistry, 2014. **79**(1): p. 507-532.
35. O'Day, P.A., *Chemistry and Mineralogy of Arsenic*. Elements, 2006. **2**(2): p. 77-83.

## CHAPTER 1

36. Swash, P. and A. Monhemius, *The scorodite process: A technology for the disposal of arsenic in the 21st century* In *Effluent Treatment in the Mining Industry*. Sánchez, M.A.; Vergara, F.; Castro, S.H., Eds., Universidad de Concepción: Concepción, Chile. 1998.
37. Mandal, B.K., 7 - *Changing Concept of Arsenic Toxicity with Development of Speciation Techniques*, in *Handbook of Arsenic Toxicology*, S.J.S. Flora, Editor. 2015, Academic Press: Oxford. p. 179-201.
38. Gasanov, A.A. and A.V. Naumov, *World and Russian markets of arsenic*. Russian Journal of Non-Ferrous Metals, 2016. **57**(7): p. 670-680.
39. Binkowski, L.J., *Arsenic, As*, in *Mammals and Birds as Bioindicators of Trace Element Contaminations in Terrestrial Environments: An Ecotoxicological Assessment of the Northern Hemisphere*, E. Kalisińska, Editor. 2019, Springer International Publishing: Cham. p. 463-481.
40. Sarkar, A. and B. Paul, *The global menace of arsenic and its conventional remediation - A critical review*. Chemosphere, 2016. **158**: p. 37-49.
41. Agency, U.S.E.P., *Response to Requests to Cancel Certain Chromated Copper Arsenate (CCA) Wood Preservative Products and Amendments to Terminate Certain Uses of other CCA Products*. Federal Register, 2003. **68**: p. pp. 17366-17372.
42. Hughes, M.F., et al., *Arsenic Exposure and Toxicology: A Historical Perspective*. Toxicological Sciences, 2011. **123**(2): p. 305-332.
43. Asselin, E. and R. Shaw, *Chapter 41 - Developments in Arsenic Management in the Gold Industry*, in *Gold Ore Processing (Second Edition)*, M.D. Adams, Editor. 2016, Elsevier. p. 739-751.
44. Bissen, M. and F.H. Frimmel, *Arsenic — a Review. Part I: Occurrence, Toxicity, Speciation, Mobility*. Acta hydrochimica et hydrobiologica, 2003. **31**(1): p. 9-18.
45. Murcott, S., *Arsenic Contamination in the World: An International Sourcebook 2012*. 2012, IWA Publishing.
46. Díaz, A.J., J. Serrano, and E. Leiva, *Bioleaching of Arsenic-Bearing Copper Ores*. Minerals, 2018. **8**(5).
47. Nazari, A.M., R. Radzinski, and A. Ghahreman, *Review of arsenic metallurgy: Treatment of arsenical minerals and the immobilization of arsenic*. Hydrometallurgy, 2016.
48. Comisión Nacional del Medio Ambiente, G.d.c., *Normas de Emision para la Regulacion de Contaminantes Asociados a las Descargas de Residuos Liquidos a Aguas Marinas y Continentales Superficiales*, M.S.G.d.l. Presidencia, Editor. 2001.
49. Cui, J., et al., *A new process of continuous three-stage co-precipitation of arsenic with ferrous iron and lime*. Hydrometallurgy, 2014. **146**: p. 169-174.
50. Canada, G.o., *Metal Mining Effluent Regulations, Canada Gazette* 2002. p. 1412-1462.
51. 357/2005, C.R., *Resolução do CONAMA para a classificação dos corpos de água para o seu enquadramento, bem como estabelecimento das condições e padrões de lançamento de efluentes*. 2005: Brasilia. p. 58–63.
52. Gutiérrez, C., *Standards and Thresholds for Waste Water Discharges in Mexico*, in *Standards and Thresholds for Impact Assessment*, M. Schmidt, et al., Editors. 2008, Springer Berlin Heidelberg: Berlin, Heidelberg. p. 113-124.
53. Council, N.R.M.M., *National Water Quality Management Strategy, Australian Drinking Water*

- Guidelines version 3.4.* 2001.
54. Squibb, K.S. and B.A. Fowler, *CHAPTER 7 - The toxicity of arsenic and its compounds*, in *Biological and Environmental Effects of Arsenic*, B.A. Fowler, Editor. 1983, Elsevier: Amsterdam. p. 233-269.
  55. IARC, *Summaries & evaluations: Arsenic and arsenic compounds (Group 1)*. 1987(Lyon, International Agency for Research on Cancer, (IARC Monographs on the Evaluation of Carcinogenic Risks to Humans, Supplement 7)): p. p.100.
  56. Vahter, M., *Mechanisms of arsenic biotransformation*. Toxicology, 2002. **181-182**: p. 211-217.
  57. Hallberg, K.B., H.M. Sehlin, and E.B. Lindström, *Toxicity of arsenic during high temperature bioleaching of gold-bearing arsenical pyrite*. Applied Microbiology and Biotechnology, 1996. **45**(1): p. 212.
  58. Oremland, R.S. and J.F. Stolz, *The Ecology of Arsenic*. Science, 2003. **300**(5621): p. 939-944.
  59. Sehlin, H.M. and E.B. Lindström, *Oxidation and reduction of arsenic by Sulfolobus acidocaldarius strain BC*. FEMS Microbiology Letters, 1992. **93**(1): p. 87-92.
  60. Okibe, N., et al., *Simultaneous oxidation and immobilization of arsenite from refinery waste water by thermoacidophilic iron-oxidizing archaeon, Acidianus brierleyi*. Minerals Engineering, 2013. **48**: p. 126-134.
  61. Rodríguez-Freire, L., et al., *Flexible bacterial strains that oxidize arsenite in anoxic or aerobic conditions and utilize hydrogen or acetate as alternative electron donors*. Biodegradation, 2012. **23**(1): p. 133-143.
  62. Silver, S. and L.T. Phung, *Genes and enzymes involved in bacterial oxidation and reduction of inorganic arsenic*. Applied and Environmental Microbiology, 2005. **71**(2): p. 599-608.
  63. Anguita, J.M., et al., *A new aerobic chemolithoautotrophic arsenic oxidizing microorganism isolated from a high Andean watershed*. Biodegradation, 2018. **29**(1): p. 59-69.
  64. Zhu, Y.-G., et al., *Linking Genes to Microbial Biogeochemical Cycling: Lessons from Arsenic*. Environmental Science & Technology, 2017. **51**(13): p. 7326-7339.
  65. Casiot, C., et al., *Bacterial immobilization and oxidation of arsenic in acid mine drainage (Carnoulès creek, France)*. Water Research, 2003. **37**(12): p. 2929-2936.
  66. Duquesne, K., et al., *Immobilization of arsenite and ferric iron by Acidithiobacillus ferrooxidans and its relevance to acid mine drainage*. Applied and Environmental Microbiology, 2003. **69**(10): p. 6165-6173.
  67. Bruneel, O., et al., *Mediation of arsenic oxidation by Thiomonas sp. in acid-mine drainage (Carnoulès, France)*. Journal of applied microbiology, 2003. **95**(3): p. 492-499.
  68. USEPA, *Toxicity characteristic leaching procedure (TCLP) method 1311*. 1992, EPA Publication SW-846.
  69. Valenzuela, A., *Arsenic management in the metallurgical industry*. 2000, Université Laval.
  70. Leist, M., R.J. Casey, and D. Caridi, *The management of arsenic wastes: problems and prospects*. Journal of Hazardous Materials, 2000. **76**(1): p. 125-138.
  71. Bissen, M. and F.H. Frimmel, *Arsenic — a Review. Part II: Oxidation of Arsenic and its Removal in Water Treatment*. Acta hydrochimica et hydrobiologica, 2003. **31**(2): p. 97-107.
  72. Filippou, D. and G.P. Demopoulos, *Arsenic immobilization by controlled scorodite precipitation*.

## CHAPTER 1

- JOM, 1997. **49**(12): p. 52-55.
73. De Klerk, R.J., et al., *Continuous circuit coprecipitation of arsenic(V) with ferric iron by lime neutralization: Process parameter effects on arsenic removal and precipitate quality*. Hydrometallurgy, 2012. **111-112**: p. 65-72.
74. Basha, C.A., et al., *Removal of arsenic and sulphate from the copper smelting industrial effluent*. Chemical Engineering Journal, 2008. **141**(1): p. 89-98.
75. Mohan, D. and C.U. Pittman, *Arsenic removal from water/wastewater using adsorbents—A critical review*. Journal of Hazardous Materials, 2007. **142**(1): p. 1-53.
76. Eguez, E.H. and E.H. Cho, *Adsorption of arsenic on activated charcoal*. JOM Journal of the Minerals, Metals and Materials Society, 1987. **39**(7): p. 38-41.
77. Mondal, P., C. Balomajumder, and B. Mohanty, *A laboratory study for the treatment of arsenic, iron, and manganese bearing ground water using Fe<sup>3+</sup> impregnated activated carbon: Effects of shaking time, pH and temperature*. Journal of Hazardous Materials, 2007. **144**(1-2): p. 420-426.
78. Molnár, L.u., E. Virčíkova, and P. Lech, *Experimental study of As(III) oxidation by hydrogen peroxide*. Hydrometallurgy, 1994. **35**(1): p. 1-9.
79. Chai, L.-Y., et al., *Arsenic Behaviors and Pollution Control Technologies in Aqueous Solution*, in *Arsenic Pollution Control in Nonferrous Metallurgy*, L.-Y. Chai, Editor. 2019, Springer Singapore: Singapore. p. 29-120.
80. Guo, F., Q. Wang, and G.P. Demopoulos, *Kinetics of iron(III)-catalyzed oxidation of arsenic(III) in acidic solutions with SO<sub>2</sub>/O<sub>2</sub> gas mixture using different iron sources*. Hydrometallurgy, 2019. **189**: p. 105130.
81. Zhang, W., P. Singh, and D.M. Muir, *SO<sub>2</sub>/O<sub>2</sub> as an oxidant in hydrometallurgy*. Minerals Engineering, 2000. **13**(13): p. 1319-1328.
82. Stolz, J.F., et al., *Arsenic and Selenium in Microbial Metabolism\**. Annu. Rev. Microbiol., 2006. **60**: p. 107-130.
83. Higashidani, N., et al., *Speciation of arsenic in a thermoacidophilic iron-oxidizing archaeon, Acidianus brierleyi, and its culture medium by inductively coupled plasma–optical emission spectroscopy combined with flow injection pretreatment using an anion-exchange mini-column*. Talanta, 2014. **122**: p. 240-245.
84. Agency, U.S.E.P., *Arsenic Treatment Technology Evaluation Handbook for Small Systems*, O.o. water, Editor. 2003: Washington, DC.
85. Jia, Y. and G.P. Demopoulos, *Adsorption of Silver onto Activated Carbon from Acidic Media: Nitrate and Sulfate Media*. Industrial & Engineering Chemistry Research, 2003. **42**(1): p. 72-79.
86. Ahumada, E., et al., *Catalytic oxidation of Fe(II) by activated carbon in the presence of oxygen.: Effect of the surface oxidation degree on the catalytic activity*. Carbon, 2002. **40**(15): p. 2827-2834.
87. Huang, C. and P. Fu, *Treatment of arsenic (V)-containing water by the activated carbon process*. Journal (Water Pollution Control Federation), 1984: p. 233-242.
88. Lorenzen, L., J.S.J. van Deventer, and W.M. Landi, *Factors affecting the mechanism of the adsorption of arsenic species on activated carbon*. Minerals Engineering, 1995. **8**(4): p. 557-569.
89. Jahromi, F.G. and A. Ghahreman, *Effect of Surface Modification with Different Acids on the Functional*

- Groups of AF 5 Catalyst and Its Catalytic Effect on the Atmospheric Leaching of Enargite*. Colloids and Interfaces, 2019. **3**(2).
90. Kolthoff, I., *Properties of active charcoal reactivated in oxygen at 400°*. The Journal of the American Chemical Society, 1932. **54**.
  91. Lamb, A.B. and L.W. Elder, *THE ELECTROMOTIVE ACTIVATION OF OXYGEN*. Journal of the American Chemical Society, 1931. **53**(1): p. 137-163.
  92. Choi, Y., A.G. Gharelar, and N. Ahern, *Method for arsenic oxidation and removal from process and waste solutions*. 2014, Google Patents.
  93. Choi, Y., A. Ghahremaninezhad, and N. Ahern. *Process for activated carbon-assisted oxidation of arsenic species in process solutions and waste waters*. in *COM 2014-Conference of Metallurgists*. 2014.
  94. Markets, R.a., *Global and China Activated Carbon Industry Report, 2018-2023*. 2018: China. p. 138.
  95. Rawlings, D.E. and D.B. Johnson, *Biomining*. 2006: Springer Berlin Heidelberg.
  96. Johnson, D.B., *Biomining—biotechnologies for extracting and recovering metals from ores and waste materials*. Current Opinion in Biotechnology, 2014. **30**: p. 24-31.
  97. Donati, E.R., C. Castro, and M.S. Urbieto, *Thermophilic microorganisms in biomining*. World Journal of Microbiology and Biotechnology, 2016. **32**(11): p. 179.
  98. Gericke, M., J.W. Neale, and P.J. van Staden, *A Mintek perspective of the past 25 years in minerals bioleaching*. Journal of the Southern African Institute of Mining and Metallurgy, 2009. **109**: p. 567-585.
  99. Dopson, M. and D.S. Holmes, *Metal resistance in acidophilic microorganisms and its significance for biotechnologies*. Applied Microbiology and Biotechnology, 2014. **98**(19): p. 8133-8144.
  100. Hackl, R.P.N.V., CA), Wright, Frank R. (North Vancouver, CA), Bruynesteyn, Albert (North Vancouver, CA), *Bacteria for oxidizing multimetallic sulphide ores*. 1992, GB Biotech Inc. (Burnaby, CA): United States.
  101. Dopson, M., B.E. Lindström, and K.B. Hallberg, *Chromosomally encoded arsenical resistance of the moderately thermophilic acidophile Acidithiobacillus caldus*. Extremophiles, 2001. **5**(4): p. 247-255.
  102. Dinkla, I.J.T., et al., *Quantifying microorganisms during biooxidation of arsenite and bioleaching of zinc sulfide*. Minerals Engineering, 2013. **48**: p. 25-30.
  103. Casiot, C., et al., *Geochemical Processes Controlling the Formation of As-Rich Waters Within a Tailings Impoundment (Carnoulès, France)*. Aquatic Geochemistry, 2003. **9**(4): p. 273-290.
  104. Lebrun, E., et al., *Arsenite oxidase, an ancient bioenergetic enzyme*. Molecular biology and evolution, 2003. **20**(5): p. 686-693.
  105. Okibe, N., et al., *Microbial formation of crystalline scorodite for treatment of As (III)-bearing copper refinery process solution using Acidianus brierleyi*. Hydrometallurgy, 2014. **143**: p. 34-41.
  106. Tanaka, M. and N. Okibe, *Factors to Enable Crystallization of Environmentally Stable Bioscorodite from Dilute As(III)-Contaminated Waters*. Minerals, 2018. **8**(1): p. 23.
  107. Plessis, C.A.d., J.D. Batty, and D.W. Dew, *Commercial Applications of Thermophile Bioleaching*, in *Biomining*, D.E. Rawlings and D.B. Johnson, Editors. 2007, Springer Berlin Heidelberg: Berlin, Heidelberg. p. 57-80.

## CHAPTER 1

108. Twidwell, L., *Treatment of Arsenic-Bearing Minerals and Fixation of Recovered Arsenic Products: A Review*. 2018.
109. Twidwell, L.G. and J.W. McCloskey, *Removing arsenic from aqueous solution and long-term product storage*. JOM, 2011. **63**(8): p. 94.
110. Jambor, J.L. and J.E. Dutrizac, *Occurrence and Constitution of Natural and Synthetic Ferrihydrite, a Widespread Iron Oxyhydroxide*. Chemical Reviews, 1998. **98**(7): p. 2549-2586.
111. Jia, Y., et al., *Infrared spectroscopic and X-ray diffraction characterization of the nature of adsorbed arsenate on ferrihydrite*. Geochimica et Cosmochimica Acta, 2007. **71**(7): p. 1643-1654.
112. Twidwell, L., R.G. Robins, and J. Hohn, *The Removal of Arsenic from Aqueous Solution by Coprecipitation with Iron (III)*. 2005.
113. Swash, P.M., *The hydrothermal precipitation of arsenical solids in the Ca-Fe-AsO<sub>4</sub>-SO<sub>4</sub> system at elevated temperatures*. 1996, Imperial College of Science, Technology and Medicine, University of London, London.
114. Paktunc, D. and K. Bruggeman, *Solubility of nanocrystalline scorodite and amorphous ferric arsenate: Implications for stabilization of arsenic in mine wastes*. Applied Geochemistry, 2010. **25**(5): p. 674-683.
115. Dove, P.M., Rimstidt, J.D., *The solubility and stability of scorodite, FeAsO<sub>4</sub> · 2H<sub>2</sub>O*. American Mineralogist, 1985. **70**(7-8): p. 838-844.
116. Demopoulos, G.P., *On the preparation and stability of Scorodite*. R.G. Reddy, V. Ramachandran (Eds.), Arsenic Metallurgy, TMS, Warrendale, PA (2005), , 2005: p. 25-50.
117. Gomez, M.A., et al., *The effect of copper on the precipitation of scorodite (FeAsO<sub>4</sub>·2H<sub>2</sub>O) under hydrothermal conditions: Evidence for a hydrated copper containing ferric arsenate sulfate-short lived intermediate*. Journal of Colloid and Interface Science, 2011. **360**(2): p. 508-518.
118. Swash, P. and A. Monhemius, *Hydrothermal precipitation from aqueous solutions containing iron (III), arsenate and sulphate*, in *Hydrometallurgy'94*. 1994, Springer. p. 177-190.
119. Demopoulos, G.P., *Arsenic Immobilization Research Advances: Past, Present and Future*. Canadian Institute of Mining, Metallurgy and Petroleum,, 2014.
120. Singhania, S., et al., *Acidity, valency and third-ion effects on the precipitation of scorodite from mixed sulfate solutions under atmospheric-pressure conditions*. Metallurgical and Materials Transactions B, 2006. **37**(2): p. 189-197.
121. Demopoulos, G., et al. *The atmospheric scorodite process*. in *Copper*. 2003.
122. Qin, W., et al., *Oxidation of arsenite (As (III)) by ferric iron in the presence of pyrite and a mixed moderately thermophilic culture*. Hydrometallurgy, 2013. **137**: p. 53-59.
123. Gonzalez Contreras, P.A., *Bioscorodite: biological crystallization of scorodite for arsenic removal*. 2012, Wageningen university: [S.l.s.n.].
124. Okibe, N., et al., *Bioscorodite crystallization using Acidianus brierleyi: Effects caused by Cu(II) present in As(III)-bearing copper refinery wastewaters*. Hydrometallurgy, 2017.



## CHAPTER 2



**PROOF OF PRINCIPLE:  
BIOLOGICAL SCORODITE PRECIPITATION THROUGH  
THE CATALYZED AS(III) OXIDATION BY GRANULAR  
ACTIVATED CARBON (GAC).**

Authors: Silvia Vega-Hernandez, Jan weijma, Cees J.N. buisman

A modified version of this chapter is published as:  
Vega-Hernandez, Silvia, Jan Weijma, and Cees JN Buisman. "Immobilization of  
arsenic as scorodite by a thermoacidophilic mixed culture via As (III)-catalyzed  
oxidation with activated carbon." *Journal of hazardous materials* 368 (2019): 221-227.  
<https://doi.org/10.1016/j.jhazmat.2019.01.051>

## CHAPTER 2

### ABSTRACT

In this study we describe the immobilization of arsenic as scorodite ( $\text{FeAsO}_4 \cdot 2\text{H}_2\text{O}$ ) by a thermophilic iron-oxidizing mixed culture from an acidic sulfate medium containing  $500 \text{ mgL}^{-1}$  of Fe(II),  $500 \text{ mgL}^{-1}$  As(III) and granular activated carbon (GAC) as the main arsenite oxidant. This study shows that crystalline scorodite can only be precipitated in the presence of the ferrous iron-oxidizing mixed culture (pH 1.3 and  $70^\circ\text{C}$ ). The efficiency of arsenite oxidation was over 99% with a maximum specific oxidation rate of  $280 \text{ mgAs(III) gGAC}^{-1} \text{ day}^{-1}$ . Ferrous iron and arsenite were also oxidized in the absence of the mixed culture, however, no scorodite precipitated under these conditions; consequently, scorodite precipitation was biologically induced. The precipitated scorodite particles had a size between 0.5 and  $10 \mu\text{m}$  with an average of  $5 \mu\text{m}$ , resulting in low settling rates. Ion activity product calculations and observations by Scanning Electron Microscopy (SEM) indicated that microbial cells served as surface for heterogeneous nucleation. The potential of the thermophilic mixed culture for the scorodite formation explored in this study provides the basis of a new approach for the treatment of As(III) polluted streams.

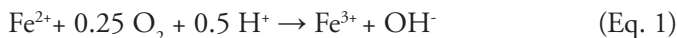
**Keywords:** Arsenic removal; Arsenite oxidation; Biogenic scorodite; ferrous iron oxidation; Granular activated carbon; Thermoacidophilic mixed culture.

## 1. INTRODUCTION

The contamination of water sources with arsenic is a matter of concern caused by its high toxicity to all forms of life [1]. Arsenic naturally exists in four oxidation states with As(III) (arsenite) as the most toxic species [2]. Due to its natural association with minerals in the earth crust, the primary anthropogenic source of arsenic emission to natural waters are mining and metallurgical activities. Especially in the processing of gold and copper ores, arsenic represents one of the major impurities and the inadequate management of arsenic solid residues often results in emission to ground or surface waters [3, 4]. Environmental regulations restrict arsenic discharge into the environment [4, 5].

The development of technologies for removal and stable disposal of the arsenic from effluents poses major challenges for the industry. Available arsenic removal technologies are based on adsorption and (co)-precipitation [6, 7]. However, these techniques are not optimal due to the large volume of solid waste generated and the unstable resultant product, which might not meet the regulatory requirements for long-term storage [8]. Crystalline scorodite ( $\text{FeAsO}_4 \cdot 2\text{H}_2\text{O}$ ) has been considered a suitable medium for the stable immobilization and long-term storage of arsenic as this mineral combines low leaching rates with high arsenic content [9, 10]. For example with an initial concentration of  $0.5 \text{ g L}^{-1}$  of As(V) and complete precipitation of As(III) from the solution as scorodite,  $1.3 \text{ g scorodite L}^{-1}$  is formed. With a density of scorodite of  $3.27 \text{ g cm}^{-3}$ , the volume of the precipitate then amounts to merely  $0.4 \text{ ml}$  per litre of treated solution.

The chemical precipitation of scorodite (mainly from As(V) (arsenate) solutions) under pressurized ( $>150 \text{ }^\circ\text{C}$ ) [11-13] and atmospheric conditions with  $T < 95 \text{ }^\circ\text{C}$  [4, 14-16] has been well-documented. On the other hand, biological crystallization of scorodite was previously demonstrated by [17] through the bio-oxidation of ferrous iron in arsenate solutions at pH 1.1-1.5 and  $70 \text{ }^\circ\text{C}$ :



Process streams often contain diluted concentrations of arsenic (between  $1$  and  $3 \text{ g L}^{-1}$ ) [18], mainly present in the trivalent form (As(III)) [19, 20]. Thus, the oxidation of As(III) to its pentavalent form (As(V)) is a requisite for the precipitation of arsenic as scorodite. Under atmospheric conditions As(III) without catalysts oxidation with oxygen results in a slow reaction [21]. Hydrogen peroxide is an effective As(III) oxidizing agent in hydrometallurgical processes [22, 23]. However, the use of expensive peroxide and its tendency to decompose in the presence of solids may limit widespread application

## CHAPTER 2

in the scorodite proces [4, 24]. As an alternative, the biological oxidation of As(III) by the thermoacidophilic archaeon *Acidianus brierleyi* in addition of Fe(II) (ferrous iron) followed by the synthesis of ferric arsenate from dilute arsenic solutions (between 0.5-1 g·L<sup>-1</sup>) was reported [19, 25, 26]. The oxidation rate was between 0.016-0.026 gAs(III) L<sup>-1</sup> day<sup>-1</sup> [19] under thermoacidophilic conditions (70° C, pH ≤ 1.5).

Activated carbon is considered an efficient catalyst for the oxidation of As(III) in acid solutions. High rates of As(III) oxidation have been reported when air or pure oxygen is used as oxidant in the presence of granulated activated carbon (GAC) at pH 1 and room temperature [27]. The use of GAC in the scorodite process could avoid the consumption of expensive hydrogen peroxide, rendering the process more competitive with alternative methods for arsenic immobilization. Although the mechanism involved in the surface catalyzed oxidation is not fully understood, it has been suggested that a strong oxidant such as hydrogen peroxide was formed in solution when water and oxygen reacted with surface functional groups of GAC [4, 28].

The scorodite process aims to immobilize the bulk of arsenic in metallurgical waste streams as a solid that is safe to store. Therefore, in this study, we have investigated the Fe(II) oxidation, As(III) oxidation and scorodite precipitation in a single step. Starting solutions contained ferrous iron, arsenite, a thermoacidophilic iron-oxidizing mixed culture, and GAC. Likewise, the contribution of the microorganisms and GAC to the oxidation of Fe(II) and As(III) and the characterization of the precipitates were examined.

## 2. EXPERIMENTAL SECTION

### 2.1. MIXED CULTURE AND MEDIA COMPOSITION

The thermoacidophilic mixed culture used in this study was kindly provided by Prof. Sandström of Luleå University (Sweden). The mixed culture was previously grown on sulfide minerals as energy source and used in bioleaching experiments at 65 °C and pH 1.6. The composition of the mixed culture is not defined but species from the genera *Sulfobacillus* and *Sulfolobales* were identified previously [29].

In this study, the mixed culture (considered as biotic condition) was inoculated at 10 % v/v in the bottles with a concentration of approximately 1·10<sup>6</sup> cell ml<sup>-1</sup>. Prior to inoculation, cells were harvested by 2-3 successive cycles of centrifugation at 10000 rpm for 15 minutes and resuspension in acidic deionized water (pH 1.3). A control with the same composition in absence of the microorganisms (considered as abiotic condition) were also included in the experiments.

The basal medium contained 3.0 mM (NH<sub>4</sub>)<sub>2</sub>SO<sub>4</sub>, 2 mM MgSO<sub>4</sub>·7H<sub>2</sub>O and 1.5 mM

$\text{KH}_2\text{PO}_4$  and 1.3 mM KCl. The medium was supplemented with 0.2% w/v yeast extract and trace elements were added according to DSM88 medium for *Sulfolobales*. The solution pH was adjusted to 1.3 with 50 mM  $\text{H}_2\text{SO}_4$ . All chemicals used were analytical- reagent grade.

Ferrous iron stock solution was prepared by dissolving ferrous sulfate heptahydrate ( $\text{FeSO}_4 \cdot 7\text{H}_2\text{O}$ ) in dilute sulphuric acid ( $\text{H}_2\text{SO}_4$ , 50 mM). Arsenic solutions were prepared from sodium arsenite standard solution Tritipur ( $0.05 \text{ mol L}^{-1} \pm 0.1\% \text{ NaAsO}_2$ ).

## 2.2. CATALYST FOR ARSENITE OXIDATION

Granular activated carbon NORIT GAC 830W (Cabot Norit Nederland B.V., Amersfoort, The Netherlands) with a particle size from 0.8-2.3 mm was used as catalyst in the experiments. The GAC was produced from coal followed by thermal activation and possesses a surface area of  $885 \text{ m}^2 \text{ g}^{-1}$ , density of  $1.06 \text{ g cm}^{-3}$ , a pore radius of 8–60  $\text{\AA}$ , a total pore volume of  $0.775 \text{ cm}^3 \text{ g}^{-1}$  according to supplier specifications. The GAC used in the experiments was washed with sulphuric acid (1 M) followed by rinsing with deionized water in order to remove impurities, before its use in experiments.

## 2.3. BATCH EXPERIMENTS

Batch experiments were carried out in serum bottles of 125 mL closed with a butyl rubber stopper and crimped aluminum seal. The flasks were filled with 50 ml of media and inoculated as described above and placed in a thermostat shaker incubator at 150 rpm and 70 °C. Samples were taken regularly for analysis of dissolved Fe(II) and Fe(III), total Fe, dissolved As(III) and As(V) and total As. Approximately 1.5 ml of liquid sample was taken with a syringe from the sealed bottles prior to the chemical analysis. At the end of the experiment, the precipitates from the bottles were collected by centrifugation, washed with 50 mM of sulphuric acid, followed by washing with DI water and dried in a vacuum oven at 60 °C temperature before solids characterization.

The biotic tests were performed in triplicate in addition to an abiotic control that was inoculated with 10 % v/v of acid sterile water. Furthermore, the results are expressed as the mean  $\pm$  value standard deviation.

## 2.4. ANALYTICAL METHODS

Liquid samples periodically withdrawn from batch bottles to monitor the concentrations

## CHAPTER 2

of iron and arsenic species in addition to the solution pH and redox potential. The samples were filtered through a 0.2  $\mu\text{m}$  cellulose acetate membrane filter and diluted with 10 mM of sulphuric acid if needed for the analyses.

Dissolved Fe(II) and Fe(III) concentrations of filtered samples were measured using Dr. Lange Cuvette test LCK 320 and a Xion 500 spectrophotometer (Hach-Lange, Germany). As(III) and As(V) concentrations were measured with an HPLC connected to a UV photospectrometer. The HPLC was an ultimate VWD 3000 RS (Dionex, Netherlands) equipped with an ion exclusion column using sulphuric acid 10 mM as the mobile phase. The concentration of arsenic species (As(III) and As(V)) in solution were measured by anionic ion exclusion chromatography. The HPLC system was an ultimate VWD 3000 RS (Dionex, Netherlands) equipped with an ion exclusion column using sulphuric acid 10 mM as the mobile phase and connected to a UV photospectrometer. The method for As(III) and As(V) analysis has been described in more detail elsewhere [30]. Total dissolved iron and arsenic of filtered samples were also quantified in the aqueous phase via inductively coupled plasma optical emission spectrometry (ICP-OES). The pH and oxido-reduction potential of the samples were measured with glass electrodes QP181X and QR480X-Pt (Prosense, Netherlands) respectively.

Samples of the synthesized precipitates and the granules were collected at the end of the experiment for the solids characterization. Carbon granules were manually separated (by sieving), while the produced precipitates were collected by centrifugation. Both solid samples were three times washed with 50 mM of sulphuric acid and rinsed with deionized water, respectively. Finally, these samples were dried in a vacuum oven 60°C before the analyses. The particle size distribution was measured by a laser diffraction particle size analyzer (SALD-2300, Shimadzu Co., Japan). The identification of the mineral phases present in the solids was performed by powder X-Ray Diffraction (XRD). The XRD analysis was performed with a Bruker D2 PHASER diffractometer (Bruker Axs) with Cu-K $\alpha$  radiation generated at 30 kV - 10 mA in the angular range -3 — 160 ° (2 $\theta$ ) with a step size of  $\pm 0.02$  ° and acquisition time of 1 s per step. The X-ray diffractogram was evaluated by the software DIFFRAC.EVA V4 (Bruker Axs). The morphology of the solids was investigated by scanning electron microscopy coupled with energy dispersive X-ray spectrometry (SEM-EDX). The samples were analysed at an accelerating voltage of 2.0 kV, and electron beam current of 50 pA, at room temperature, in a field emission scanning electron microscope (Magellan 400, FEI, Eindhoven, the Netherlands) equipped with an X-Max/AZtec X-ray analyser detector for energy dispersive X-ray (Oxford Instruments Analytical, High Wycombe, England).

### 3. RESULTS AND DISCUSSION

#### 3.1. AS(III) OXIDATION MEDIATED BY GAC AND THE MIXED CULTURE

In the absence of GAC, the mixed culture was unable to oxidize As(III) under the studied conditions (data not shown). Batch experiments were performed to determine the influence of 9 gL<sup>-1</sup> of GAC on the oxidation of As(III) with and without the thermoacidophilic mixed culture and in the absence of Fe(II). The toxicity of Arsenic for thermoacidophilic microorganisms has been reported for species of the genus *Sulfolobus* and *Acidianus*, unable to sustain growth in solutions with As(III) as the only energy source. [19, 29, 31, 32].

With GAC, As(III) was depleted within 3 days to less than 30 mgL<sup>-1</sup> with and without the culture at a similar zero order rate of 153 mgL<sup>-1</sup>.day<sup>-1</sup> and 149 mgL<sup>-1</sup>.day<sup>-1</sup> respectively (Figure 1). At day 4 the concentration of As(III) decreased to less than 0.5 mg.L-1 (HPLC detection limit) in both cases, while the As(V) concentration remained stable at 395±20 mgL<sup>-1</sup> and 433±12 mgL<sup>-1</sup>, for the incubation with the mixed culture and the abiotic control, respectively. Since 463 (biotic) and 471 mgL<sup>-1</sup> As(III) (abiotic) were present at time 0 (t=0), about 70 and 40 mgL<sup>-1</sup> of As were missing from the mass balance at day 9, respectively. Because there were no precipitates visible in the bottles, most likely some As had adsorbed as As(V) to the GAC and also to microbial cells (~30 mgL<sup>-1</sup>) in the experiment with the mixed culture (bio-adsorption and accumulation). With 40 mgL<sup>-1</sup> As(V) adsorbed to 20 g.L<sup>-1</sup> of GAC, the adsorption capacity estimated is 2 mg.g<sup>-1</sup> activated carbon, which is within the range of reported values [33]. Thus, with the As(III) depletion rate representing the As(III) oxidation rate, the latter amounts also to approximately 150 mgL<sup>-1</sup>.day<sup>-1</sup>, corresponding to a specific arsenite oxidation rate of 0.44 mmol e<sup>-</sup>.gGAC<sup>-1</sup>.day<sup>-1</sup> under the experimental conditions.

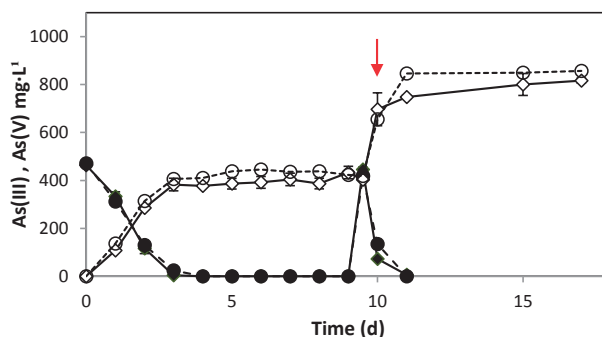


**Figure 1.** Oxidation of As(III) to As(V) with and without the mixed culture (solid and dashed lined respectively) in the presence of 9 gL<sup>-1</sup> of GAC. Closed symbols: As(III), open symbols: As(V). Error bars indicate standard deviation of the biotic triplicates and the red arrow indicates the addition of arsenite in the experiment.

## CHAPTER 2

Arsenite oxidation continued when As(III) was added to the bottles on day 9 (red arrow in Figure 1). Within 2 days As(III) was depleted at an average rate of  $280 \text{ mg}\cdot\text{L}^{-1}\cdot\text{day}^{-1}$  without the culture and  $230 \text{ mg}\cdot\text{L}^{-1}\cdot\text{day}^{-1}$  with the culture, which is markedly higher than the initial oxidation rate. It may be speculated that, despite pre-washing, impurities were washed from the surface of the GAC by the acid solution in the batch, thereby increasing the number of active surface sites available. The mass balance for dissolved As was again incomplete for the experiment with the culture, where approximately  $450 \text{ mg}\cdot\text{L}^{-1}$  As(III) was added on day 9, and only  $406 \text{ mg}\cdot\text{L}^{-1}$  As(V) accumulated between day 9 and day 17. In the abiotic experiment, the addition of approximately  $420 \text{ mg}\cdot\text{L}^{-1}$  As(III) was followed by accumulation of  $433 \text{ mg}\cdot\text{L}^{-1}$  of As(V) in solution. The latter suggests that the adsorption equilibrium was reached. The catalyzed oxidation of As(III) by activated carbon in batch and continuous reactors was reported previously [27]. With a concentration of dry GAC around  $165 \text{ g}\cdot\text{L}^{-1}$  previously wetted at pH 1 and  $40^\circ\text{C}$  in addition of oxygen or air, a zero order oxidation rate of  $0.05 \text{ gAs(III)}\cdot\text{gGAC}^{-1}\cdot\text{d}^{-1}$  can be estimated. Although the concentrations of As(III) and GAC used in this study were 18 times lower than in the mentioned study, also a zero reaction order was observed with an oxidation rate of  $0.017 \text{ gAs(III)}\cdot\text{gGAC}^{-1}\cdot\text{day}^{-1}$ . In the proposed mechanism for the arsenic oxidation catalyzed by activated carbon, the oxidation takes place by the formation hydrogen peroxide. This reaction occurs when oxygen reacts with the activated carbon in solution [4, 28].

In this scenario, oxygen plays an important role as electron acceptor for arsenite oxidation with activated carbon. The oxidation of As(III) mediated by GAC under anaerobic conditions was assessed (data not shown) and the concentration of As(III) ( $500 \text{ mg}\cdot\text{L}^{-1}$ ) remained constant in solution during the test. This results are in accordance with the arsenic oxidation mechanism aforementioned.

### 3.2. AS(III) OXIDATION WITH GAC AND SCORODITE PRECIPITATION WITH AND WITHOUT ADDITION OF THE MIXED CULTURE

Approximately  $500 \text{ mg}\cdot\text{L}^{-1}$  of As(III) was oxidized in biotic experiments containing  $9 \text{ g}\cdot\text{L}^{-1}$  GAC and about  $450 \text{ mg}\cdot\text{L}^{-1}$  Fe(II) (Figure 2A and 2C). Until day 3, As(III) depletion rates were similar to the experiments without Fe(II) ( $\sim 150 \text{ mg}\cdot\text{L}^{-1}\cdot\text{d}^{-1}$  As(III), Figure 1), indicating that As(III) oxidation followed the same mechanism; The oxidation of Fe(II) was also apparent from the start of the experiment. Thus, As(III) and Fe(II) oxidation did not compete for a possible common electron acceptor or catalytic sites on the GAC. After day 3 the As(III) depletion became slower (Figure 2A), with an average rate of only  $27 \text{ mg}\cdot\text{L}^{-1}\cdot\text{d}^{-1}$  with microbial cells, and a higher average rate of  $50 \text{ mg}\cdot\text{L}^{-1}\cdot\text{d}^{-1}$  without the cells. Only after 6 and 7 days for the biotic and abiotic experiment respectively, As(III)

was below  $0.5 \text{ mgL}^{-1}$ , while in the experiment without Fe(II) this concentration was reached after only 4 days. Thus, oxidation of As(III) was hindered from day 3 onwards, probably by the precipitation of ferric arsenate on the GAC which was apparent from the removal of 40% of total arsenic and Fe from solution in the biotic experiments between day 2-4 (Figure 2B and 2D).

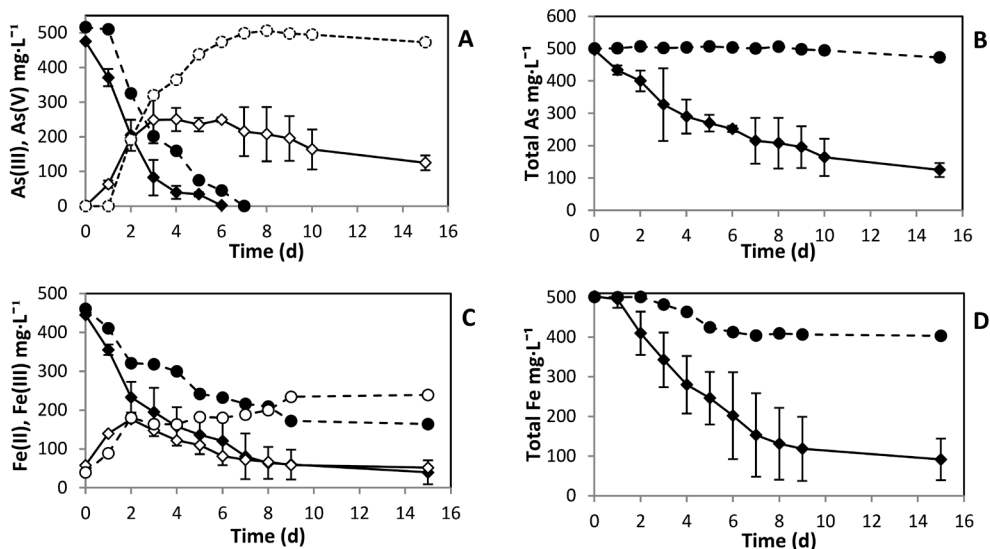


**Figure 2.** Oxidation of  $500 \text{ mgL}^{-1}$  As(III) with and without of the mixed culture (solid and dashed lined respectively) with  $500 \text{ mgL}^{-1}$  Fe(II) and  $9 \text{ gL}^{-1}$  of GAC. As(III) and As(V) dissolved (A), total As dissolved (B), Fe(II) dissolved (C) and Fe(III) dissolved (D). Error bars indicate standard deviation of the biotic triplicates.

The oxidation of Fe(II) in addition of GAC proceeded simultaneously with As(III) oxidation, with and without the mixed culture. However, Fe(II) oxidation proceeded faster in biotic experiments. Under the same experimental conditions, in absence of GAC, the biotic oxidation of Fe(II) proceeded at a slower rate (data not shown). Fe(II) oxidation stopped on day 9, with 60 (biotic) and  $172 \text{ mgL}^{-1}$  (abiotic) remaining in solution (Figure 2B). 61% Fe(II) was oxidized in the presence of GAC and 87% with GAC and the mixed culture, indicating that Fe(II) oxidation due to GAC-catalyzed oxidation was predominant.

From day 3 onwards, results of biotic experiments began to deviate from the abiotic control with respect to the dissolved concentrations of total arsenic and total iron (Figure 2B and D). With the culture, As(V) and Fe(III) started to decrease (Figure 2A and 2C), indicating the onset of ferric arsenate precipitation while without the culture

## CHAPTER 2

both ions further accumulated, revealing that the microorganisms played a crucial role in the precipitation process. A milky colloidal-like suspension was observed at day 4 in the biotic experiment while the control bottles (without inoculum) remained clear during the experiment (Figure S1). The volume based particle size distribution of the solids collected at day 14 from biotic experiments showed an average particle size of 5  $\mu\text{m}$  (ranging from 0.5 to 10  $\mu\text{m}$ ) (Figure S2). Observations with scanning electron microscope (SEM) showed the presence of particles with various morphologies, mostly agglomerates with an average size  $\leq 5 \mu\text{m}$  (Figure 3A and B). Mass balances for dissolved Fe(II, III) and As(III, V) on day 0 and 15 in the biotic experiment showed that 411  $\text{mgL}^{-1}$  of Fe and 375  $\text{mgL}^{-1}$  of As were removed from solution, at a molar ratio Fe/As of 1.47. Because the theoretical Fe/As molar ratio in scorodite is 1, this indicates that at least part of the Fe has not precipitated as scorodite. However, the mineral phase present in the solids collected after the experiment were identified by XRD as scorodite, while the presence of other precipitates were not indicated in the diffractogram. (Figure S3). The analysis of the Fe and As content of the fine particles revealed a ratio of Fe/As of 1.3. These results suggest that Fe also precipitated as amorphous phases which were not identified by XRD.

The saturation ratio for scorodite was calculated as the ratio of ion activity product (IAP) of Fe(III) and As(V) in solution to the solubility product of the salt ( $K_{\text{sp}}$ ). The saturation ratio in the biotic experiments ranged from 1.5 to 3.3 between days 2 until day 9, while the saturation index in the abiotic experiment was higher than biotic bottles throughout the experiment (Table S1). In spite of the higher saturation index, the solution of the abiotic test remained clear throughout the experiment. Therefore, while in both abiotic and biotic experiments the solution was oversaturated, only in the latter scorodite precipitated. Apparently, with the saturation ratio remaining below 3 in biotic experiments, both biotic and abiotic solutions were in a metastable state, but only in the biotic experiment the precipitation of scorodite took place, suggesting that precipitation of scorodite was biologically influenced. We postulate that microbial cells served as surface for heterogeneous nucleation, which is supported by the presence of bacillus-like microorganisms closely attached to the scorodite precipitates as observed by SEM (Figure 3C). The nucleation of scorodite or precursors on microbial cell surface was also proposed as one of the possible mechanisms in the bioscorodite process starting with As(V) solutions [18]. In addition, it has been also mentioned, that cell surface of live and dead or cell debris could also serve as nucleation sites of minerals [34, 35].

The IAP (Figure 4) increased between day 2 and day 5, largely due to the increased activity of As(V) (Table S1). Precipitates were visible in the bottles from day 4 onwards, furthermore around day 9 light green-grey precipitates were observed in the bottles, at the same time that the IAP reached values around  $10^{-22}$  (Figure S1B) which represents the

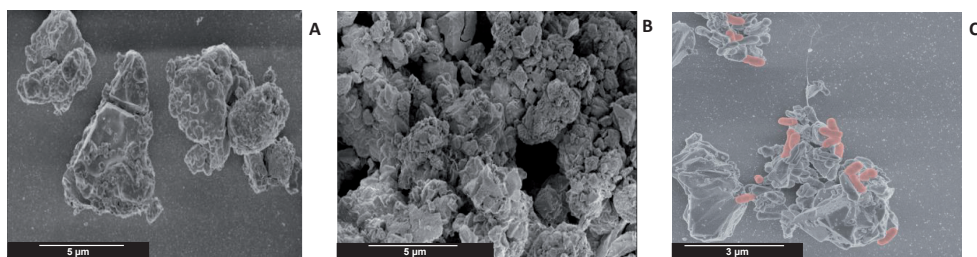


**Figure 3.** SEM photograph of the scorodite precipitates obtained at 70 °C from the bulk solution in biotic experiments with 9 gL<sup>-1</sup> GAC, 500 mgL<sup>-1</sup> As(III) and Fe(II) respectively. Image of the solids agglomerated performed with 10000X magnification (A and B) and microorganisms (*Bacillus*) (coloured red) attached to the precipitates with 25000X magnification (C).

$K_{sp}$  reported for scorodite [17]. Approximately 75% of As was removed from solution in the biotic experiments at day 16. The presence of 12.7 mg of Fe and 10.3 mg of As per gram of activated carbon was estimated from the digestion of the granules of activated carbon, accounting for 25% Fe and 20% As removed from solution. White precipitates were visible on the dry GAC collected at day 16 (Figure 5A). Likewise, the image of the surface granule indicated the deposition of crystalline colloidal scorodite  $\leq 1\mu\text{m}$  (Figure 5B), which was also supported by the content of Fe and As on the above-mentioned precipitates, determined by EDX (Figure S4). Although most of the Fe and As was precipitated as fine particles, a fraction was associated to the GAC. Considering an adsorption of As(V) of maximally 1.1 mg:gGAC<sup>-1</sup>, the amount precipitated as scorodite is at least 9.3 mg:gGAC<sup>-1</sup>. Therefore, besides the adsorptive and oxidative capacity GAC also served as a surface for heterogeneous nucleation.

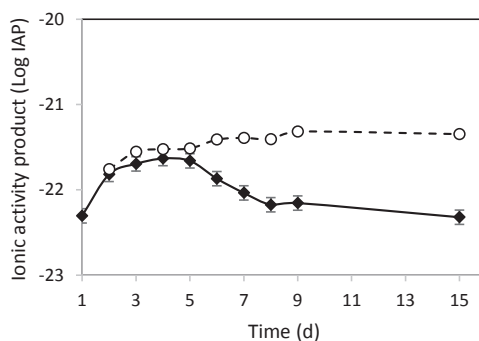


**Figure 4.** Ion activity product of scorodite precipitates in biotic and abiotic experiments at 70 °C (solid and dashed lines respectively). Error bars indicate standard deviation of the biotic triplicates.

### 3.3. AS(III) OXIDATION WITH GAC AND SCORODITE PRECIPITATION IN THE PRESENCE OF AUTOCLAVED MIXED CULTURE

To shed light on the possible mechanism behind the generation of scorodite precipitates by the mixed culture in this study, active biomass ( $1 \times 10^6$  cells  $\text{ml}^{-1}$ ) was autoclaved and 10% v/v was added to batch bottles (triplicates) with  $9 \text{ gL}^{-1}$  of GAC. A control with autoclaved acidic water (pH 1.2) was also included (Figure 6).

As(III) was oxidized with similar rates in the bottles inoculated with the autoclaved mixed culture and the control (Figure 6A). The concentrations of total arsenic remained constant during the experiment and the solution in the bottles also remained clear indicating that no precipitation occurred. A brownish solution was observed in the bottles inoculated with autoclaved mixed culture, typical for acidic Fe(III) solutions. The higher initial concentration of Fe in the biotic autoclaved test compared to the control experiment without the autoclaved inoculum (Figure 6C) was due to the remaining concentration of Fe from the inoculum. In spite of some fluctuations in the oxidation of iron between the bottles with autoclaved inoculum (Figure 6C), the total concentration of dissolved Fe species also remained fairly constant with autoclaved cells and the control (Figure 6C) as observed in the abiotic control of previous experiments. In addition, these results indicate that for the precipitation of ferric arsenate, in particular scorodite, the presence of the cell material which remains after autoclaving, does not suffice for onset of precipitation. Thus, only intact biological material matter induces scorodite precipitation.

**Figure 5.** Picture of solids collected at day 16 (A) and SEM photograph of the GAC surface (B) from biological test with  $9 \text{ gL}^{-1}$  GAC,  $500 \text{ mgL}^{-1}$  As(III) and Fe(II) respectively. Scorodite precipitates obtained at  $70 \text{ }^\circ\text{C}$ . SEM photograph was performed with 10000X magnification.

A possible explanation builds upon our previous observations [36] when deposited jarosite and scorodite precipitates were found on the surface of iron-oxidizing *Sulfolobales*. Such precipitates could function as seeds for scorodite precipitation. Different from the above mentioned study [36], in the present work fine particles of scorodite were formed, rather than well-settleable precipitates. Thus, in our experiments nucleation appears to have been dominant over crystal growth. This aspect will be the focus of follow up work.

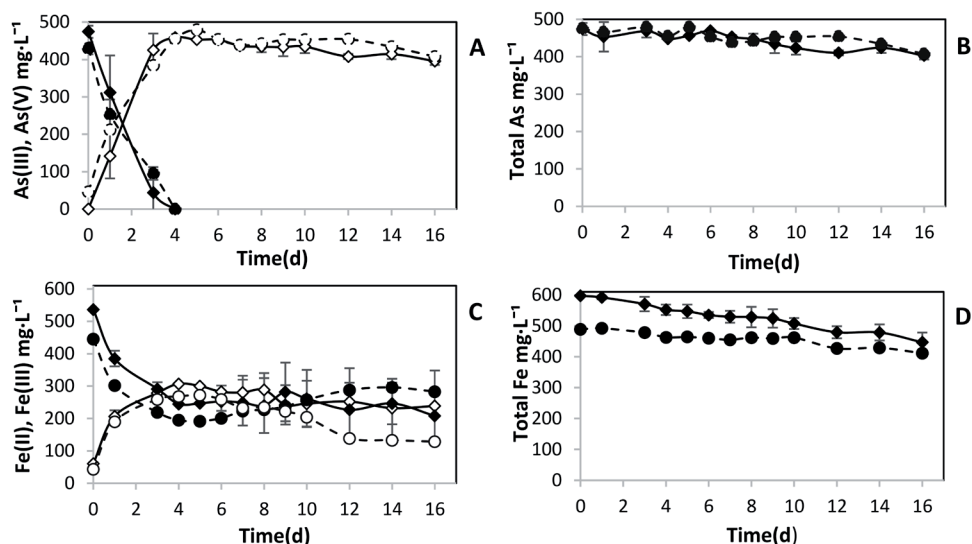


**Figure 6.** Oxidation of 500 mg·L<sup>-1</sup> As(III) and Fe(II) with and without the autoclaved mixed culture (solid and dashed lined respectively) and 9 g·L<sup>-1</sup> GAC. Dissolved As(III) and As(V) (A), total dissolved As (B), dissolved Fe(II), Fe(III) (C) and total dissolved Fe (D). Error bars indicate standard deviation of the biotic replicates.

The formation of scorodite in our study was dependent on the presence of the microorganisms. In our previous work, we observed that the precipitation of crystalline scorodite from As(V) solutions was controlled by the biological oxidation of Fe(II) [17]. Here, the use of GAC as catalyst mitigated the toxicity of As(III) but also affected the oxidation of Fe(II); therefore, an efficient combination of GAC in the process might be beneficial to control the saturation index of scorodite and thus, the particle size. The results obtained provide the basis of a new method for the management of As(III) polluted streams.

#### 4. CONCLUSIONS

In this work, we researched the precipitation of scorodite from sulfate solutions with a thermophilic iron oxidizing mixed culture and granular activated carbon as catalyst for arsenite oxidation. Our new findings showed that biologically induced crystallization is the main mechanism for the precipitation of scorodite. Furthermore, high removal of arsenic (> 90%) was achieved when the mixed culture was combined with 9 g·L<sup>-1</sup> GAC and Fe(II) as electron donor. In addition, scorodite was the main mineral phase identified in the precipitates neglecting the presence of other contaminants. Batch experiments showed that the oxidation of As(III) to As(V) is continuously

## CHAPTER 2

catalyzed by activated carbon under aerobic thermoacidophilic conditions similar to previous studies.

## SUPPORTING INFORMATION OF CHAPTER 2

**Table S1.** Calculated saturation index in batch experiments at 70 °C with 9 gL<sup>-1</sup> GAC, 500 mgL<sup>-1</sup> As(III) and Fe(II) respectively.

Day		Log IAP ( $\alpha_{Fe^{3+}} \cdot \alpha_{AsO_4^{3-}}$ )	SI		Log IAP ( $\alpha_{Fe^{3+}} \cdot \alpha_{AsO_4^{3-}}$ )	SI
0		0	0.0		0	0.0
1	Biotic	-22.38	0.4	Abiotic	0	0.0
2		-21.74	1.8		-21.8	1.8
3		-21.68	<b>2.1*</b>		-21.6	2.7
4		-21.49	<b>3.3*</b>		-21.5	3.0
5		-21.53	<b>3.0*</b>		-21.4	4.3
6		-22.07	0.9		-21.4	4.5
7		-22.33	0.5		-21.3	5.0
8		-22.50	0.3		-21.3	5.5
9		-22.50	0.3		-21.2	6.3
15		-22.59	0.3		-21.2	6.3

\*:visible appearance of colloidal in the biotic bottles

**Table S2.** Fe mass balance in biotic experiments at 70 °C with 9 gL<sup>-1</sup> GAC, 500 mgL<sup>-1</sup> As(III) and Fe(II) respectively.

		Biotic	Control
Total Fe measured $t_{(0)}$	(mg)	50.30	50.09
Total Fe measured $t_{(15)}$	(mg)	12.85	40.3
Total Fe in precipitates*	(mg)	27.35*	0
Total Fe adsorbed on GAC	(mg)	11.9	12.2
Difference (error)	(%)	3.4	5
Fe/As Molar ratio precipitate		1.3	0

\*: 100% of the precipitates assumed as scorodite

**Table S3.** As mass balance in in biotic experiments at 70 °C with 9 gL<sup>-1</sup> GAC, 500 mgL<sup>-1</sup> As(III) and Fe(II) respectively.

		Biotic	Control
Total As measured $t_{(0)}$	(mg)	50.08	50.06
Total As measured $t_{(15)}$	(mg)	14.00	43.76
Total As in precipitates*	(mg)	28.30*	0
Total Fe adsorbed on GAC	(mg)	9.8	9.9
Difference	(%)	3.4	7
Fe/As Molar ratio precipitate		1.3	0

\*: 100% of the precipitates assumed as scorodite

**Table S4.** Hydrolysis constants for arsenate and ferric iron used in this study for the IAP calculation [17, 37, 38].

	pK
<b>Arsenate</b>	
$H_3AsO_4 = H_2AsO_4^- + H^+$	2.24
$H_2AsO_4^- = HAsO_4^{2-} + H^+$	6.86
$HAsO_4^{2-} = AsO_4^{3-} + H^+$	11.49
<b>Ferric Iron</b>	
$Fe^{3+} + H_2O = Fe(OH)^{2+} + H^+$	2.19
$Fe(OH)^{2+} + H_2O = Fe(OH)_2^+ + H^+$	3.48
$Fe(OH)_2^+ + H_2O = Fe(OH)_3 + H^+$	6.33
$Fe(OH)_3 + H_2O = Fe(OH)_4^- + H^+$	9.6

### SUPPORTING EQUATIONS.

Equations 1, 2 and 3 were used for the calculation of the Ion Activity Product (IAP) of the scorodite precipitates [17].

$$IAP_{\text{scorodite}} = (a_{Fe^{3+}})(a_{AsO_4^{3-}}) \quad (\text{Eq 1})$$

$$a_{AsO_4^{3-}} = \frac{Arsenate_{total}}{1 + \frac{a_{H^+}}{K_3} + \frac{(a_{H^+})^2}{K_2K_3} + \frac{(a_{H^+})^3}{K_1K_2K_3}} \quad (\text{Eq 2})$$

$$a_{Fe^{3+}} = \frac{Ferric_{total}}{1 + \frac{K_1}{a_{H^+}} + \frac{K_2K_3}{(a_{H^+})^2} + \frac{K_1K_2K_3}{(a_{H^+})^3} + \frac{K_1K_2K_3K_4}{(a_{H^+})^4}} \quad (\text{Eq 3})$$



**Figure S1.** Precipitates visualized in the batch bottle of the biotic experiments at day 4(A), and day 14 (B) and bottle of abiotic experiment at day 16 (C) at 70 °C with 9 gL<sup>-1</sup> GAC, 500 mgL<sup>-1</sup> As(III) and Fe(II) respectively.

## CHAPTER 2

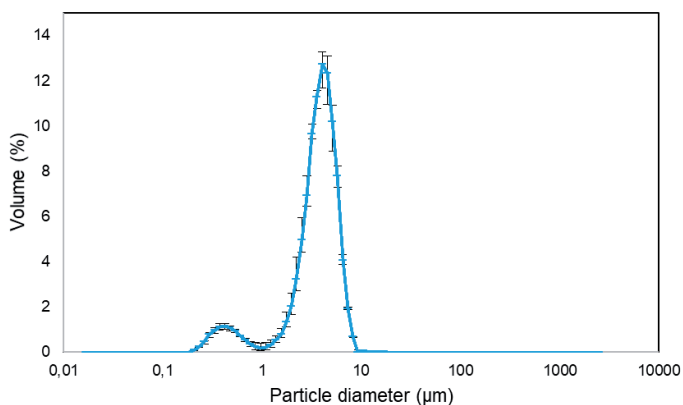


**Figure S2.** Volume based particle size distribution of the precipitates collected from biotic experiments at day 14. Error bars show standard deviation of the triplicates

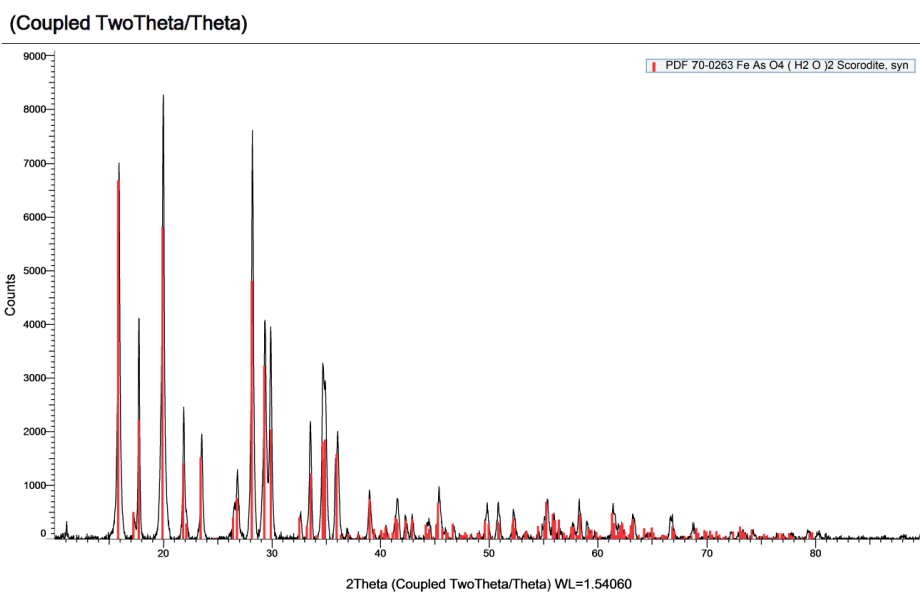


**Figure S3.** X-ray diffractogram of the scorodite precipitates obtained at 70 °C in biotic experiments 9 gL<sup>-1</sup> GAC, 500 mgL<sup>-1</sup> As(III) and Fe(II) respectively. No other precipitates were identified besides scorodite in the solids collected.

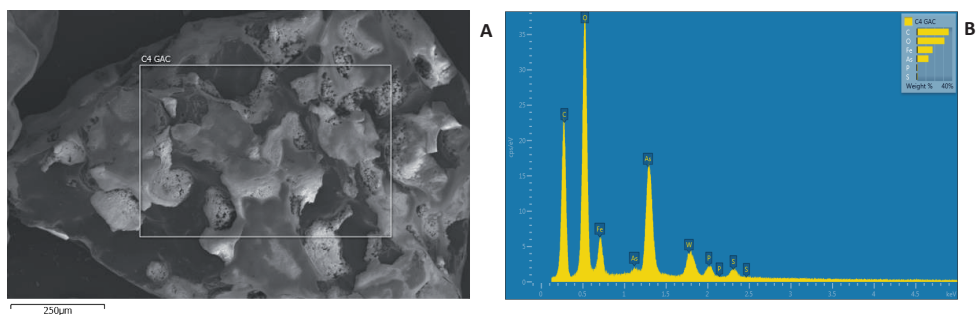


**Figure S4.** SEM photograph (A) and EDX analysis of the activated carbon granule collected at day 16 from biotic experiments with 9 gL<sup>-1</sup> GAC, 500 mgL<sup>-1</sup> As(III) and Fe(II) respectively.

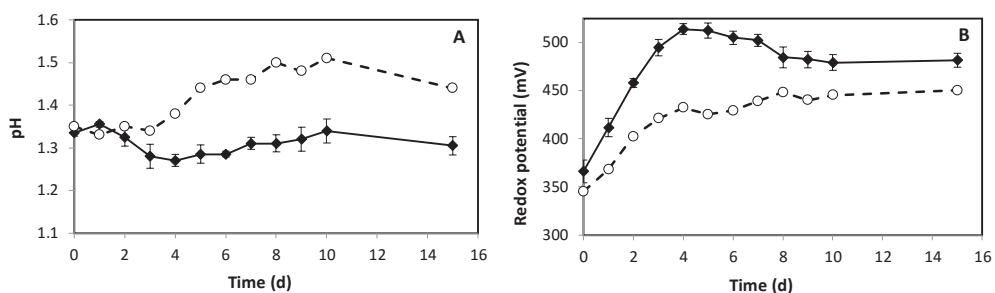


**Figure S5.** Changes in pH and redox potential in biotic and abiotic experiments (solid and dashed line respectively) 9 gL<sup>-1</sup> GAC, 500 mgL<sup>-1</sup> As(III) and Fe(II) respectively. Error bars indicate standard deviation of the biotic replicates.

## REFERENCES

1. Jain, C.K. and I. Ali, *Arsenic: occurrence, toxicity and speciation techniques*. Water Research, 2000. **34**(17): p. 4304-4312.
2. Singh, R., S. Singh, P. Parihar, V.P. Singh, and S.M. Prasad, *Arsenic contamination, consequences and remediation techniques: A review*. Ecotoxicology and Environmental Safety, 2015. **112**: p. 247-270.
3. Riveros, P., J. Dutrizac, and P. Spencer, *Arsenic disposal practices in the metallurgical industry*. Canadian Metallurgical Quarterly, 2001. **40**(4): p. 395-420.
4. Nazari, A.M., R. Radzinski, and A. Ghahreman, *Review of arsenic metallurgy: Treatment of arsenical minerals and the immobilization of arsenic*. Hydrometallurgy, 2016.
5. Agorhom, E.A., J.P. Lem, W. Skinner, and M. Zanin, *Challenges and opportunities in the recovery/rejection of trace elements in copper flotation—a review*. Minerals Engineering, 2015. **78**: p. 45-57.
6. Höll, W.H., *Mechanisms of arsenic removal from water*. Environmental Geochemistry and Health, 2010. **32**(4): p. 287-290.
7. Mohan, D. and C.U. Pittman, *Arsenic removal from water/wastewater using adsorbents—A critical review*. Journal of Hazardous Materials, 2007. **142**(1): p. 1-53.
8. Welham, N.J., K.A. Malatt, and S. Vukcevic, *The stability of iron phases presently used for disposal from metallurgical systems—A review*. Minerals Engineering, 2000. **13**(8): p. 911-931.
9. Fujita, T., S. Fujieda, K. Shinoda, and S. Suzuki, *Environmental leaching characteristics of scorodite synthesized with Fe(II) ions*. Hydrometallurgy, 2012. **111-112**: p. 87-102.
10. Shinoda, K., T. Tanno, T. Fujita, and S. Suzuki, *Coprecipitation of large scorodite particles from aqueous Fe (II) and As (V) solution by oxygen injection*. Materials transactions, 2009. **50**(5): p. 1196-1201.
11. Demopoulos, G., F. Lagno, Q. Wang, and S. Singhania. *The atmospheric scorodite process*. in *Copper*. 2003.
12. Dutrizac, J. and J. Jambor, *The synthesis of crystalline scorodite, FeAsO<sub>4</sub> · 2H<sub>2</sub>O*. Hydrometallurgy, 1988. **19**(3): p. 377-384.
13. Monhemius, A.J. and P.M. Swash, *Removing and stabilizing as from copper refining circuits by hydrothermal processing*. JOM, 1999. **51**(9): p. 30-33.
14. Fujita, T., R. Taguchi, M. Abumiya, M. Matsumoto, E. Shibata, and T. Nakamura, *Novel atmospheric scorodite synthesis by oxidation of ferrous sulfate solution. Part I*. Hydrometallurgy, 2008. **90**(2): p. 92-102.
15. Fujita, T., R. Taguchi, M. Abumiya, M. Matsumoto, E. Shibata, and T. Nakamura, *Novel atmospheric scorodite synthesis by oxidation of ferrous sulfate solution. Part II. Effect of temperature and air*. Hydrometallurgy, 2008. **90**(2): p. 85-91.
16. Demopoulos, G.P., D.J. Droppert, and G. Van Weert, *Precipitation of crystalline scorodite (FeAsO<sub>4</sub> · 2H<sub>2</sub>O) from chloride solutions*. Hydrometallurgy, 1995. **38**(3): p. 245-261.
17. Gonzalez-Contreras, P., J. Weijma, R.v.d. Weijden, and C.J.N. Buisman, *Biogenic Scorodite Crystallization by Acidianus sulfidivorans for Arsenic Removal*. Environmental Science & Technology,

2010. **44**(2): p. 675-680.
18. Gonzalez-contreras, P.A., *Bioscorodite: biological crystallization of scorodite for arsenic removal*. 2014.
  19. Okibe, N., M. lindKoga, K. Sasaki, T. Hirajima, S. Heguri, and S. Asano, *Simultaneous oxidation and immobilization of arsenite from refinery waste water by thermoacidophilic iron-oxidizing archaeon, Acidianus brierleyi*. Minerals Engineering, 2013. **48**: p. 126-134.
  20. Harris, B., *The removal and stabilization of arsenic from aqueous process solutions: Past, present and future*. Minor Elements 2000. 2000. 3-20.
  21. Molnár, L.u., E. Virčíkova, and P. Lech, *Experimental study of As(III) oxidation by hydrogen peroxide*. Hydrometallurgy, 1994. **35**(1): p. 1-9.
  22. Bissen, M. and F.H. Frimmel, *Arsenic — a Review. Part II: Oxidation of Arsenic and its Removal in Water Treatment*. Acta hydrochimica et hydrobiologica, 2003. **31**(2): p. 97-107.
  23. Debekaussen, R., Droppert, D., Demopoulos, and G. P., *Ambient pressure hydrometallurgical conversion of arsenic trioxide to crystalline scorodite*. CIM bulletin, 2001. **94**: p. 116-122.
  24. Demopoulos, G.P., *Arsenic Immobilization Research Advances: Past, Present and Future*. Canadian Institute of Mining, Metallurgy and Petroleum,, 2014.
  25. Tanaka, M. and N. Okibe, *Factors to Enable Crystallization of Environmentally Stable Bioscorodite from Dilute As(III)-Contaminated Waters*. Minerals, 2018. **8**(1): p. 23.
  26. Okibe, N., M. Koga, S. Morishita, M. Tanaka, S. Heguri, S. Asano, K. Sasaki, and T. Hirajima, *Microbial formation of crystalline scorodite for treatment of As (III)-bearing copper refinery process solution using Acidianus brierleyi*. Hydrometallurgy, 2014. **143**: p. 34-41.
  27. Choi, Y., A. Ghahremaninezhad, and N. Ahern. *Process for activated carbon-assisted oxidation of arsenic species in process solutions and waste waters*. in *COM 2014-Conference of Metallurgists*. 2014.
  28. Choi, Y., A.G. Gharelar, and N. Ahern, *Method for arsenic oxidation and removal from process and waste solutions*. 2014, Google Patents.
  29. Lindström, E.B., Å. Sandström, and J.-E. Sundkvist, *A sequential two-step process using moderately and extremely thermophilic cultures for biooxidation of refractory gold concentrates*. Hydrometallurgy, 2003. **71**(1): p. 21-30.
  30. Gonzalez-Contreras, P., I. Gerrits-Benneheij, J. Weijma, and C.J. Buisman, *HPLC inorganic arsenic speciation analysis of samples containing high sulfuric acid and iron levels*. Toxicological & Environ Chemistry, 2011. **93**(3): p. 415-423.
  31. Escobar, B., E. Huenupi, I. Godoy, and J.V. Wiertz, *Arsenic precipitation in the bioleaching of enargite by Sulfolobus BC at 70 °C*. Biotechnology Letters, 2000. **22**(3): p. 205-209.
  32. Higashidani, N., T. Kaneta, N. Takeyasu, S. Motomizu, N. Okibe, and K. Sasaki, *Speciation of arsenic in a thermoacidophilic iron-oxidizing archaeon, Acidianus brierleyi, and its culture medium by inductively coupled plasma–optical emission spectroscopy combined with flow injection pretreatment using an anion-exchange mini-column*. Talanta, 2014. **122**: p. 240-245.
  33. Mondal, P., C. Majumder, and B. Mohanty, *Treatment of arsenic contaminated water in a batch reactor by using Ralstonia eutropha MTCC 2487 and granular activated carbon*. Journal of hazardous materials, 2008. **153**(1): p. 588-599.
  34. Jimenez-Lopez, C., K.B. Chekroun, F. Jroundi, M. Rodríguez-Gallego, J.M. Arias, and M.T.

## CHAPTER 2

- González-Muñoz, *Myxococcus xanthus* Colony Calcification: An Study to Better Understand the Processes Involved in the Formation of this Stromatolite-Like Structure, in *Advances in Stromatolite Geobiology*. 2011, Springer Berlin Heidelberg: Berlin, Heidelberg. p. 161-181.
35. Picard, A., A. Gartman, D.R. Clarke, and P.R. Girguis, *Sulfate-reducing bacteria influence the nucleation and growth of mackinawite and greigite*. *Geochimica et Cosmochimica Acta*, 2018. **220**: p. 367-384.
  36. Gonzalez-Contreras, P., J. Weijma, and C.J. Buisman, *Kinetics of ferrous iron oxidation by batch and continuous cultures of thermoacidophilic Archaea at extremely low pH of 1.1–1.3*. *Applied microbiology and biotechnology*, 2012. **93**(3): p. 1295-1303.
  37. Dove, P.M., Rimstidt, J.D., *The solubility and stability of scorodite, FeAsO<sub>4</sub> · 2H<sub>2</sub>O*. *American Mineralogist*, 1985. **70**(7-8): p. 838-844.
  38. Krause, E., Ettl, V.A., *Solubility and stability of scorodite, FeAsO<sub>4</sub>·2H<sub>2</sub>O: new data and further discussion*. *American Mineralogist* 1988. **73**(7-8): p. 850-854.

**PROOF OF PRINCIPLE:** BIOLOGICAL SCORODITE PRECIPITATION THROUGH THE CATALYZED AS(III) OXIDATION BY GRANULAR ACTIVATED CARBON (GAC).

## CHAPTER 3



# EVALUATING THE EFFECT OF GAC IN THE BIOLOGICAL CRYSTALLIZATION OF SCORODITE

Authors: Silvia Vega-Hernandez, Jan Weijma, Cees J.N. Buisman

A modified version of this chapter is published as:  
Vega-Hernandez, Silvia, Jan Weijma, and Cees J N. Buisman. "Particle size control of the biogenic scorodite during the GAC-catalysed As (III) oxidation for efficient arsenic removal in acid wastewaters." *Water Resources and Industry* (2020): 100128. <https://doi.org/10.1016/j.wri.2020.100128>

## CHAPTER 3

### ABSTRACT

The synthesis of biogenic scorodite combined with oxidation of As(III) catalysed by granular activated carbon (GAC) was previously demonstrated. However, the colloidal size of the formed scorodite particles is still a bottleneck, as it would hinder the easy separation of the precipitates in a full-scale application. Here, we studied the effect of GAC concentration on biological scorodite precipitation at thermoacidophilic conditions in batch experiments. Higher arsenic removal efficiency and precipitation of larger and more stable scorodite particles were found only in biotic tests and at low catalyst concentration of  $4 \text{ g L}^{-1}$ . Furthermore, with  $4 \text{ g L}^{-1}$  GAC, the Fe and As predominantly precipitated in solution while with  $20 \text{ g L}^{-1}$  GAC the Fe and As predominantly precipitated on the GAC. For experiments with 4 and  $20 \text{ g L}^{-1}$  of GAC, the average particle size was 66 and  $2.6 \mu\text{m}$ , respectively. This could be explained by the lower saturation level of the solution at the lower GAC level. This study shows that the oxidative catalytic capacity of GAC can be used to influence crystallisation of scorodite.

**Keywords:** Arsenite oxidation; activated carbon; biological iron oxidation; saturation control; biological crystallization; scorodite.

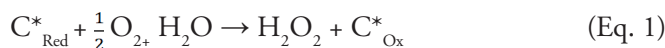
## 1. INTRODUCTION

Arsenic (As) is a toxic metalloid which is widely dispersed throughout the earth's crust where it is commonly associated with ores of Cu, Zn, Au and Ag [1]. The mining and metallurgical industries exploiting these ores contribute substantially to the economic development of metal-exporting countries [2]. However, it results in the generation of acid effluents with high concentrations of As between 500-10,000 ppm, mainly in the trivalent form, As(III) [3]. The removal and immobilization of arsenic is commonly accomplished by co-precipitation with lime and ferric salts [4]. However, the precipitated arsenic-rich solids are chemically not entirely stable. Therefore, the suitability of such precipitates for long-term storage has been questioned, as uncontrolled emissions of arsenic from stored arsenic-rich solid waste results in unacceptable environmental hazards [5, 6](Riveros et al., 2001). Due to the increasing worldwide metal demand and the current trend of exploiting low-grade ores, more arsenic-containing waste is generated. Hence, a proper management of these residues for the disposal and storage becomes even more urgent.

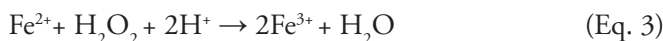
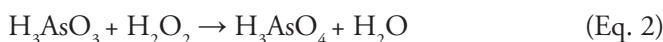
The mineral scorodite, crystalline ferric arsenate dihydrate with formula  $\text{FeAsO}_4 \cdot 2\text{H}_2\text{O}$ , has been proposed as a suitable carrier medium for stable immobilization and long-term storage of arsenic, as it combines low solubility with high arsenic content [7, 8]. In previous studies of our group, the biological crystallization of scorodite starting from ferrous iron (Fe(II)) and arsenate (As(V)) containing solutions inoculated with thermoacidophilic iron-oxidizing microbial cultures was demonstrated [9].

Considering that arsenite (As(III)) is the predominant arsenic species in acidic metallurgical wastewater, the efficient oxidation of arsenite to arsenate is required to achieve removal of arsenic as scorodite. Biological As(III) oxidation under thermoacidophilic conditions has been scarcely reported [10, 11], only Okibe and co-workers have described biological oxidation of As(III) by the archaea *Acidianus brierleyi* [12-14]. As an alternative, we previously found that granular activated carbon (GAC) was effective as catalyst for As(III) oxidation under thermoacidophilic conditions in the presence of air. Interestingly, when Fe(II) and the microbial mixed culture were also present, scorodite was ultimately formed [15]. The catalytic As(III) oxidation by granular activated carbon (GAC) in the presence of air or oxygen in acidic solutions was reported previously [16-18], as well as its application as catalyst for enhanced leaching of sulfide minerals [17, 19]. It has been proposed that hydrogen peroxide is formed at the surface of the activated carbon [20], according to:

## CHAPTER 3



Where  $C_{\text{red}}^*$  and  $C_{\text{Ox}}^*$  stands for reduced and oxidized functional groups on the carbon surface, respectively. Subsequently, hydrogen peroxide can oxidize As(III) and Fe(II) according to:



In our preliminary experiments, both As(III) and a fraction of Fe(II) were oxidized by GAC in the absence of an Fe(II)-oxidizing thermoacidophilic mixed culture [15]. However, the formed As(V) and Fe(III) remained in solution, while under the same conditions but in the presence of a thermoacidophilic mixed culture, As(V) was depleted from solution and precipitated as scorodite. The scorodite precipitate consisted of colloidal crystallite agglomerates with a size of <5  $\mu\text{m}$ , with settling rates below 0.01 m/h. The small particle size was attributed to the relatively high degree of saturation of the solution with respect to scorodite [15]. The poor settling behaviour makes separation of the particles from the process stream in practice difficult and costly. Furthermore, particle size may negatively affect the stability of scorodite [8, 21, 22].

Therefore, it is desirable to obtain precipitates with a larger particle size in the scorodite biocrystallisation process. To this purpose, we investigated the possible effect of the GAC catalyst concentration in the oxidation process and the biological precipitation of arsenic as scorodite at pH 1.2-1.3 and 70°C.

## 2. MATERIALS AND METHODS

### 2.1. INOCULUM AND MEDIUM COMPOSITION

A thermoacidophilic iron-oxidizing mixed culture (Chapter 2), to which the archaeal strain *Acidianus brierleyi* (DSM 1651) was added, was acclimatized to growth medium containing 6.8 mM (510  $\text{mg L}^{-1}$ ) of As(III). The microbial culture composition has been described earlier [23]. The acclimatized culture was inoculated in batch bottles containing the growth medium with GAC and Fe(II) and As(III) at a molar ratio of 1.29. The growth medium for the mixed culture was prepared as described in Chapter 2.

The growth medium was additionally supplied with 8.8 mM (490  $\text{mg L}^{-1}$ ) ferrous iron

and 6.8 mM (510 mg L<sup>-1</sup>) arsenic (As(III)), giving a Fe/As molar ratio of 1.29. Ferrous iron and arsenite stock solutions were prepared as previously reported in Chapter 2. Arsenate stock solutions were prepared from disodium arsenate heptahydrate (Na<sub>2</sub>HAsO<sub>4</sub>·7H<sub>2</sub>O) (Fluka, Switzerland). All used chemicals were analytical-reagent grade.

## 2.2. BATCH EXPERIMENTS

Batch experiments were carried out in 250 mL serum bottles closed with a butyl rubber stopper and crimped aluminum seal. The bottles were supplied with 4 or 20 g L<sup>-1</sup> granulated activated carbon (GAC). Bottles for abiotic experiments were filled to a final volume of 100 ml with growth medium containing Fe(II) and As(III). Bottles for biotic tests contained 90 ml growth medium with Fe(II), As(III) and 10 ml of the pre-cultivated thermoacidophilic mixed culture with a concentration of 1·10<sup>7</sup> cell ml<sup>-1</sup>. A summary of the conditions used in the batch experiments is shown in Table 1. The cell concentration in the bottles was determined by direct counting using a Neubauer chamber. The headspace (150 ml) of the bottles consisted of air, implying that at the start, oxygen was present in excess by a factor of 2 with respect to the maximum amount needed for full oxidation of As(III) and Fe(II). The bottles were placed in a thermostat shaker incubator at 150 rpm and 70 °C during the experiment and samples were taken regularly for analysis of pH, Eh, and dissolved Fe and As species. Since the pH fluctuated between 1.24 and 1.3 during the biotic and abiotic experiments, adjustment of pH of the solution was not necessary.

The biotic tests were performed in duplicate in addition to an abiotic control that was inoculated with 10 % v/v of acid sterile water. Furthermore, the results are expressed as the mean ± value standard deviation.

**Table 1.** Summary of characteristics of the experiment.

Concentration of GAC g L <sup>-1</sup>	As species	Ratio Fe(II):As(III)	Gas
4	As(III)	1.29	Air
20	As(III)	1.29	Air

The precipitates were collected from the bottles at the end of the experiments. First, the carbon granules were manually separated (by sieving) and washed with acid water (50 mM of sulphuric acid) in order to release any solid particle that might be deposited on the GAC. The precipitates were separated from the liquid phase by settling and centrifugation. The collected precipitates were washed with 50 mM sulphuric acid, followed by washing with deionized water and dried in a vacuum oven at 60°C before

## CHAPTER 3

characterization. Liquid samples were filtered over a 0.2  $\mu\text{m}$  cellulose acetate membrane filter before analysis. The pH and redox potential of the samples were measured with glass electrodes QP181X and QR480X-Pt triple billed junction (vs. Ag/AgCl) (Prosense, the Netherlands), respectively.

### 2.3. PRE-TREATMENT OF GAC AS CATALYST FOR ARSENITE OXIDATION

Granular activated carbon NORIT GAC 830W (Cabot Norit Nederland B.V., Amersfoort, the Netherlands) with a particle size ranging from 0.8-2.3 mm was used as catalyst for arsenite oxidation. The GAC was produced from coal followed by thermal activation and possesses a surface area of  $885 \text{ m}^2 \text{ g}^{-1}$ , density of  $1.06 \text{ g cm}^{-3}$ , a pore radius of 8–60 Å, a total pore volume of  $0.775 \text{ cm}^3 \text{ g}^{-1}$  (specifications provided by supplier). Before the pre-treatment, the GAC samples were firstly sieved to an average particle size of 0.8-1.4 mm. In order to remove impurities, the granules were washed with sulphuric acid (1 M) followed by deionized water before its use in the experiments.

### 2.4. CHEMICAL ANALYSIS

Fe(II) and Fe(III) concentrations in solution were measured using Dr. Lange Cuvette test LCK 320 and a Xion 500 spectrophotometer (Hach-Lange, Germany). As(III) and As(V) concentrations in solution were measured with an HPLC connected to a UV photospectrometer. The HPLC was an ultimate VWD 3000 RS (Dionex, the Netherlands) equipped with an ion exclusion column using 10 mM sulphuric acid as the mobile phase. The concentration of  $\text{H}_2\text{O}_2$  was measured by a semi-quantitative measurement using reagent strips (Quantofix).

The Fe and As content of the activated carbon and of precipitates was determined after microwave digestion with aqua regia with inductively coupled plasma-optical emission spectrometry (ICP-OES) equipped with a megapixel (MPX) CCD detector (VISTA-MPX CCD Simultaneous, VARIAN Inc.).

### 2.5. CHARACTERIZATION OF THE SOLIDS

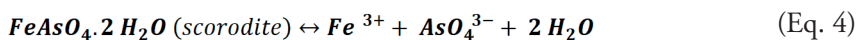
The method for identification of crystalline phases with X-Ray Diffraction (XRD) was previously described in Chapter 2. Phase identification was assessed with the software DIFFRAC.EVA V4.1.1 (Bruker Axs) and crystallography open database. The same

software was used to calculate crystallinity of solid samples based on peak to noise ratio's. Fourier transform infrared (FT-IR) spectra of the samples were obtained with a Varian Scimitar 1000 FT-IR spectrometer equipped with a deuterated triglycine sulfate (DTSG) detector. The measurement resolution was set at  $4\text{ cm}^{-1}$ , and the spectra were collected in the ATR (Attenuated Total Reflection) mode in the range  $4000\text{--}650\text{ cm}^{-1}$  with 128 co-added scans. ATR was performed on a PIKE MIRacle ATR with a diamond w/ZnSe lens single reflection plate. The sample chamber was purged with  $\text{N}_2$  during 10 min before the scanning. The structural  $\text{H}_2\text{O}$  content of the solids was determined with a Thermogravimetric Analyser (Perkin-Elmer TGA7 equipped with Pyris software). The thermal gravimetrical analysis was performed with 10 mg of air-dried powdered material at a heating rate of  $10^\circ\text{C min}^{-1}$  from  $20^\circ\text{C}$  to  $600^\circ\text{C}$  under an air atmosphere. Particle size distribution was measured with a Shimadzu Particle Size Analyzer SALD-2300.

The morphology of the precipitates was investigated with scanning electron microscopy (SEM). The samples were fixed on sample holders by carbon adhesive tabs and subsequently coated with about 10 nm of carbon (K950X, Quorum Technologies). Samples were analysed at SE detection 2 kV, 50 pA, WD 5 mm at room temperature, in a field emission scanning electron microscope (Magellan 400, FEI, Eindhoven, the Netherlands). The arsenic leachability of the precipitates was evaluated with the standard toxicity characterization leaching procedure (TCLP) of US Environmental Protection Agency (USEPA) [24]. The test was conducted at  $30^\circ\text{C}$  and an acetate buffer at pH 4.98 was used as extraction solution at a solid to liquid mass ratio of 20. Samples were withdrawn after 24 hours and after 30 days. The sampling volume was replaced by fresh leaching solution.

## 2.6. CALCULATION OF ION ACTIVITY PRODUCT

The ion activity product (IAP), defined as the product of the ferric and arsenate ion concentration in solution was calculated considering the congruent dissolution of mineral scorodite defined as:



The saturation index of the solution is defined as the ratio between the IAP of ferric arsenate in the solution the solubility product ( $K_{\text{sp}}$ ) of scorodite.

$$\text{IAP}_{\text{scorodite}} = (a\text{Fe}^{3+})(a\text{AsO}_4^{3-}) \quad (\text{Eq. 5})$$

## CHAPTER 3

$$Ksp_{scorodite} = (aFe^{3+})(aAsO_4^{3-}) \text{ at equilibrium} \quad (\text{Eq. 6})$$

$$SI = IAP_{scorodite} / Ksp_{scorodite} \quad (\text{Eq. 7})$$

Equations 8 and 9 were used to calculate the activity of arsenate and ferric ions in solution respectively. Values for dissociation constants are shown in Table S1.

$$aAsO_4^{3-} = \frac{Arsenate_{total}}{1 + \frac{a_{H^+}}{K_3} + \frac{(a_{H^+})^2}{K_2 K_3} + \frac{(a_{H^+})^3}{K_1 K_2 K_3}} \quad (\text{Eq. 8})$$

$$aFe^{3+} = \frac{Ferric_{total}}{1 + \frac{K_1}{a_{H^+}} + \frac{K_2 K_3}{(a_{H^+})^2} + \frac{K_1 K_2 K_3}{(a_{H^+})^3} + \frac{K_1 K_2 K_3 K_4}{(a_{H^+})^4}} \quad (\text{Eq. 9})$$

### 3. RESULTS AND DISCUSSION

#### 3.1. AS(III) AND FE(II) OXIDATION WITHOUT GAC

Arsenite oxidation was evaluated in batch tests containing 0, 4 and 20 g L<sup>-1</sup> GAC with initial concentrations of 510 mg L<sup>-1</sup> As(III) and 490 mg L<sup>-1</sup> Fe(II) (Figure 1A). Without GAC and without the culture, As(III) was not oxidized (Figure 1A.), while only 7% of the Fe(II) was oxidized in 16 days. Without GAC but with the culture, 228 mg L<sup>-1</sup> As(III) was removed from solution. The As(V) concentration increased, reaching a maximum of 79 mg L<sup>-1</sup> on day 7 and subsequently decreased to 17 mg L<sup>-1</sup> on day 16 (data not shown). The formed As(V) in solution, did not match the depleted As(III), implying that the total As concentration in solution decreased as shown in Figure 1B. In the same experiment, 275 mg L<sup>-1</sup> Fe(II) was removed, while only 11 mg L<sup>-1</sup> Fe(III) accumulated from start to end. These results indicate that the mixed culture could oxidize As(III) to some extent when grown on Fe(II) as energy source. Without Fe(II), the culture did not oxidize As(III) (data not shown). Hardly any As(III) and Fe(II) was oxidized after day 9, revealing the inability of the culture to oxidize As(III) to low concentrations under the applied conditions. The results furthermore reveal that Fe and As precipitated to some extent, with a molar ratio of 1.0 to 1.4 of Fe-precipitated: As-precipitated.

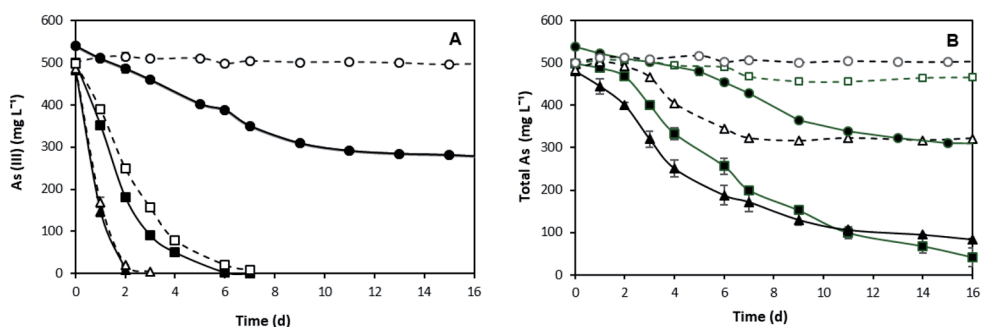


**Figure 1.** Arsenite oxidation catalysed by GAC (A) and total arsenic removal B) in the batch tests containing 0 ( $\circ$  abiotic,  $\bullet$  biotic), 4 ( $\square$  abiotic,  $\blacksquare$  biotic), and 20 ( $\Delta$  abiotic,  $\blacktriangle$  biotic)  $\text{g L}^{-1}$  GAC. Solid and dashed lines correspond to biotic and abiotic experiments, respectively. Error bars indicate standard deviation of the mean.

**Table 2.** Rates of As(III) oxidation obtained as a function of the catalyst (GAC) concentrations in 2 days of batch experiment, with the mixed culture (biotic) and the abiotic control (C).

	unit	4 $\text{g L}^{-1}$ Biotic	4 $\text{g L}^{-1}$ Abiotic	20 $\text{g L}^{-1}$ Biotic	20 $\text{g L}^{-1}$ Abiotic
Max. volumetric As(III) oxidation rate day 0-2	$\text{mg L}^{-1} \text{d}^{-1}$	160	125	236	232
As(III) oxidized after 2 days	%	64	50	98	96
Specific As(III) oxidation rate day 0-2	$\text{mgAs gGAC}^{-1} \text{d}^{-1}$	40	31	11	11

### 3.2. AS(III) AND FE(II) OXIDATION IN THE PRESENCE OF 4 AND 20 $\text{G L}^{-1}$ GAC

With 4  $\text{g L}^{-1}$  of GAC, a zero order oxidation rate of 160 and 125  $\text{mg L}^{-1} \text{d}^{-1}$  As(III) was estimated in biotic and abiotic experiments, respectively, until an As(III) concentration of 100  $\text{mg L}^{-1}$  was reached (Figure 1A). The difference in abiotic and biotic rate can be explained by the contribution of microbially induced As(III) oxidation, because in the absence of GAC an initial As(III) oxidation rate of 27  $\text{mg L}^{-1} \text{d}^{-1}$  was found (Figure 1A). With 20  $\text{g L}^{-1}$  GAC, As(III) oxidation was almost complete within 2 days with no difference in the depletion curve between the biotic and abiotic experiments (Figure 1A). Furthermore, around 1  $\text{mg L}^{-1}$  of hydrogen peroxide was detected in the bottles with 20  $\text{g L}^{-1}$  of GAC immediately after the addition of the granules to the solution (Figure S1), confirming that equations 1 and 2 play a role in the oxidation of As(III) [6, 15].

## CHAPTER 3

With 4 g L<sup>-1</sup> of GAC in the biotic experiment, a specific oxidation rate of 40±1 mgAs gGAC<sup>-1</sup> d<sup>-1</sup> was calculated, which decreased with almost a factor of 4 in the bottles with 20 g L<sup>-1</sup> GAC (Table 2). Thus, in the experiment with 20 g L<sup>-1</sup> GAC, the catalyst did not exert its maximum oxidation capacity, indicating a limitation. Possibly the oxidation was hampered by the presence of ferric precipitates on the GAC surface, as with 20 g L<sup>-1</sup> GAC, 7 times more ferric was associated to the GAC at the end of the experiment (day 16), compared to the experiment with 4 g L<sup>-1</sup> (Table 3).

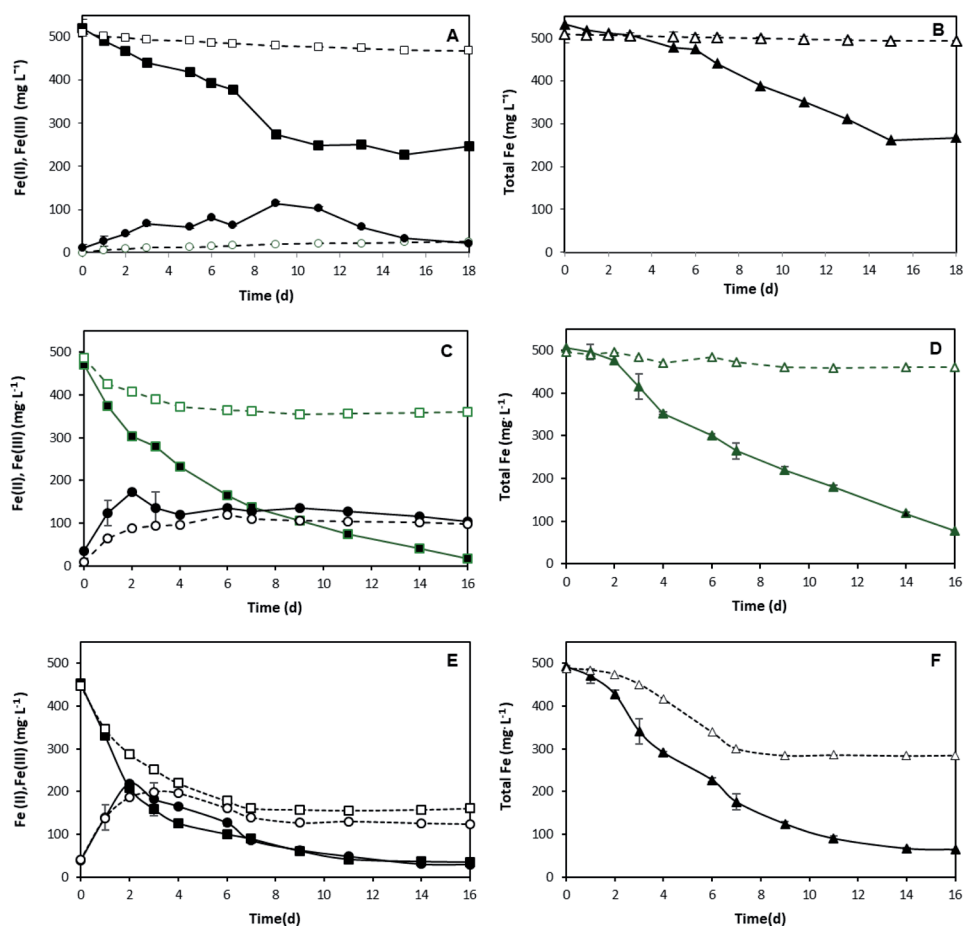


**Figure 2.** Ferrous iron oxidation and Fe precipitation (solid and dashed line respectively) containing 0 g L<sup>-1</sup> GAC (A and B), 4 g L<sup>-1</sup> of GAC (C and D) and 20 g L<sup>-1</sup> GAC (E and F). Fe(II): □ abiotic, ■ biotic, Fe(III): ○ abiotic, ● biotic, Total Fe: △ abiotic, ▲ biotic. Solid and dashed lines correspond to biotic and abiotic experiments, respectively. Error bars indicate standard deviation of the mean.

It is noted that some adsorption of arsenic on GAC was observed at the beginning of the experiments as the As(III) concentration ( $520 \pm 10 \text{ mg L}^{-1}$ ) decreased immediately after the addition of the GAC. The adsorption amounted to  $1.5 \pm 0.5 \text{ mg}$  arsenic per gram of GAC, which lies in the range ( $0.16\text{--}3.5 \text{ mgAs/gGAC}^{-1}$ ) reported in literature [25-27]. Although at lower GAC concentration the amount of adsorbed arsenic is negligible, it becomes more substantial with increasing concentration of the catalyst, such as in the bottles with  $20 \text{ g L}^{-1}$  of GAC, where only  $470 \text{ mg L}^{-1}$  As(III) was measured at the beginning of the experiment.

In the biotic experiment with  $4 \text{ g L}^{-1}$  of GAC,  $453 \text{ mg L}^{-1}$  (96%) of Fe(II) was oxidized in 16 days while in the abiotic experiment this was only  $123 \text{ mg L}^{-1}$  (25%) (Figure 2C). Thus, the contribution of the microbial culture to Fe(II) oxidation was dominant compared to the contribution of GAC. With  $20 \text{ g L}^{-1}$  of GAC, the difference was less pronounced with 64% and 93% Fe(II) oxidized in the abiotic and biotic experiment, respectively (Figure 2E). Still, this reveals that Fe(II) can also be oxidized with GAC as catalyst, even though oxidation of As(III) was much faster in our experiments when both ions were present (Figure 1A, Figure 2C, Figure 2E).

### 3.3. EFFECT OF GAC ON FE AND AS PRECIPITATION

In the biotic experiment with  $4 \text{ g L}^{-1}$  GAC, the solution became opaque and the first greenish precipitates, resembling the colour of scorodite, were visible with the naked eye after 4 days. In the biotic experiment with  $20 \text{ g L}^{-1}$  GAC, removal of As was evident already after day 1 (Figure 1B), and colloidal-like precipitates were visible after 2 days (Figure 3B). In abiotic experiments, the solution remained transparent (Figure 3), in agreement with previous results (Chapter 2).

Table 3 and 4 show the mass balance of As and Fe in the bottles, and their distribution in the solution (dissolved Fe and As species), in the precipitates, and associated with the GAC (predominantly as precipitate, and adsorbed, as explained in section 3.2). After 16 days in the biotic experiment with  $4 \text{ g L}^{-1}$  GAC, 76% of the Fe and 78% of the As was present in the precipitate and only 8% of the Fe and 10% of the As was found in the GAC. The remainder of Fe (16%) and As (12%) remained in solution. Thus, precipitation in the solution was predominant with only little precipitation on the GAC. With  $20 \text{ g L}^{-1}$  of GAC, 34% of the Fe and 34% of the As was present in the precipitate while 54% of the Fe and 49% of the As was found in the GAC, revealing that with the higher GAC concentration, precipitation on the GAC was predominant over precipitation in solution.

## CHAPTER 3

**Table 3.** Fe mass balance in biotic and abiotic experiments containing 4 g L<sup>-1</sup> and 20 g L<sup>-1</sup> of GAC, respectively with 510 mg L<sup>-1</sup> As(III) and 490 mg L<sup>-1</sup> Fe(II) at 70°C and pH 1.3.

		Biotic 4 g L <sup>-1</sup> GAC	Abiotic 4 g L <sup>-1</sup> GAC	Biotic 20 g L <sup>-1</sup> GAC	Abiotic 20 g L <sup>-1</sup> GAC
Fe in solution t <sub>(0)</sub>	mg/bottle	50.5	49.6	48.9	49.3
Fe in solution t <sub>(16)</sub>	mg/bottle (%)	8.2 (16)	45.9 (90)	6.4 (13)	27.1 (53)
Fe in precipitates t <sub>(16)</sub> *	mg/bottle (%)	39.2* (76)	0.0 (0)	17.2 (34)	0.0
Fe associated with GAC t <sub>(16)</sub>	mg/bottle (%)	3.9 (8)	5.2 (10)	26.8 (54)	23.7 (47)
Recovery**	%	102	103	103	103

\* 100% of the precipitates assumed as scorodite as indicated by XRD analysis.

\*\* Recovery = 100%\*(Fe in solution t<sub>(16)</sub> + Fe in precipitates t<sub>(16)</sub> + Fe associated with GAC t<sub>(16)</sub>)/(Fe in solution t<sub>(0)</sub>).

With 4 g L<sup>-1</sup> of GAC in the abiotic experiment, only 10% of Fe and As was associated with the GAC after 16 days, with the remainder still in solution mainly as Fe(II) and As(V). With 20 g L<sup>-1</sup> of GAC, 47% of Fe and 34% of As was associated with the GAC. Interestingly, the amount of Fe associated with the GAC is similar for both conditions with 13 and 12 mgFe gGAC<sup>-1</sup> for 4 and 20 g L<sup>-1</sup> of GAC respectively. For As, these values are 12 and 8 mgAs gGAC<sup>-1</sup>, respectively. In both abiotic experiments, arsenite and ferrous oxidation stopped around day 7, and the concentrations of Fe(II), Fe(III), As(III) and As(V) did not change after this day, revealing that precipitation had also stopped.

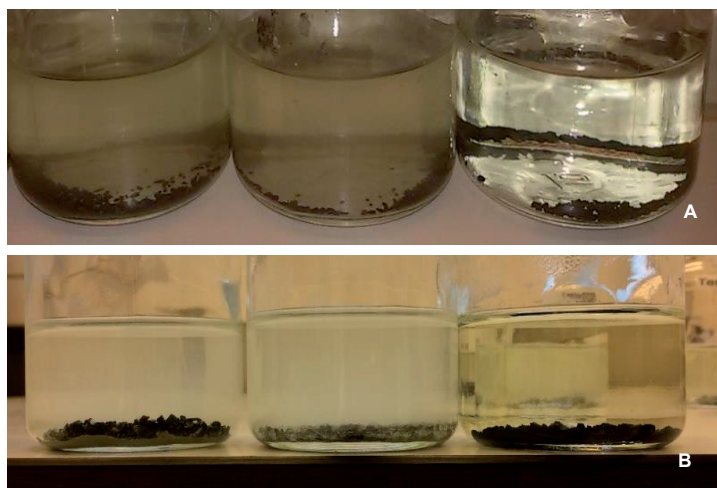


**Figure 3.** Photo of batch bottles with 4 g L<sup>-1</sup> (A) and 20 g L<sup>-1</sup> (B) of GAC at day 10. Duplicates of the biotic test are in the middle and left, to right the chemical control.

The above results suggest that in the abiotic experiments the Fe-As precipitates covered oxidation sites on the GAC surface, thereby preventing further oxidation and subsequent precipitation. In the biotic experiments, the Fe(II)-oxidizing microorganisms ‘compete’ with the GAC for Fe(II). Clearly, at the higher GAC concentration of 20 g L<sup>-1</sup>, more Fe(II) is oxidized by the GAC and more Fe precipitates on the GAC rather than in solution. With 4 g L<sup>-1</sup> of GAC, the oxidation and precipitation of Fe on GAC does not appear to be affected by the microorganisms as the biotic and abiotic show similar amounts of Fe and As on the GAC (Table 3 and 4). This is also true for Fe with 20 g L<sup>-1</sup> of GAC, and to a lesser extent for As. The Fe-As precipitates on the GAC had a molar ratio of 1.0-1.9 (Table 4).

**Table 4.** Arsenic mass balance in biotic and abiotic experiments containing 4 g L<sup>-1</sup> and 20 g L<sup>-1</sup> of GAC with 510 mg L<sup>-1</sup> As(III) and 490 mg L<sup>-1</sup> Fe(II) at 70°C and pH 1.3.

		<b>Biotic</b> <b>4 g L<sup>-1</sup> GAC</b>	<b>Abiotic</b> <b>4 g L<sup>-1</sup> GAC</b>	<b>Biotic</b> <b>20 g L<sup>-1</sup> GAC</b>	<b>Abiotic</b> <b>20 g L<sup>-1</sup> GAC</b>
<b>As in solution t<sub>(0)</sub></b>	mg/bottle	49.9	49.8	47.2	47.0
<b>As in solution t<sub>(16)</sub></b>	mg/bottle (%)	6.1 (12)	46.6 (90)	8.6 (17)	32.2 (66)
<b>As in precipitates t<sub>(16)</sub><sup>*</sup></b>	mg/bottle (%)	40.5* (78)	0.0 (0)	17.2 (34)	0.0 (0)
<b>As associated with GAC t<sub>(16)</sub></b>	mg/bottle (%)	5.2 (10)	4.9 (10)	24.9 (49)	16.6 (34)
<b>Recovery**</b>	%	103	103	107	104
<b>Fe/As ratio of precipitates</b>	mol/mol	1.2	-	1.35	-
<b>Fe/As ratio of GAC</b>	mol/mol	1.0	1.4	1.4	1.9

\* 100% of the precipitates assumed as scorodite as indicated by XRD analysis.

\*\* Recovery = 100%\*(As in solution t<sub>(16)</sub> + As in precipitates t<sub>(16)</sub> + As associated with GAC t<sub>(16)</sub>)/(As in solution t<sub>(0)</sub>).

From the aforementioned the following scheme emerges; in the presence of GAC and the iron-oxidizing culture, the GAC and the microorganisms compete for Fe(II). Following microbial oxidation, the Fe(III) precipitates with As(V) in the solution or on the cell surface, while Fe(II) oxidized by the GAC, precipitates with As(V) on the surface of the GAC, thereby inactivating the GAC.

### 3.4. CHARACTERIZATION OF THE PRECIPITATES

The concentration of GAC influenced the As(III) and Fe(II) oxidation rates, and consequently, also the saturation state of the solution is affected (Figure 4A). The saturation index (SI) of the solution, calculated from ratio of IAP and the K<sub>sp</sub> of scorodite (10<sup>-22</sup>) [28], ranged between 1-1.4, reaching the maximum value on day 2 in the biotic

experiments with 4 g L<sup>-1</sup> GAC, which coincided with the onset of depletion of As and Fe from solution (Figure 4B). Furthermore, the IAP in solution reached values close to -22 observed between day 1-7 (Figure 4A) which are in the range of reported  $K_{sp}$  values for scorodite (10<sup>-22</sup>) [9, 29-31], indicating that the solution was only slightly oversaturated in that period.

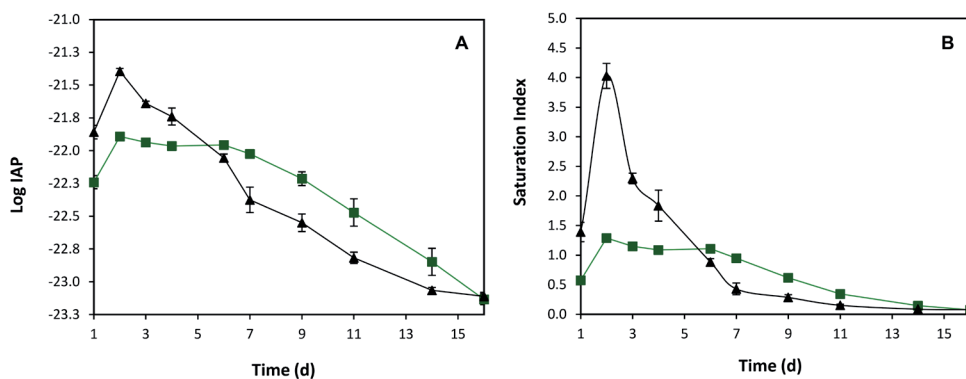


**Figure 4.** Calculated ion activity product (Log IAP) (A) and saturation index (B) in biotic batch tests containing 4 g L<sup>-1</sup> GAC (■) and 20 g L<sup>-1</sup> GAC (▲) with 510 mg L<sup>-1</sup> As(III) and 490 mg L<sup>-1</sup> Fe(II). Error bars indicate standard deviation of the mean.

The particle size distribution (PSD) of precipitates collected at the end of the biotic experiments is shown in Figure 5. With 4 g L<sup>-1</sup> GAC the average particle size was 66  $\mu$ m, while with 20 g L<sup>-1</sup> GAC it was only 2.6  $\mu$ m, with a substantial colloidal fraction with particle sizes under 1  $\mu$ m. Apparently, as the higher saturation index with 20 g L<sup>-1</sup> GAC, nucleation was favoured over crystal growth, thereby yielding particles with small crystal size [32].

The XRD analysis of the precipitates confirmed that scorodite was formed in all biotic experiments (Figure 6). However, sharper peaks were found in the diffractogram of solids from the experiment with 4 g L<sup>-1</sup> GAC compared to experiments with 20 g L<sup>-1</sup>, indicating a higher crystallinity. The computed crystallinity of the samples by crystallography open database (COD) indicated 83% and 54% of crystallinity in the precipitates collected from experiments with 4 and 20 g L<sup>-1</sup> of GAC, respectively.

The higher background or “hump” observed in the diffractogram of precipitates with 20 g L<sup>-1</sup> GAC is indicative either of poorly crystalline material or fine carbon particles present in the sample since a similar pattern was detected in the XRD of the raw GAC (Figure S2A). Besides, in the diffractogram a broad peak in the region  $2\theta$ : 10.7° could

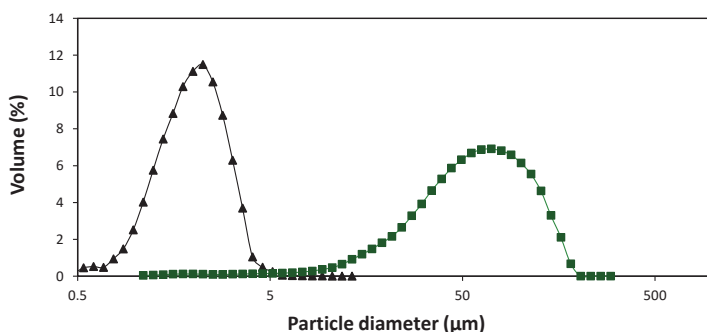


**Figure 5.** Particle size distribution volume based on the precipitates collected at day 16 from biotic experiments containing 4 (■) and 20 g L<sup>-1</sup> (▲) of GAC with As(III).

not be identified in the database, but this peak was also observed in the pattern of carbon granules washed with sulphuric acid (Figure S2B).

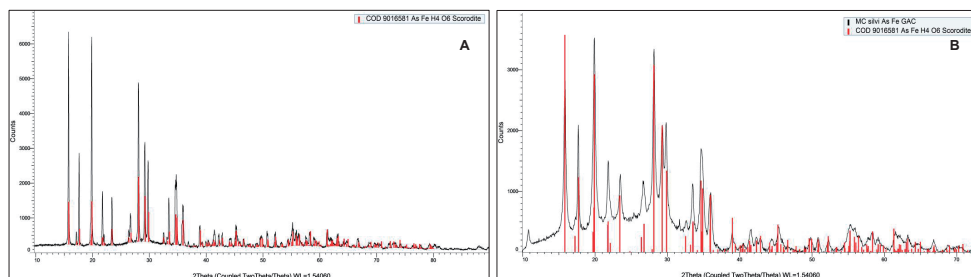


**Figure 6.** XRD diffractogram of solids collected from biotic tests containing 4 and 20 g L<sup>-1</sup> GAC (6A and 6B, respectively) with 510 mg L<sup>-1</sup> As(III) and 490 mg L<sup>-1</sup> Fe(II).

The Fe/As molar ratio of the synthesized solids measured by ICP-OES was 1.2 and 1.35 respectively (Table 4). The structural water content of the precipitates was also determined by thermogravimetric analysis (TGA) (Figure 7). The TGA curve of the precipitates collected from bottles with 4 g L<sup>-1</sup> GAC showed the inflection point between 160 and 240°C with a calculated weight loss of 15.4% (Figure 7A), this value is close to the theoretical value of 15.6% corresponding to 2 molecules of water in mineral scorodite. Between 245 and 500°C the water loss was 2.3%. This was also observed in a previous study of our group [9] in which we suggested that this was due to the presence of organic matter. The water content of the precipitates collected from experiments supplied with 20 g L<sup>-1</sup> GAC was around 18.5% with the inflection point between 130–230°C. This higher value implies the formation of poorly crystalline phases rather than fully crystallized scorodite [33].

The FT-IR analysis of the precipitates displayed peaks at 819 and 795  $\text{cm}^{-1}$  (Figure 7B and 7D), characteristic for arsenate stretching and bending bands ( $\nu_3\text{AsO}_4^{3-}$ ) in agreement with the reported bands for biogenic and mineral scorodite [9, 34, 35]. Another vibration band observed at 1054  $\text{cm}^{-1}$  in Figure 7B was related to phosphate or organic material [36]. The vibration bands for sulfate were absent in the spectra of the biogenic precipitates with 4  $\text{g L}^{-1}$  GAC, indicating that the sample was free of sulfate. Contrarily, a strong band occurring at 983  $\text{cm}^{-1}$  in the spectra of solids collected from 20  $\text{g L}^{-1}$  of GAC in Figure 7D indicated the presence of sulfate in the precipitates. Presumably, this was due to the presence of basic ferric arsenate sulfate [37].

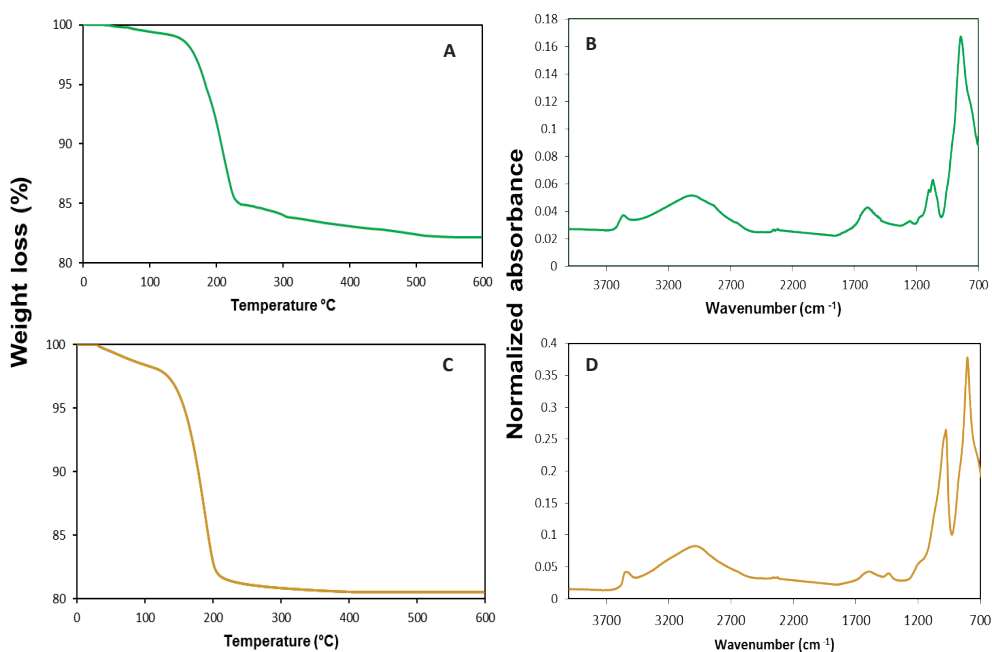


**Figure 7.** Characterization of the scorodite precipitates obtained in batch experiments: TGA and FT-IR analysis of solids collected from biotic tests with 4  $\text{g L}^{-1}$  (A and B) and 20  $\text{g L}^{-1}$  of GAC (C and D) respectively. The structural water content measured by TGA was calculated from the mass loss between 150 and 250  $^{\circ}\text{C}$ .

Bending vibration of the water molecule in the solids were also found at 1619  $\text{cm}^{-1}$  and 1587  $\text{cm}^{-1}$  (Figure 7B and D, respectively). Both values are in agreement with those reported previously [36, 38]. Furthermore, the bands displayed at 2964  $\text{cm}^{-1}$  and 2997  $\text{cm}^{-1}$  correlate to the O-H bond between crystalline water groups and oxygen of the arsenate molecules that occurs in the region 2900-3080, as well the similar stretch bands observed at 3518-3520  $\text{cm}^{-1}$  coincide with weaker O-H bond between oxygen atoms in

crystalline water (Figure 7B and D) [39].

Scanning electron microscopy of the precipitates collected at day 16, revealed the presence of solids with the typical dipyramidal habit of scorodite (Figure 8A and 8B). In addition, rod-shaped microorganisms associated with the scorodite precipitates and the GAC surface were found (Figure S3). This observation supports the hypothesis that the microbial surface served as heterogeneous nucleation, perhaps after adsorption of ferric and arsenate ions.

The results of the arsenic leaching test revealed that the scorodite precipitates collected from the experiment with  $4 \text{ g L}^{-1}$  GAC leached around  $0.87 \pm 0.2 \text{ mg L}^{-1}$  of As after 24 hours. Similarly, a concentration of  $0.91 \pm 0.07 \text{ mg L}^{-1}$  As was measured in leachate samples after 30 days. These results revealed that the produced scorodite was stable under the studied conditions. In contrast, the leaching of the solids produced in experiments with  $20 \text{ g L}^{-1}$  GAC showed an increase from  $3.63 \text{ mg L}^{-1}$  As after 24 hours to  $5.11 \pm 0.15 \text{ mg L}^{-1}$  As at the end of the leaching tests. The leached concentration of arsenic with these precipitates was above the permissible US EPA level of  $5 \text{ mg L}^{-1}$  As.

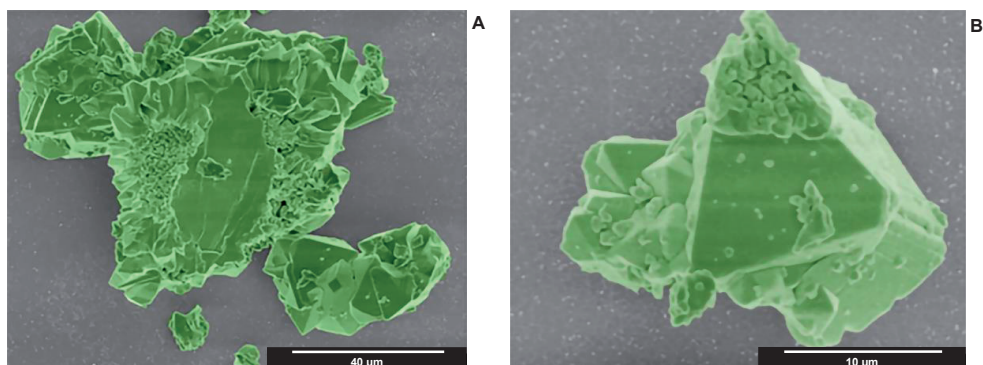


**Figure 8.** Scanning electron microscopy of the scorodite precipitates (manually colored in green) collected from biotic experiments containing  $4 \text{ g L}^{-1}$  GAC with As(III)

Although the difference in the leaching behaviour of scorodite (produced under atmospheric or hydrothermal conditions) has been attributed to different factors such as particle size and the molar Fe/As, the crystallinity of the precipitates seem to be an important parameter determining leaching characteristics of scorodite [7, 29]. The formation of poorly crystalline phases has been explained by the fast precipitation rate caused by the rapid Fe(II) oxidation which consequently affects the saturation of the solution allowing nucleus formation over the growth of the crystal [40, 41]. The uncontrolled precipitation as observed in biotic tests with  $20 \text{ g L}^{-1}$  GAC led to

## CHAPTER 3

the formation of fine precipitates, identified mainly as scorodite by powder diffraction analysis. Due to the low computed crystallinity of these solids (54%), it is possible that non-crystalline phases have developed along with scorodite, triggering the fast leaching of arsenic [42].

### 4. CONCLUSIONS

The results presented here demonstrate the impact of the concentration of GAC on the precipitation of scorodite starting from As(III) and Fe(II) containing medium, inoculated with thermoacidophilic iron-oxidizing microorganisms. With higher GAC concentrations, the contribution of GAC-catalysed iron oxidation increases relative to microbial oxidation. Fe(II) oxidized by GAC has a tendency to precipitate with As(V), formed through GAC-catalysed oxidation of As(III), on the surface of the GAC. This results in inactivation of the oxidative capacity of the GAC. With higher GAC concentrations, relatively more Fe and As precipitate on the catalyst.

Furthermore, higher GAC concentrations result in higher Fe(II) and As(III) oxidation rates and higher concentrations of Fe(III) and As(V), resulting in a higher saturation state of the solution with respect to scorodite. In turn, this results in the formation of smaller scorodite particles which are less stable. The controlled biological oxidation of Fe(II) achieved in the experiments with 4 g L<sup>-1</sup> GAC allowed to keep the saturation index below 1.5, leading to the formation of settleable particles which As leaching behaviour that comply with the USEPA limit value, even after 30 days.

The proposed mechanism is a potential option for the treatment of diluted As(III) acid streams. Therefore, future studies aim to reproduce and scale-up the process for the continuous treatment of As(III)-containing acid streams.

SUPPORTING INFORMATION OF CHAPTER 3

**Table S1.** Hydrolysis constants for arsenate and ferric iron used in this study for the IAP calculation [9, 28, 30].

Arsonate	pK
$H_3AsO_4 = H_2AsO_4^- + H^+$	2.24
$H_2AsO_4^- = HAsO_4^{2-} + H^+$	6.86
$HAsO_4^{2-} = AsO_4^{3-} + H^+$	11.49
Ferric Iron	
$Fe^{3+} + H_2O = Fe(OH)^{2+} + H^+$	2.19
$Fe(OH)^{2+} + H_2O = Fe(OH)_2^+ + H^+$	3.48
$Fe(OH)_2^+ + H_2O = Fe(OH)_2 + H^+$	6.33
$Fe(OH)_3 + H_2O = Fe(OH)_4^- + H^+$	9.6

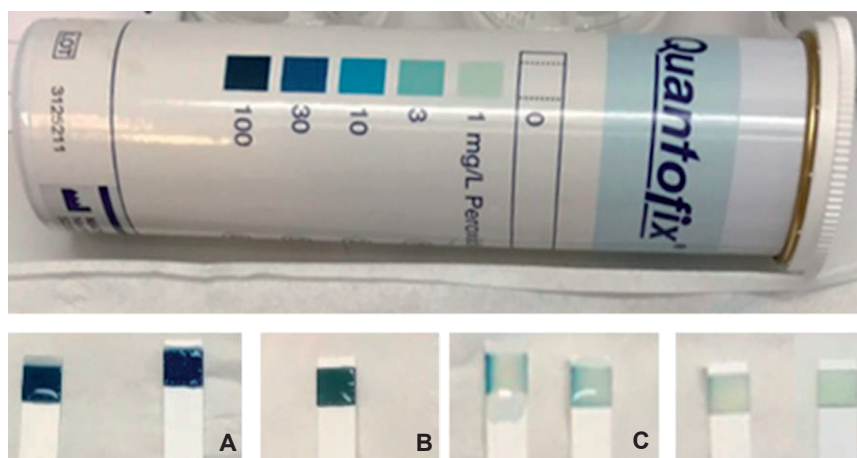


**Figure S1.** Hydrogen peroxide quantification: hydrogen peroxide reagent 30 wt% (A), 20 g L<sup>-1</sup> GAC in 1M H<sub>2</sub>SO<sub>4</sub> (B), 20 g L<sup>-1</sup> GAC (C) and 4 g L<sup>-1</sup> GAC (D) in culture media containing 510 mg L<sup>-1</sup> As(III) and 490 mg L<sup>-1</sup> Fe(II).

## CHAPTER 3

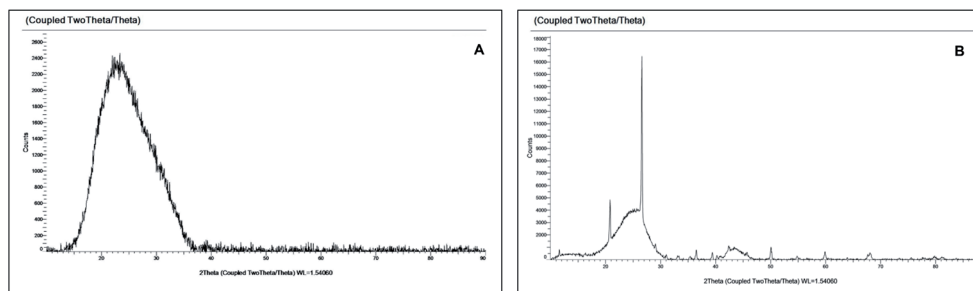


**Figure S2.** XRD diffractogram of the raw activated carbon (A) and the pre-treated activated carbon granules by water wash (B).

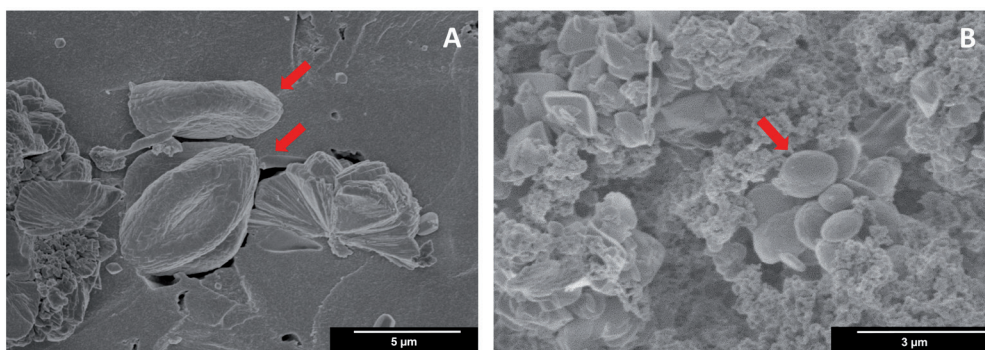


**Figure S3.** SEM images of rod-shaped microorganisms (indicated with red arrows) on the surface of the activated carbon granules from test with 4 g L<sup>-1</sup> GAC (A) and the biogenic precipitates obtained from tests with 20 g L<sup>-1</sup> GAC

## REFERENCES

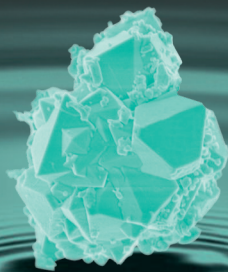
1. Gupta, D.K., S. Tiwari, B.H.N. Razafindrabe, and S. Chatterjee, *Arsenic Contamination from Historical Aspects to the Present*, in *Arsenic Contamination in the Environment: The Issues and Solutions*, D.K. Gupta and S. Chatterjee, Editors. 2017, Springer International Publishing: Cham. p. 1-12.
2. Dold, B., *Sustainability in metal mining: from exploration, over processing to mine waste management*. *Reviews in Environmental Science and Bio/Technology*, 2008. **7**(4): p. 275.
3. Nazari, A.M., R. Radzinski, and A. Ghahreman, *Review of arsenic metallurgy: Treatment of arsenical minerals and the immobilization of arsenic*. *Hydrometallurgy*, 2017. **174**: p. 258-281.
4. Park, J.H., Y.-S. Han, and J.S. Ahn, *Comparison of arsenic co-precipitation and adsorption by iron minerals and the mechanism of arsenic natural attenuation in a mine stream*. *Water Research*, 2016. **106**: p. 295-303.
5. Riveros, P., J. Dutrizac, and P. Spencer, *Arsenic disposal practices in the metallurgical industry*. *Canadian Metallurgical Quarterly*, 2001. **40**(4): p. 395-420.
6. Nazari, A.M., R. Radzinski, and A. Ghahreman, *Review of arsenic metallurgy: Treatment of arsenical minerals and the immobilization of arsenic*. *Hydrometallurgy*, 2016.
7. Fujita, T., S. Fujieda, K. Shinoda, and S. Suzuki, *Environmental leaching characteristics of scorodite synthesized with Fe(II) ions*. *Hydrometallurgy*, 2012. **111-112**: p. 87-102.
8. Paktunc, D. and K. Bruggeman, *Solubility of nanocrystalline scorodite and amorphous ferric arsenate: Implications for stabilization of arsenic in mine wastes*. *Applied Geochemistry*, 2010. **25**(5): p. 674-683.
9. Gonzalez-Contreras, P., J. Weijma, R.v.d. Weijden, and C.J.N. Buisman, *Biogenic Scorodite Crystallization by *Acidianus sulfidivorans* for Arsenic Removal*. *Environmental Science & Technology*, 2010. **44**(2): p. 675-680.
10. Sehlin, H.M. and E.B. Lindström, *Oxidation and reduction of arsenic by *Sulfolobus acidocaldarius* strain BC*. *FEMS Microbiology Letters*, 1992. **93**(1): p. 87-92.
11. Lebrun, E., M. Brugna, F. Baymann, D. Muller, D. Lièremont, M.-C. Lett, and W. Nitschke, *Arsenite oxidase, an ancient bioenergetic enzyme*. *Molecular biology and evolution*, 2003. **20**(5): p. 686-693.
12. Okibe, N., M. Koga, K. Sasaki, T. Hirajima, S. Heguri, and S. Asano, *Simultaneous oxidation and immobilization of arsenite from refinery waste water by thermoacidophilic iron-oxidizing archaeon, *Acidianus brierleyi**. *Minerals Engineering*, 2013. **48**: p. 126-134.
13. Okibe, N., M. Koga, S. Morishita, M. Tanaka, S. Heguri, S. Asano, K. Sasaki, and T. Hirajima, *Microbial formation of crystalline scorodite for treatment of As (III)-bearing copper refinery process solution using *Acidianus brierleyi**. *Hydrometallurgy*, 2014. **143**: p. 34-41.
14. Tanaka, M. and N. Okibe, *Factors to Enable Crystallization of Environmentally Stable Bioscorodite from Dilute As(III)-Contaminated Waters*. *Minerals*, 2018. **8**(1): p. 23.
15. Vega-Hernandez, S., J. Weijma, and C.J.N. Buisman, *Immobilization of arsenic as scorodite by a thermoacidophilic mixed culture via As(III)-catalyzed oxidation with activated carbon*. *Journal of*

## CHAPTER 3

- Hazardous Materials, 2019. **368**: p. 221-227.
16. Choi, Y., A. Ghahremaninezhad, and N. Ahern. *Process for activated carbon-assisted oxidation of arsenic species in process solutions and waste waters*. in *COM 2014-Conference of Metallurgists*. 2014.
  17. Jahromi, F.G. and A. Ghahreman, *In-situ oxidative arsenic precipitation as scorodite during carbon catalyzed enargite leaching process*. Journal of Hazardous Materials, 2018. **360**: p. 631-638.
  18. Bissen, M. and F.H. Frimmel, *Arsenic — a Review. Part II: Oxidation of Arsenic and its Removal in Water Treatment*. Acta hydrochimica et hydrobiologica, 2003. **31**(2): p. 97-107.
  19. Jahromi, F.G., D.H. Cowan, and A. Ghahreman, *Lanxess Lewatit® AF 5 and activated carbon catalysis of enargite leaching in chloride media; a parameters study*. Hydrometallurgy, 2017. **174**: p. 184-194.
  20. Ahumada, E., H. Lizama, F. Orellana, C. Suárez, A. Huidobro, A. Sepúlveda-Escribano, and F. Rodríguez-Reinoso, *Catalytic oxidation of Fe(II) by activated carbon in the presence of oxygen.: Effect of the surface oxidation degree on the catalytic activity*. Carbon, 2002. **40**(15): p. 2827-2834.
  21. Sun, Y., Q. Yao, X. Zhang, H. Yang, N. Li, Z. Zhang, and Z. Hao, *Insight into mineralizer modified and tailored scorodite crystal characteristics and leachability for arsenic-rich smelter wastewater stabilization*. RSC Advances, 2018. **8**(35): p. 19560-19569.
  22. Fujita, T., R. Taguchi, M. Abumiya, M. Matsumoto, E. Shibata, and T. Nakamura, *Effect of pH on atmospheric scorodite synthesis by oxidation of ferrous ions: Physical properties and stability of the scorodite*. Hydrometallurgy, 2009. **96**(3): p. 189-198.
  23. Lindström, E.B., Å. Sandström, and J.-E. Sundkvist, *A sequential two-step process using moderately and extremely thermophilic cultures for biooxidation of refractory gold concentrates*. Hydrometallurgy, 2003. **71**(1): p. 21-30.
  24. USEPA, *Toxicity characteristic leaching procedure (TCLP) method 1311*. 1992, EPA Publication SW-846.
  25. Leist, M., R.J. Casey, and D. Caridi, *The management of arsenic wastes: problems and prospects*. Journal of Hazardous Materials, 2000. **76**(1): p. 125-138.
  26. Radzinski, R.L., *An investigation into the activated carbon-catalyzed arsenic oxidation process*. 2017, Queen's University (Canada).
  27. Eguez, H.E. and E.H. Cho, *Adsorption of arsenic on activated charcoal*. JOM Journal of the Minerals, Metals and Materials Society, 1987. **39**(7): p. 38-41.
  28. Dove, P.M., Rimstidt, J.D., *The solubility and stability of scorodite, FeAsO<sub>4</sub>·2H<sub>2</sub>O*. American Mineralogist, 1985. **70**(7-8): p. 838-844.
  29. Langmuir D., M.J.a.R.J., *Solubility products of amorphous ferric arsenate and crystalline scorodite (FeAsO<sub>4</sub>·2H<sub>2</sub>O) and their application to arsenic behavior in buried mine tailings*. Geochimica et Cosmochimica Acta, 2006. **70**(12): p. 2942 - 2956.
  30. Krause, E., Ettel, V.A., *Solubility and stability of scorodite, FeAsO<sub>4</sub>·2H<sub>2</sub>O: new data and further discussion*. American Mineralogist 1988. **73**(7-8): p. 850-854.
  31. Robins, R.G., P.M. Dove, J.D. Rimstidt, D.K. Nordstrom, and G.A. Parks, *Solubility and stability of scorodite, FeAsO<sub>4</sub>·2H<sub>2</sub>O; discussions and replies*. American Mineralogist, 1987. **72**(7-8): p. 842-855.

32. Shibata, E., N. Onodera, T. Fujita, and T. Nakamura, *Elusion Tests of Scorodite Synthesized by Oxidation of Ferrous Ions*. Resources Processing, 2012. **59**(1): p. 42-48.
33. Le Berre, J.F., R. Gauvin, and G.P. Demopoulos, *A study of the crystallization kinetics of scorodite via the transformation of poorly crystalline ferric arsenate in weakly acidic solution*. Colloids and Surfaces A: Physicochemical and Engineering Aspects, 2008. **315**(1): p. 117-129.
34. Gomez, M.A., Assaouidi, H., Becze, L., Cutler, J. N. and Demopoulos, G. P., *Vibrational spectroscopy study of hydrothermally produced scorodite (FeAsO<sub>4</sub>·2H<sub>2</sub>O), ferric arsenate sub-hydrate (FAsH; FeAsO<sub>4</sub>·0.75H<sub>2</sub>O) and basic ferric arsenate sulfate (BFAS; Fe[(AsO<sub>4</sub>)<sub>1-x</sub>(SO<sub>4</sub>)<sub>x</sub>(OH)<sub>x</sub>·wH<sub>2</sub>O)*. Journal of Raman Spectroscopy, 2010. **41**((2)): p. p. 212-221.
35. Povarennykh, A.S., *The use of infrared spectra for the determination of minerals*. Am. Mineral., 1978. **63**: p. 956-959.
36. Ondruš, P., R. Skála, C. Viti, F. Veselovský, F. Novák, and J. Jansa, *Parascorodite, FeAsO<sub>4</sub>·2H<sub>2</sub>O—a new mineral from Kaňk near Kutná Hora, Czech Republic*, in *American Mineralogist*. 1999. p. 1439.
37. Gomez, M.A., L. Becze, M. Celikin, and G.P. Demopoulos, *The effect of copper on the precipitation of scorodite (FeAsO<sub>4</sub>·2H<sub>2</sub>O) under hydrothermal conditions: Evidence for a hydrated copper containing ferric arsenate sulfate-short lived intermediate*. Journal of Colloid and Interface Science, 2011. **360**(2): p. 508-518.
38. Baghurst, D.R., J. Barret, E. Coleyshaw Esther, P. Griffith William, D. Mingos, and M. P., *Microwave techniques for the synthesis and deuteration of minerals, with particular reference to scorodite, FeAsO<sub>4</sub>·2H<sub>2</sub>O*, in *Mineralogical Magazine*. 1996. p. 821.
39. Gonzalez-contreras, P.A., *Bioscorodite: biological crystallization of scorodite for arsenic removal*. 2014.
40. Fujita, T., R. Taguchi, M. Abumiya, M. Matsumoto, E. Shibata, and T. Nakamura, *Novel atmospheric scorodite synthesis by oxidation of ferrous sulfate solution. Part II. Effect of temperature and air*. Hydrometallurgy, 2008. **90**(2): p. 85-91.
41. Myerson, A.S. and R. Ginde, 2 - *Crystals, crystal growth, and nucleation*, in *Handbook of Industrial Crystallization (Second Edition)*, A.S. Myerson, Editor. 2002, Butterworth-Heinemann: Woburn. p. 33-65.
42. Harris, B., *The removal and stabilization of arsenic from aqueous process solutions: Past, present and future*. Minor Elements 2000. 2000. 3-20.

## CHAPTER 4



# **SCALE-UP OF THE BIOSCORODITE CRYSTALLIZATION FOR THE CONTINUOUS TREATMENT OF DILUTED AS(III) STREAMS.**

Authors: Silvia Vega-Hernandez, Irene Sánchez-Andrea,  
Jan weijma, Cees J.N. buisman

**Manuscript submitted for publication**

### ABSTRACT

The generation and treatment of arsenic-rich wastewater from metallurgical processes remain a serious environmental challenge. In this study, we focused on an integrated green process for the continuous oxidation of diluted As(III)-containing acid solutions and the simultaneous biological precipitation of scorodite ( $\text{FeAsO}_4 \cdot 2\text{H}_2\text{O}$ ); using a continuous laboratory-scale airlift reactor operated at thermophilic conditions and fed with Fe(II) as an electron donor. As(III) oxidation catalyzed by granular activated carbon (GAC), biological Fe(II) oxidation and scorodite crystallization took place simultaneously in the reactor, allowing the treatment of influent solution containing  $0.65 \text{ g} \cdot \text{L}^{-1}$  As(III). At a hydraulic retention time of 2.2 days, a stable arsenite oxidation efficiency of 99% was achieved, while the removal of total arsenic was 93%. The good sedimentation properties of the obtained scorodite precipitates due to the large average size ( $250 \text{ }\mu\text{m}$ ), allowed the easy harvesting of the precipitates from the reactor. The crystal structure of the solids was comparable to the mineral scorodite with an increase of the crystallinity during the experiment, which reflected the low arsenic release of  $0.4 \text{ mg} \cdot \text{L}^{-1}$  after 60 days of leaching, evaluated by the standard USEPA leaching method. The analysis of the microbial composition in the reactor suspension and the precipitates indicated the dominance of the thermoacidophilic archaea of the genus *Acidianus*. Microorganisms associated with the precipitates were observed by scanning electron microscopy, suggesting that the precipitation in our system was biologically mediated. The stability achieved in the process and the produced scorodite make it a sustainable alternative for arsenic fixation in metallurgical effluents.

**Keywords:** *Acidianus*, Activated carbon; Airlift Reactor, Arsenite oxidation; Thermoacidophilic; Scorodite

## 1. INTRODUCTION

Arsenic is a hazardous contaminant of global concern commonly released to the acid wastewater derived from the processing of base metal ores (i.e., Cu, Zn, Cd, Pb) [1]. Health effects due to exposure to As species are severe and include skin and lung cancer, neurological effects, hypertension and cardiovascular diseases [2]. Accordingly, the World Health Organization has set a very low standard of 10 ppb for drinking water. To protect the environment and drinking water resources, hydrometallurgical process streams containing arsenic concentrations (mainly As(III)) in the range 500-10000 ppm [3, 4] must be treated prior to the reuse of the water in the process or the disposal of the treated effluent in tailings facilities [5]. The removal and stabilization of this toxic element still is a significant and continuous challenge for the non-ferrous extractive metallurgical industry. Traditional methods to remove arsenic from industrial wastewaters and metallurgical operations include lime neutralization and chemical coprecipitation of arsenate with ferric iron [6]. Recent technologies, including adsorption/desorption, encapsulation, electrocoagulation have been developed and are widely applied to treat As-containing streams. However, the main disadvantage is the cost of such processes, the high iron dose needed and the amount of unstable generated waste [7, 8].

The precipitation of arsenic and iron as scorodite ( $\text{FeAsO}_4 \cdot \text{H}_2\text{O}$ ) is regarded as the preferred route for arsenic fixation due to the high arsenic content, high stability, low iron consumption and good settling properties of the product [9, 10]. Different methods for chemical precipitation of scorodite, mainly from As(V) solutions under hydrothermal and atmospheric conditions have been described [6, 11]. Similarly, under ambient conditions, the precipitation of biogenic scorodite from As(V) solutions was demonstrated [4, 12-14]. In the biogenic process, the saturation control is given by the biological oxidation of Fe(II) leading to the synthesis of crystalline scorodite at 70°C in the absence of primary seeds.

The oxidation state of arsenic is of importance for the design of effective removal strategies. Since As(III), the most mobile form of arsenic, is often present in the acid stream [5, 15], a primary oxidation step is required. The growth of thermoacidophilic archaea of the *Sulfolobaceae* family (e.g. *Acidianus sulfidivorans* and *Acidianus brierleyi*) by the oxidation of iron and sulfur as energy source has been widely described. In contrast, arsenite oxidizing activity has been scarcely reported, and at low rates for *Acidianus* and *Sulfolobus* spp. [4, 14, 16-20], which still represents a drawback for the scale-up and development of the biological process. On the other hand, hydrogen peroxide is an efficient oxidant of As(III) in sulfate media [21]; however, it is an expensive consumable

## CHAPTER 4

for the process. Alternatively, the catalytic oxidation of As(III) in acidic solutions by activated carbon in the presence of oxygen at ambient conditions has been reported [22, 23]. With this concept, oxidation efficiencies up to 99% were reported using a catalyst ratio between 1/17-1/30.

We have previously investigated the feasibility of precipitating scorodite from Fe(II) and As(III) solutions through the simultaneous As(III) oxidation by granular activated carbon (GAC) and Fe(II) oxidation by a thermoacidophilic iron oxidizing mixed culture in batch experiments (Chapter 2). Furthermore, the effect of GAC on the particle size of the biologically synthesized scorodite (Chapter 3) was also assessed. For further scale up and use in metallurgical industry, the development of a continuous process will be essential. In this work, we aim to develop such a continuous process for precipitation of biogenic scorodite in an airlift reactor fed with an diluted As(III) and Fe(II) containing acidic solutions. The scorodite produced in the continuous reactor was examined for its chemical composition and long-term stability through the toxicity leaching test procedure.

## 2. MATERIALS AND METHODS

### 2.1. MIXED CULTURE AND GROWTH MEDIA.

Enrichments culture of thermoacidophilic archaeon from Chapter 2 and Chapter 3 were used as inoculum in this study. The reactor was inoculated with 10% v/v of the thermoacidophilic mixed culture pre-grown in growth medium (Chapter 2) containing  $0.5 \text{ g L}^{-1}$  Fe(II) and  $0.5 \text{ g L}^{-1}$  As(III) at a pH of 1.3 and  $70^\circ\text{C}$ . Cell numbers were monitored during the experiment through cell counting using Burkler chamber (Germany). The medium fed to the reactor, ferrous iron stock solution and arsenite solutions were prepared as described previously (Chapter 2).

The granular activated carbon (NORIT GAC 830W) used in the experiments was sieved to particle sizes between 0.8-1.4 mm and washed with sulphuric acid (1 M) followed by rinsing with deionized water in order to remove impurities. The characteristics of the used GAC were reported earlier (Chapter 2).

### 2.2. AIRLIFT REACTOR SET-UP AND OPERATION.

An airlift reactor with 9 L of working volume was used in this work. The reactor temperature was controlled at  $70 \pm 2^\circ\text{C}$  with a heating bath (Julabo F25, Germany).

The pH was controlled at  $1.2 \pm 0.1$  using  $\text{H}_2\text{SO}_4$  (5 M) and NaOH (5 M) solutions. Air and oxygen were supplied to the reactor giving an inlet concentration of 27.5%  $\text{O}_2$  in the mixed gas. Therefore, the feed gas flow rate was controlled by separate mass flow controllers (Brooks thermal mass flow meter, type 5850 E,  $0\text{--}60 \text{ L h}^{-1}$ ). The gas was recycled at  $60 \text{ L h}^{-1}$ , with a membrane pump (KNF N828) providing a superficial air velocity in the riser of  $0.59 \text{ m s}^{-1}$ . The water vapour in the bleed air was condensed with a reflux condenser connected to a cooling bath (Julabo F25, Germany) and the condensate was returned by gravity to the reactor. The reactor was operated without external recirculation of liquid or solids.

Redox potential (Eh, mV) and pH were measured with glass electrodes (QR480X-Pt billed-triple junction (vs. Ag/AgCl in saturated KCl) and QP181X-triple junction, respectively; Prosense, the Netherlands). Slope calibration of the pH electrode was done with pH 1 and 4 buffers. Dissolved oxygen was measured using an oxygen dipping probe DPPSt3 (Presens, Germany) connected to a Fibox-3 fiber optic oxygen transmitter (Presens, Germany). The oxygen sensor was calibrated at 0% with nitrogen and at 100% with water-saturated air.

The airlift reactor was operated in three consecutive stages (I) day 1-12, batch mode (II) day 13-33, continuous mode with a hydraulic retention time (HRT) of 3.1 days and (III) day 34-98, continuous mode with an HRT of 2.2 days.

The influent media composition varied between batch and continuous operation. In stage I (batch operation), about 1 g of Fe(II)  $\text{L}^{-1}$  and 1 g of As(III)  $\text{L}^{-1}$  were added giving a molar ratio Fe/As of 1.29. When the reactor was switched to continuous operation (stage II and III), the concentrations were decreased to 0.63 g of Fe(II)  $\text{L}^{-1}$  and 0.65 g of As(III)  $\text{L}^{-1}$  (Fe/As: 1.3). No external crystal seeds were added to the bioreactor.

## 2.3. METHODS

### 2.3.1. IRON AND ARSENIC ANALYSIS.

Fe(II), Fe(III), As(III), As(V), total dissolved Fe and As species in the reactor of filtered ( $0.45 \mu\text{m}$ ) reactor samples, and As and Fe content of solid samples were prepared and analyzed as described previously in Chapter 2.

## CHAPTER 4

### 2.3.2. CHARACTERIZATION OF THE PRECIPITATES

The collected solids were washed with 50 mM of sulphuric acid, followed by washing with deionized water and dried at room temperature before characterization and the leaching test. Characterization of the solids with particle size distribution (PSD) analysis, XRD, FT-IR, TGA and SEM-EDX were carried out as described previously in Chapter 3.

### 2.3.3. TOXICITY CHARACTERISTIC LEACHING PROCEDURE

The solubility of the produced bioscorodite was assessed with the standard Toxicity Characteristic Leaching Procedure (TCLP) of EPA [24]. Serum bottles containing acetate buffer at pH 4.95 as leaching medium and a fixed solid: liquid ratio of 20% w/w were used. The bottles were shaken at 20°C. Samples were taken after 20 hours, 7 days and 60 days and sampling volume was replaced with fresh acetate medium.

### 2.3.4. MICROBIAL COMMUNITY ANALYSIS

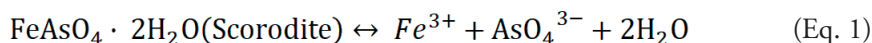
In order to assess the microbial composition, two different samples were withdrawn from the reactor and processed for DNA extraction. On one hand, 5 mL of the bulk solution were centrifuged at 13,400 *g* for 10 min, supernatant was discarded, and the pellet was resuspended in 250  $\mu$ L of sterile Milli-Q water, this sample was termed “Biomass”. On the other hand, 1 g of the mineral fraction was washed with Milli-Q water; this sample was termed “Solid”. DNA was extracted in triplicates with the FastDNA Spin Kit for Soil (MP Biomedicals, OH) according to manufacturer’s protocol. DNA was then cleaned with the Zymo DNA Clean & Concentrator kit (Zymo Research, CA). PCR was performed as described elsewhere [25]. The demultiplexed Illumina Hiseq reads of the 16S rRNA gene amplicon sequencing were deposited at the European Nucleotide Archive (ENA) under study PRJEB32058 in fastq format with accession numbers ERX3291747- ERX3291752.

A multiple alignment of the sequences was performed using Muscle v3.7 [26] with the default parameters. This multiple alignment was used to create an approximate maximum-likelihood tree using FastTree v2.1.8. [27] with default parameters. The tree was visualized with iTOL [28]. For the identity network, using the multiple sequence alignment created for the phylogenetic tree, a pairwise distance was calculated using Clustal Omega - 1.2.3 [29] for all detected 16 rRNA sequences and threshold was settled

at 0.9 for the clustering. Network visualizations were constructed using Cytoscape (v. 3.7.1) [30]

## 2.4. CALCULATION OF THE ION ACTIVITY PRODUCT

The Ion Activity Product (IAP) of the reactants of scorodite was calculated based on Eq.1 as described elsewhere [13].



## 3. RESULTS AND DISCUSSION

### 3.1. ARSENITE AND FERROUS IRON OXIDATION EFFICIENCY IN ALR

The airlift reactor was operated in batch mode during the first 12 days at an initial pH  $1.2 \pm 0.1$  with GAC ( $4 \text{ g}\cdot\text{L}^{-1}$ ) using starting concentrations of  $1 \text{ g}\cdot\text{L}^{-1}$  As(III) and  $1 \text{ g}\cdot\text{L}^{-1}$  Fe(II), resulting in a molar ratio Fe/As of 1.29. As(III) oxidation started immediately and 42% of As(III) was depleted within one day (Figure 1A). Overall As(III) and Fe(II) oxidation during stage I amounted to 83% and 76%, respectively (Figure 1A,C). Simultaneous with arsenite oxidation and Fe(II) oxidation, precipitation of dissolved As took place (Figure 1A). Iron and arsenic precipitated during the first 8 days at an approximate ratio Fe/As: of 1.3, however, between day 8 and 12 this ratio increased to 4. This was coupled to a change in the pH of the solution, which increased to 1.4 at day 9 and to the increase of the redox potential from +0.35 to +0.43 mV. On day 12, 66% of the initial arsenic and 65% of iron had precipitated at an average molar ratio for Fe/As of 2.3 (Figure 2).

On day 13 the reactor was switched to continuous operation with an HRT of 3.1 days, with an influent medium containing  $0.65 \text{ g}\cdot\text{L}^{-1}$  As(III) and  $0.63 \text{ g}\cdot\text{L}^{-1}$  Fe(II). The pH fluctuated between 1.18 and 1.24, which was maintained during continuous operation. From day 12-16, the formation of a gelatinous ferric phase was observed along with greenish precipitates collected from the reactor (Figure S1). X-ray diffraction analysis of solid samples collected at day 12 revealed the presence of amorphous ferric arsenate phases and scorodite (Figure S2). From day 17 until the end of the experiment, the concentration of Fe(II) in the feed was adjusted to achieve a Fe/As molar ratio of 1.3, and formation of the gelatinous phase was no longer observed. The precipitation of poorly crystalline phases is unwanted in the process. However, two routes determining

the fate of these phases has been considered to take place in the crystallization process, first the solubilization in the acid media or secondly, its conversion into crystalline phases [31-33] of which, the first one is the most likely to occur. The formation of amorphous phases may influence directly or indirectly the precipitation of scorodite [33]. Of the oxidized Fe, only 40% was precipitated, while 45% of As precipitated, achieving an average removal of  $0.24 \pm 0.08 \text{ g}\cdot\text{L}^{-1} \text{ d}^{-1}$  of Fe and  $0.28 \pm 0.04 \text{ g}\cdot\text{L}^{-1} \text{ d}^{-1}$  As (Figure 1B and 1D). The precipitation in stage II apparently was limited by the oxidation of As(III) which fluctuated between 50 and 60%. The molar Fe/As precipitation rate ranged between 0.9 and 1.4 in stage II (Figure 3A) and the absence of visible precipitates in the effluent indicated that precipitates were effectively retained in the reactor.

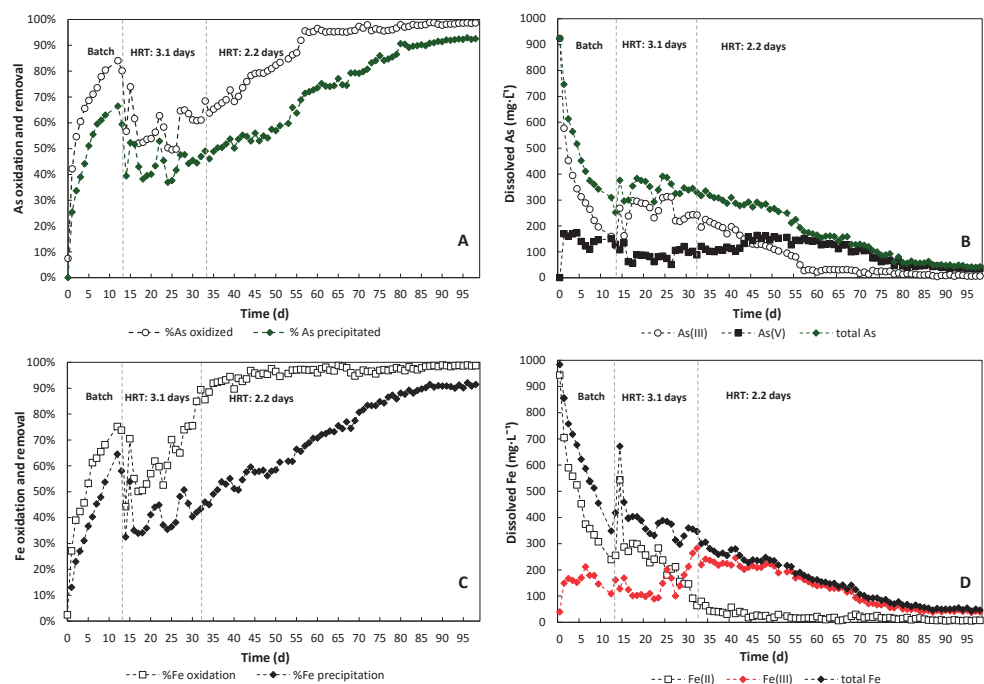


**Figure 1.** Overall arsenic and iron oxidation and removal in the airlift reactor during batch and continuous operation (from day 13 onwards at 70°C). A: As(III) oxidation and removal efficiency B: As(III), As(V) and total dissolved As species, C: Fe(II) oxidation and removal efficiency, D: Fe(II), Fe(III) and total dissolved Fe species in the airlift reactor.

The decrease of the HRT to 2.2 days at day 31 marked the start of stage III. At the same time, the oxygen flow rate was increased to  $4.7 \text{ L}\cdot\text{h}^{-1}$  and the recycle gas flow was switched to  $100 \text{ L}\cdot\text{h}^{-1}$ , giving a dissolved oxygen concentration in the reactor of  $4.0 \pm 0.1 \text{ mg O}_2 \text{ L}^{-1}$ . The increased recycle flow resulted in the effective lifting and better distribution of

the activated carbon granules, which had partially settled to the reactor bottom in stage II. The arsenite oxidation increased during stage III until a stable situation was observed from day 58 until the end of the experiment (day 98). An average oxidation rate of  $0.641 \text{ g}\cdot\text{L}^{-1} \text{ d}^{-1}$  of As(III) was found, corresponding to an oxidation efficiency of 99%. In the case of ferrous iron conversion, the rates were not markedly influenced by the improved mixing of the granules in the reactor. The oxidation efficiency increased around 16% during the last phase of continuous operation and a plateau was reached after day 50 with approximately 98.4% of the Fe(II) oxidized (Figure 1D). This was reflected also in the ORP which reached a maximum of  $+0.65 \text{ mV}$  during this phase. As shown in Figure 2, the increment of ORP due to the increased ferrous oxidation was also coupled to the growth of the iron oxidizing mixed culture, expressed by the increased quantity of planktonic cells during batch and continuous operation.

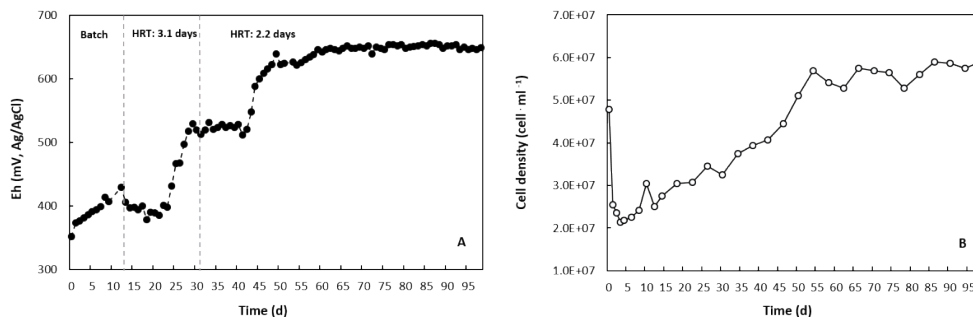


**Figure 2.** Redox potential (mV, Pt vs. Ag/AgCl in saturated KCl) and microbial growth measured as cell density ( $\text{cell}\cdot\text{ml}^{-1}$ ) in the airlift reactor during the catalyzed As(III) oxidation and biological scorodite precipitation at  $70^\circ\text{C}$ .

Once the oxidation and precipitation rates improved in stage III of reactor operation, the concentration of total dissolved iron and arsenic concentrations considerably decreased to an average of  $0.047 \pm 0.01 \text{ g}\cdot\text{L}^{-1}$ ; of which, As(III) and Fe(II) were low, ranging around  $0.01 \text{ g}\cdot\text{L}^{-1}$ . During stage III the reactor content turned to light green, typical for scorodite (Figure S3). The concentration of dissolved arsenic and iron in the effluent solution was also monitored (Figure S4) resulting in similar concentrations of total iron and arsenic around  $0.04 \pm 0.018 \text{ g}\cdot\text{L}^{-1}$ . The concentration of As is too high to allow for direct discharge. Thus, a post treatment like co-precipitation with ferrihydrite will be needed in practice.

Oxidation of As(III) is essential in the process of arsenic immobilization however, this alone doesn't ensure the effective removal of arsenic from solution. It must follow

## CHAPTER 4

either by adsorption or the precipitation. Traditionally the fixation of arsenic from relative dilute arsenic streams is accomplished by the co-precipitation of the oxidized As(V) with Fe(III) and neutralization, which results in a mixture of amorphous arsenical ferrihydrite with molar Fe/As ratio of 3-5 and thus substantial amounts of waste (i.e. arsenate bearing ferrihydrite plus gypsum). With the scorodite process, the Fe:As molar ratio of the compact precipitate is (close to) 1, implying a much lower Fe consumption and a lower volume of the solid waste residue. A single oxidation and precipitation system in the airlift reactor at 70°C for the precipitation of scorodite particles of good settling properties offers more advantages compared to separate units than only the prevented investment cost for the separate As(III) oxidation reactor. For example, the airlift reactor is effective for mass transfer of oxygen, by recycling the effluent gas, providing sufficient oxygen for both arsenite and ferrous iron oxidation. Less equipment is needed in the single stage process, i.e. less pumps, mass/gas flow controllers, sensors etc. The airlift is a also well-mixed system and was suitable to keep both scorodite crystals and GAC particles suspended, without attrition of the GAC particles. Furthermore, it has been shown that the use of air-lift reactors is beneficial for crystallization processes with respect to crystal growth [34]. Airlift and gas-lift bioreactors are already applied on a full scale for over 20 years, also in metallurgical operations and can be considered proven technology [35, 36]. For application of the biological scorodite process, the airlift reactor design may need some modification for collection and separation of the scorodite solids. Incorporation of a settling in the reactor of a settling compartment designed could represent a suitable to remove particles above a cut-off sedimentation rate (or particle size). After day 59 until the end of the experiment, the ORP was very stable at +649±4 mV. This coincided with high oxidation efficiencies for As(III) and Fe(II) (Figure 1), a high As(V):As(III) molar ratio (Figure S6) and a low Fe(II) concentration (Figure S7). The ORP may represent a suitable parameter for monitoring process performance and as a control parameter, for instance to adjust the HRT.

### 3.2. ARSENIC PRECIPITATION

The saturation of the solution was evaluated using the ion activity product (IAP) of ferric arsenate. Scorodite mostly precipitated in the reactor at log(IAP) values from -21.5 to -22.3 (Figure 3). The IAP decreased at the start of continuous operation (stage II) due to decreasing As(V) concentrations. However, the IAP increased immediately after the arsenite oxidation rate improved, resulting in increased As(V) activity in solution, without additional changes between day 31 until day 61 of stage III where the As(III) oxidation rate reached 95.3%. Until the end of the experiment (day 98) total As precipitation rate increased to 93% and IAP values fluctuated around -22±0.5 being in

the range of IAP values previously reported [9, 13, 37].

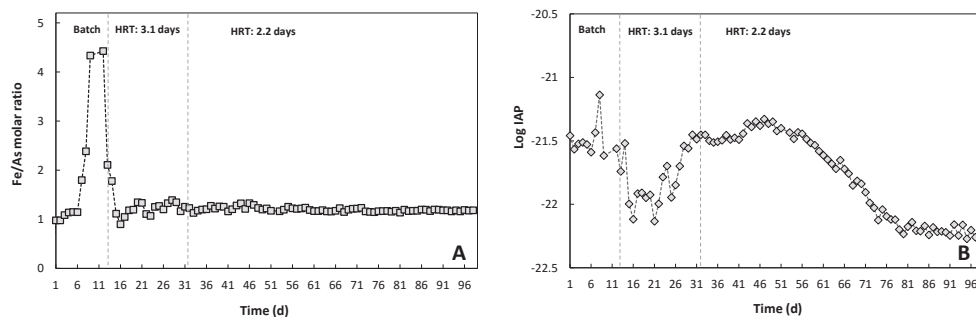


**Figure 3.** Fe/As molar ratio of Fe and As species removed from solution (A) and calculated Ion activity product (Log IAP) of biological scorodite produced in airlift reactor at 70°C.

The evolution of the particle size distribution of precipitates from the reactor is shown in Figure 4A. The average particle size was 19  $\mu\text{m}$  on day 9 (stage I, batch mode). Also particles  $<1\mu\text{m}$  were found in the sample and at the start of continuous operation (day 18) which might be attributed to the amorphous ferric arsenate solid phase formed during stage I. During continuous operation, the precipitates grew from an average particle size of 43  $\mu\text{m}$  in stage II to 230  $\mu\text{m}$  at the end of stage III. The growth of the crystals over the continuous operation indicated that crystal growth dominated over nucleation. The bioscorodite precipitates showed good settling properties and the complete deposition of 0.5  $\text{g}\cdot\text{L}^{-1}$  of solids with particle size between 15-300  $\mu\text{m}$  was achieved in 5 minutes at settling velocities between 1-228  $\text{m}\cdot\text{h}^{-1}$  in a 500 mL glass cylinder (Figure 4B).

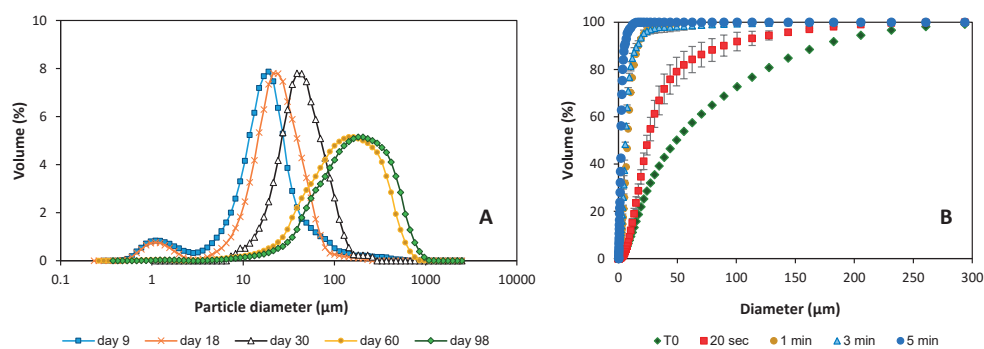


**Figure 4.** Particle size distribution (PSD) of the bioscorodite precipitates in the airlift reactor at 70°C and pH  $1.2\pm 0.1$ . (A) PSD of precipitates during batch (day 9) and continuous operation stage II (day 18-30) and III (day 60-98). (B) Settled volume of solids at different settling times as function of diameter according to Stoke's law.

## CHAPTER 4

The continuous precipitation of biogenic scorodite in the airlift reactor led to the growth of crystals aggregates which were identified as (1) the fraction that remained in suspension facilitating the precipitation of scorodite on the existing particles instead of the reactor walls and (2) the solids settled to the bottom of the reactor, which was beneficial for the collection of the solids from the solution.

### 3.3. CHARACTERIZATION OF THE PRECIPITATES

Precipitation of iron and arsenic took place during the entire experiment as revealed by the decrease of soluble total Fe and As in solution, and by the appearance of a solid phase on day 9 of batch operation. On day 12, samples taken from the reactor visually revealed two solid phases, a compact material of light green color and a gelatinous-like phase. The former settled at the bottom of the reactor while the gelatinous material was observed in suspension and the bottom of the reactor (where it was taken for the analysis).

The X-ray diffraction analysis of the both samples revealed the presence of scorodite as the main mineral phase of compact greenish precipitates (Figure S2A) and the formation of a short-lived gelatinous fraction identified as an amorphous iron arsenate phase (Figure S2B). Thus, at the precipitation ratio Fe/As of 4 in stage I, formation of other iron precipitates than scorodite were induced. Comparable XRD patterns have been obtained during arsenate adsorption studies to ferric oxides conducted at similar temperature (75°C) conditions by Jia et al. [38] and with molar Fe/As $\geq$  2. We found similar XRD pattern for ferric iron precipitates (Figure S2D) together with the scorodite precipitates from stage II (although to a lesser extent), that were no longer visible during stage III (Figure 5).

The greenish precipitates collected during stage II were also identified as scorodite (Figure S2B). While broad peaks of lower intensity were observed in the sample from stage I (Figure S2A), the sharper and narrower peaks observed in samples of stage II and stage III (Figure 5) are indicative of larger crystal size and increased crystallinity (degree of structural order) [39, 40].

The dominance of scorodite crystalline phases in the precipitates collected at the end of stage III was confirmed by the complete match of the sharp peaks to the diffraction patterns of mineral scorodite and by the high intensity counts (Figure 5A). The overall weight loss by TGA was 15.8%, close to the theoretical water content of mineral scorodite (15.6%). FT-IR analysis of the precipitates showed the characteristic peak for arsenate

bending ( $\text{V1 AsO}_4^{3-}$ ) at  $820\text{ cm}^{-1}$  [41]. Besides, 2 peaks were also observed at  $1008$  and  $1030\text{ cm}^{-1}$  which might be related to the incorporation of sulphate, possibly from the washing step of the samples prior the characterization as documented by Gonzalez-Contreras et al. [42]. The strong water stretch and bonding was identified in the region of at  $1600$  and  $2960\text{ cm}^{-1}$ .

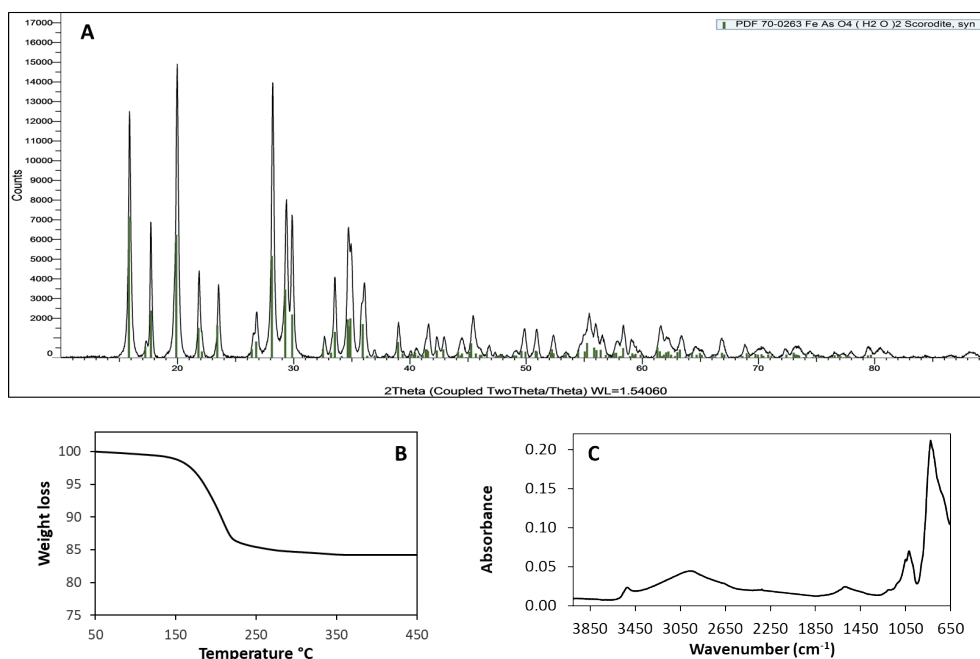


**Figure 5.** Structural characterization of bioscorodite crystals collected at the end of the continuous operation of the airlift reactor at  $70^\circ\text{C}$  and  $\text{pH } 1.2 \pm 0.1$  (A) X-ray diffraction data matching the XRD pattern. (B) Thermo Gravimetric Analyser shows the structural water content between  $170^\circ\text{C}$  and  $240^\circ\text{C}$ , at  $400^\circ\text{C}$  hydroxyl (OH) is converted to  $\text{H}_2\text{O}$ , and near to  $700^\circ\text{C}$  sulphate is converted to sulphur dioxide. (C) Fourier transform infra-red spectra of precipitates.

The morphology of the bioscorodite particles was examined by scanning electronic microscopy (SEM). The results displayed in Figure 6 indicated that the precipitated scorodite changed from an irregular to a more crystalline shape. The solids observed at beginning of stage II consisted of agglomerates with irregular structure containing crystallites of  $0.5\ \mu\text{m}$  in agreement with the particle size distribution analysis. The development of more crystalline particles was visualized in the solid aggregates at day 27 (Figure 6B). By the end of stage III, clusters of crystals and individual scorodite particles with octahedral structure were observed (Figure 6C and 6D).

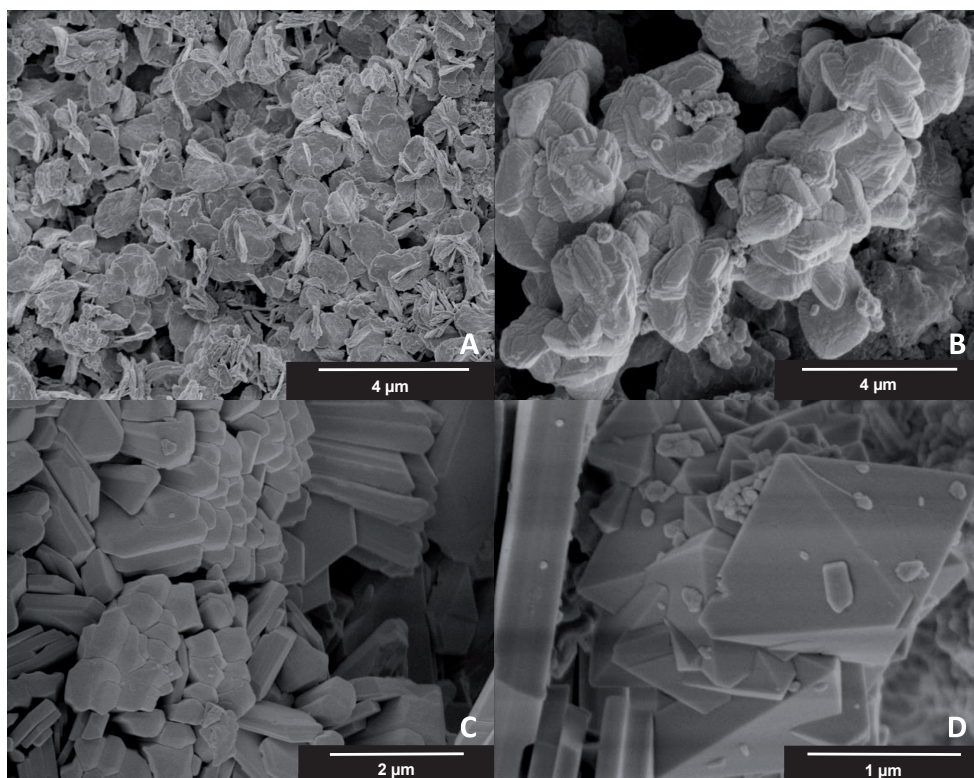


**Figure 6.** Scanning electron microscopy (SEM) of the precipitates collected during stage II at day 17 (A) and 27 (B) and during stage III at day 55 (C) and day 81 (D) of continuous operation from airlift reactor at 70°C.

As already found with the PSD analysis, precipitates collected at the end of the experiment consisted on agglomerates with sizes up to 300  $\mu\text{m}$ . The analysis of the surface of these bigger particles revealed that these consist of well-ordered planes of dipyramidal form with an estimated size of 1-2  $\mu\text{m}$  (Figure 7). This characteristic growth has been reported previously for crystalline scorodite [43] and referred as habit I by Gonzalez-Contreras et al. [13].

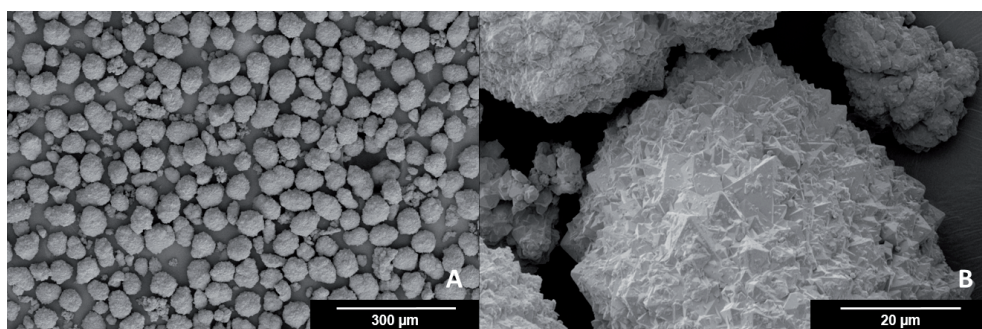


**Figure 7.** Scanning electron microscopy (SEM) of the scorodite crystals collected at the end of the experiment and surface characteristics.

The elemental composition of the precipitates was also analyzed by SEM-EDX (Figure S5), showing that Fe/As molar ratio ranged between 1.1-1.25 for the precipitates taken at day 25 and 57. The elemental composition of the precipitates collected at the end of the continuous experiment slightly changed and an average Fe/As content of 1.04 was calculated. The SEM-EDX analysis furthermore revealed the presence of P and S in small proportion of 1.6% and 0.66%wt, respectively in the solid sample. The presence of 8.21%C and 1.67%N may result from the association of microorganisms with the precipitates.

### 3.4. ARSENIC LEACHING FROM THE BIOGENIC SCORODITE PRECIPITATES

Determining the release of arsenic into solution is of environmental significance to assess if the formed precipitates are a safe medium for long term arsenic storage. The leaching of arsenic from the precipitates collected during stage I-III was evaluated by the toxicity characteristic leaching procedure (TCLP) (Figure 8).

Arsenic leaching values for all the samples was below the permissible EPA limit of 5 mgL<sup>-1</sup> of As. As shown in Figure 8, the precipitates collected during stage I (day 12) leached around 2.05 mgL<sup>-1</sup> As after 20 hours which decreased to 1.4 mgL<sup>-1</sup> after 60 days. Precipitates from stage II and III initially leached 1.5 and 0.6 mgL<sup>-1</sup> of As, respectively (20 hours), which decreased to 1.2 and 0.46 ± 0.01 mgL<sup>-1</sup> after 60 days. The higher leaching values of solids from stage I may well be due to the presence of less stable amorphous material (observed on the XRD) [10, 44, 45]. Leachability of arsenic has been associated to the crystallinity and aging time [42, 43, 46, 47], which could explain the lower leaching of solids from stage III compared to stage II.

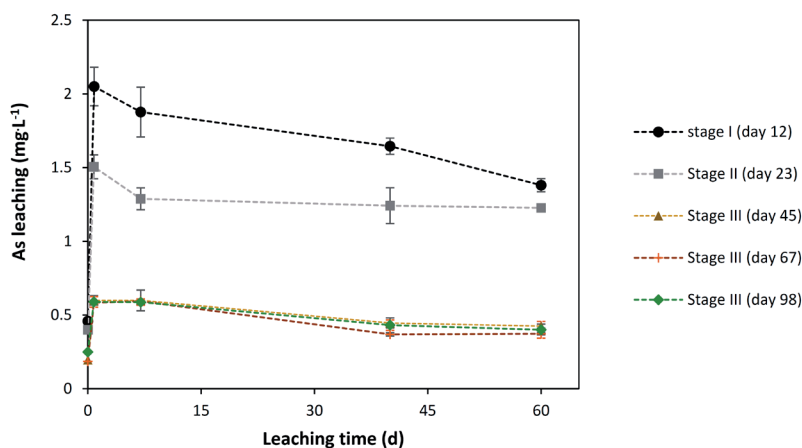


**Figure 8.** Arsenic leaching from precipitates produced in the airlift reactor during batch and continuous operation under TCLP test.

### 3.5. MICROBE-MINERAL ASSOCIATION AND MICROBIAL COMPOSITION IN AIRLIFT REACTOR

SEM images of the reactor samples from stage II and stage III showed the presence of exopolysaccharide (EPS)-like materials mediating the attachment cocci and bacillus shaped microorganisms and the produced precipitates (Figure 9A and B). Likewise, the abundance of rod-shaped cells with apparent structural cell damage was also observed during the SEM analysis (Figure 9C). These observations agreed with previous results (Chapter 2 and Chapter 3) and suggest the key role of cells in the scorodite precipitation [37] not only by providing the reactant ferric iron due to the metabolic activity but also the site for nucleation. The formation of Fe minerals has been associated with the presence of S-layer proteins at the cell envelope of some hyperthermophilic archaea (e.g., *Sulfolobus acidocaldarius*) which mediate metal interaction and the passive process of nucleation and growth on the cell surface [48]. Furthermore, EPS formation has been reported for thermoacidophilic species of *Acidianus*, *Sulfolobus*, and *Metallosphaera* [49-51], and its secretion has been suggested as a mechanism of cell protection against environmental stress such as the extreme pH conditions and from cell encrustation [52, 53]. The association of cells with solids also might facilitate biomass retention in the reactor.

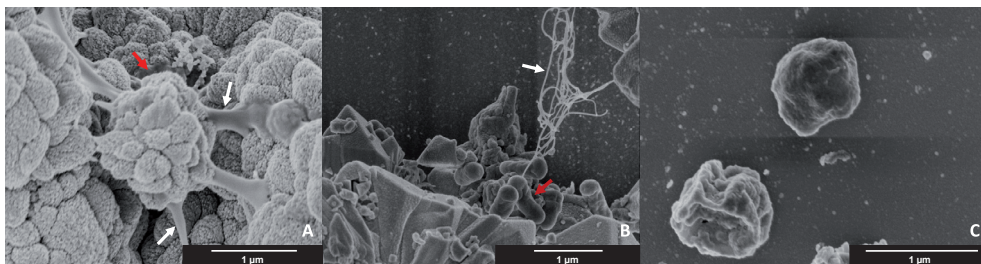


**Figure 9.** Scanning electron microscopy images of precipitates from stage II and III indicating the presence of EPS-like substances (white arrows) and coccoid-like and bacillus shaped cells adhered to the solids (red arrows) (A and B) and microorganisms from reactor suspension (C).

The microbial community composition in the reactor was analyzed by 16S rRNA sequencing of samples from the bulk solution and the solids, designated as “Biomass” and “Solid” respectively. Both samples were collected at the end of the experiment. After filtering low abundance OTUs (below 0.01%), the microbiome composition of both biomass and solids showed a relative low diversity comprising 61 OTUs in total, belonging to 24 different genera (Figure 10A and B). In the biomass sample, that was comprising the planktonic cells in the reactor, the 61 OTUs were identified, however in the solids sample only 21 OTUs were detected (Figure 10A and B).

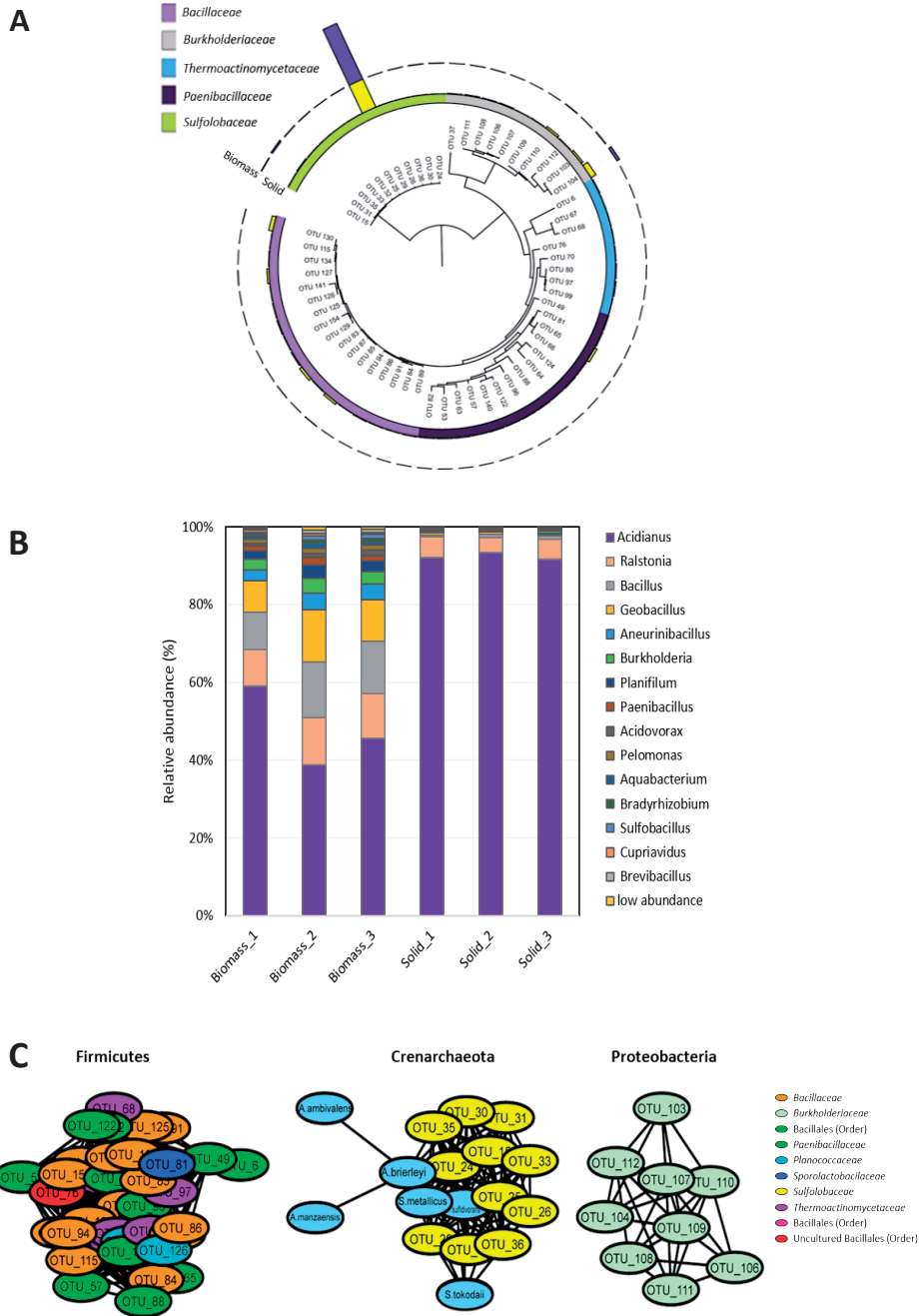


**Figure 10.** Microbiome composition of the reactor samples and scorodite precipitates named as “Biomass” and “Solid” respectively. (A) Phylogenetic tree of the OTUs (n=61) detected in the reactor samples based on an alignment of the 16S RNA gene (132 nucleotide positions). Colors

in the inner circle are indicating the taxonomic classification at Family level. Outer circles are representing the relative abundance of detected OTUs, in yellow (Biomass) and purple (Solid). Phylogenetic trees are displayed with iTOL. (B) Bar plot depicting the relative abundances at Genus level of the most abundant members of the reactor in both samples, Biomass and Solid. (C) Identity network showing the phylogenetic distance (black connecting edges) between the *Acidianus* spp. and *Sulfolobus* spp. reference strains (red nodes), previously described in acid Fe and As streams [14, 54], with OTUs identified in the reactor (colored nodes at family level).

In thermophilic bioleaching processes iron/sulfur oxidizing mixed cultures are commonly employed from which no more than three species often dominate in continuous-flow operations [55] even though under thermoacidophilic conditions (<60°C) reactions are mainly performed by archaea and only a smaller number of other bacterial species may be present [56].

Members of the *Sulfolobaceae* family (most of them annotated as *Acidianus* spp.) were the most abundant microorganisms detected in the 16S rRNA survey in both Biomass and Solid samples representing the 45.9 and 92.3% of the total microbial community (Figure 10A and B). As aforementioned, members of this genus, such as *Acidianus brierleyi* have been linked to the simultaneous ferrous iron, arsenite oxidation and to the concomitant scorodite precipitation [4, 16, 20, 57]. Similar to the iron oxidizing archaea *A. sulfidivorans*, *Metallosphaera sedula* and *sulfolobus* spp. which has been reported to mediate scorodite precipitation but in the less toxic As(V) solutions [12, 13, 58]. Phylogenetic distance analysis (Figure 10C) of the sequences from the reactor samples showed that Firmicutes, Crenarchaeota and Proteobacteria were the three main phyla clustering at 90% similarity. Furthermore, using the reference strains *Acidianus* spp. and *Sulfolobus* spp. revealed that the OTU29, highly abundant and dynamic in the Biomass and Solid samples, is clustering very close to the *S. metallicus*, *A. brierleyi*, *A. sulfidivorans* and *S. tokodaii*. Although *A. brierleyi* and *S. metallicus* were known to be part of the inoculum, further studies need to be performed to determine more precisely the taxonomic composition of this specialized community.

Besides *Acidianus* spp., the second most abundant taxa were *Ralstonia* spp., accounting for 9 and 4.8% of the total reads in the Biomass and Solid samples, respectively. Members of *Ralstonia* have been found in mine tailing sediments and associated with the oxidation of As(III) [59, 60]. Other genera, such as *Geobacillus*-related sequences also showed a high abundance, but with markedly difference within the planktonic biomass and the solid phase (9.2 and 0.5%, respectively). *Geobacillus* spp. are thermophilic, aerobes with a chemi-organotroph metabolism, also reported in mine ecosystems [61]. Other iron-oxidizing species such as *Sulfobacillus* were found in the bulk solution. Despite the low abundance (approximately 1-2% in the biomass sample), these species

## CHAPTER 4

were known to be part of the mixed culture inoculated in the reactor (Chapter 1). The optimum growth temperature (40-60°C) of *Sulfobacillus* species was below the tested conditions; however, their adaptation to adverse, or even deleterious conditions has been previously reported in thermoacidophilic leaching systems and geothermal sites [56, 62]. Moreover, previous studies have shown the beneficial interaction between *Sulfobacillus* species (e.g., *S. thermosulfidooxidans*) and acidophilic archaeon (e.g., *Acidianus* species) in the dissolution of minerals [63, 64]. Therefore, the role of this microorganism in the oxidation and/or precipitation cannot be excluded.

### 4. CONCLUSIONS

The catalyzed oxidation of arsenite by activated carbon in combination with the iron oxidizing mixed culture led to the formation of scorodite as the main product in the studied continuous airlift reactor system at pH 1.2 and 70°C. The mixing of the activated carbon granules with the bulk solution is crucial to ensure the complete oxidation of arsenite in the system. The simultaneous iron oxidation is another important parameter; In the reactor the oxidation of iron is controlled by the activity of the mixed culture, this was reflected in the increased cell concentration and the gradual increase of the iron oxidation rate, probably due to the reduced toxic effect of As(III). Under these extreme conditions mainly archaeal population were enriched in the reactor system. The high percentage of archaeal species obtained by the molecular analysis and the visualized structure EPS like material suggest that the formation of scorodite is indirectly mediated by the microbial surface or surface components (exopolymers). The biogenic scorodite produced showed similar characteristic to mineral scorodite, which was supported by the water content and the low leaching capacity. Furthermore, the quality of obtained sludge facilitated the recycling of the particles in the system, which offer significant advantages such as: (i) avoided scaling in the reactor (2) increased density of the sludge and (3) easy solid-liquid separation which allow to get a suitable material for disposal.

The obtained results provides an important step forward in the development of a sustainable and integrated approach for waste management and improvement of water quality for recycling or discharge. This in turn will contribute to reduce the environmental footprint of the mining industry.

### ACKNOWLEDGEMENTS

We want to thank Victor J. Carrión and Javier Ramiro-Garcia for their valuable advice

and support in the bioinformatics analysis.

## SUPPORTING INFORMATION OF CHAPTER 4

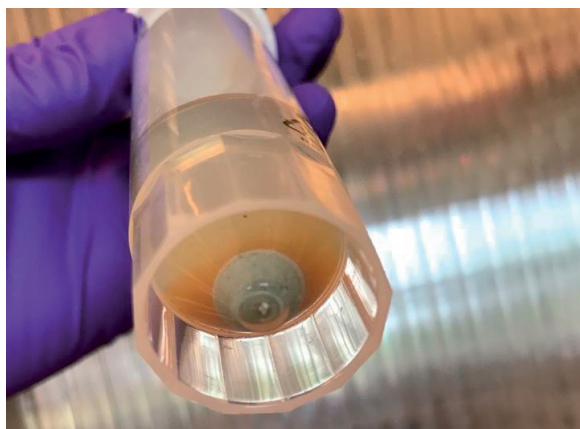


**Figure S1.** Precipitates collected from airlift reactor at day 16. Ferric precipitates (brownish) and scorodite (light green).

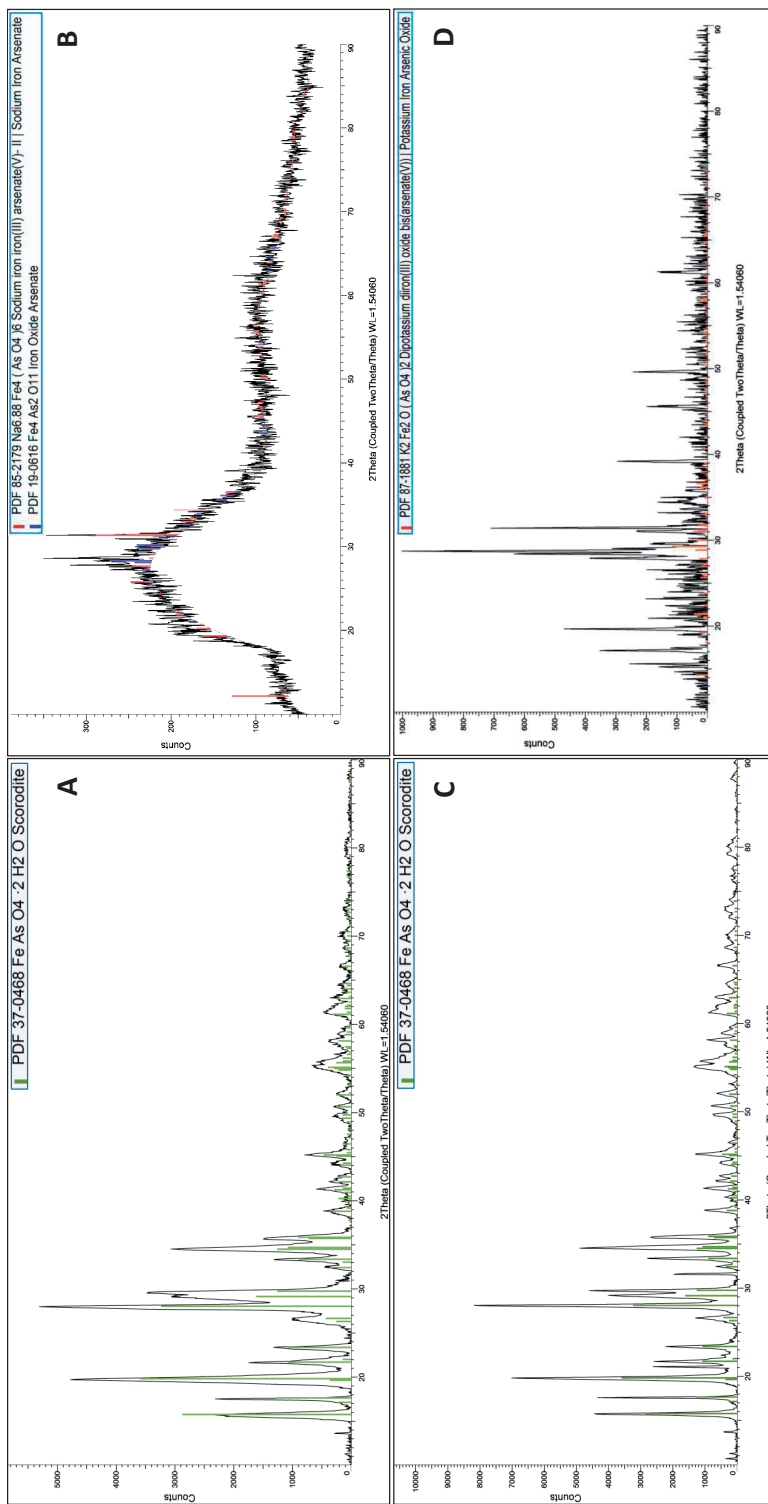


**Figure S2.** X-ray diffractogram of the crystalline and amorphous phases identified in the solids collected from batch operation at day 12 (stage I) (A and B) respectively and continuous operation of the airlift reactor at day 23 (stage II) (C and D).



**Figure S3.** Picture of the airlift reactor at day 85. Light green solution typical for scorodite precipitation systems.

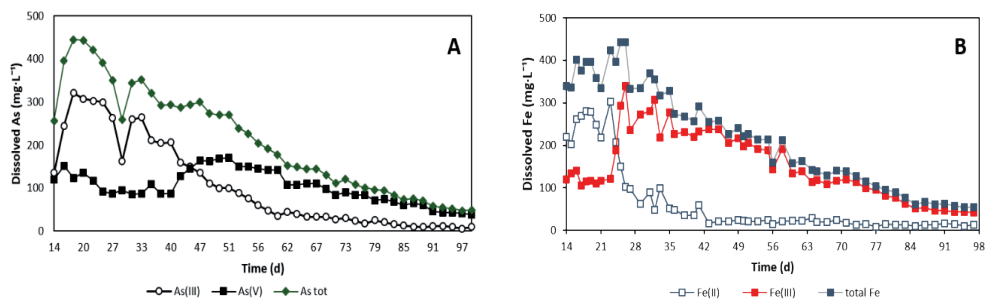


**Figure S4.** Dissolved arsenic and iron in the effluent solution.

## CHAPTER 4

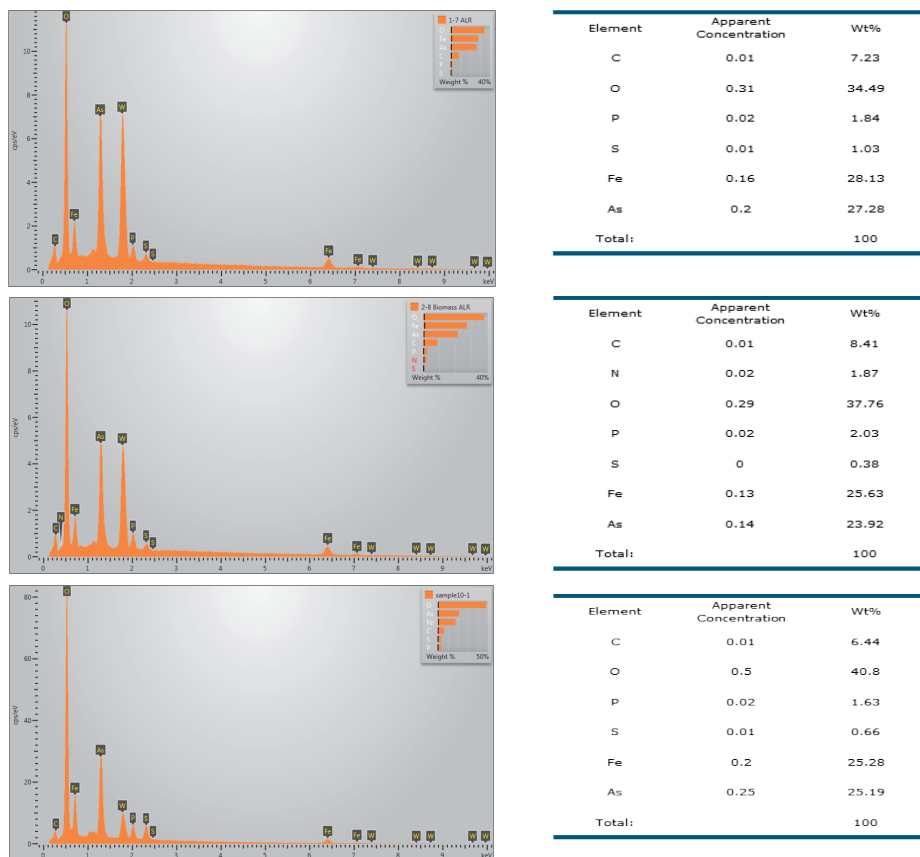


**Figure S5.** EDX analysis of bioscorodite collected from airlift reactor during continuous operation at day 25 (A), day 57 (B) and day 98 (C).

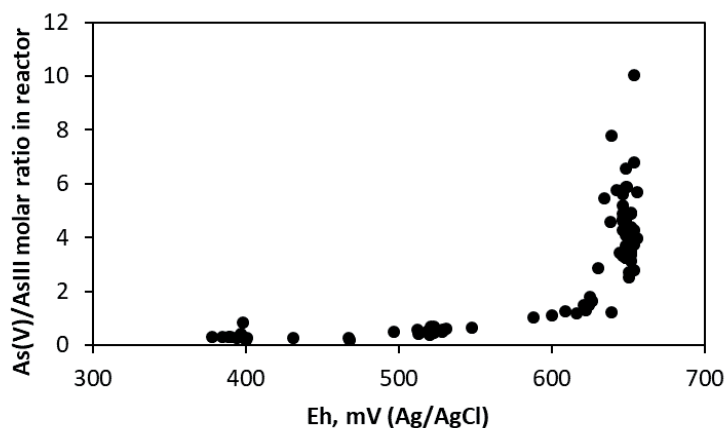


**Figure S6.** Molar ratio As(V):As(III) in the in continuous airlift reactor vs. Eh

## SCALE-UP OF THE BIOSCORODITE PROCESS IN CONTINUOUS AIRLIFT REACTOR

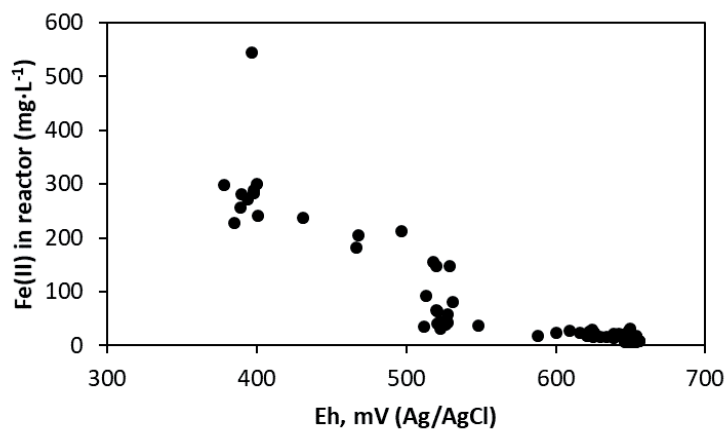


**Figure S7.** Fe(II) concentration in the continuous airlift reactor vs. Eh

**Table S1.** Development of Fe and As content of precipitates collected from the airlift reactor.

Time day	content As mg/g solid	content Fe mg/g solid	ratio Fe/As
16	228	279	1.65
25	282	247	1.17
31	274	244	1.20
43	302	290	1.29
75	268	227	1.14
98	263	226	1.15
scorodite, theoretical	325	241	1.00

## REFERENCES

1. Ding, W., H. Tong, D. Zhao, H. Zheng, C. Liu, J. Li, and F. Wu, *A novel removal strategy for copper and arsenic by photooxidation coupled with coprecipitation: Performance and mechanism*. Chemical Engineering Journal, 2020. **401**: p. 126102.
2. Vahidnia, A., G.B. van der Voet, and F.A. de Wolff, *Arsenic neurotoxicity — A review*. Human & Experimental Toxicology, 2007. **26**(10): p. 823-832.
3. Wang, A., K. Zhou, X. Zhang, D. Zhou, C. Peng, and W. Chen, *Arsenic removal from highly-acidic wastewater with high arsenic content by copper-chloride synergistic reduction*. Chemosphere, 2019: p. 124675.
4. Okibe, N., M. Koga, K. Sasaki, T. Hirajima, S. Heguri, and S. Asano, *Simultaneous oxidation and immobilization of arsenite from refinery waste water by thermoacidophilic iron-oxidizing archaeon, Acidianus brierleyi*. Minerals Engineering, 2013. **48**: p. 126-134.
5. Riveros, P., J. Dutrizac, and P. Spencer, *Arsenic disposal practices in the metallurgical industry*. Canadian Metallurgical Quarterly, 2001. **40**(4): p. 395-420.
6. Jia, Y. and G.P. Demopoulos, *Coprecipitation of arsenate with iron(III) in aqueous sulfate media: Effect of time, lime as base and co-ions on arsenic retention*. Water Research, 2008. **42**(3): p. 661-668.
7. Welham, N.J., K.A. Malatt, and S. Vukcevic, *The stability of iron phases presently used for disposal from metallurgical systems—A review*. Minerals Engineering, 2000. **13**(8): p. 911-931.
8. Mohan, D. and C.U. Pittman, *Arsenic removal from water/wastewater using adsorbents—A critical review*. Journal of Hazardous Materials, 2007. **142**(1): p. 1-53.
9. Robins, R.G., P.M. Dove, J.D. Rimstidt, D.K. Nordstrom, and G.A. Parks, *Solubility and stability of scorodite, FeAsO<sub>4</sub>·2H<sub>2</sub>O; discussions and replies*. American Mineralogist, 1987. **72**(7-8): p. 842-855.
10. Demopoulos, G.P., *On the preparation and stability of Scorodite*. R.G. Reddy, V. Ramachandran (Eds.), Arsenic Metallurgy, TMS, Warrendale, PA (2005), , 2005: p. 25-50.
11. Dutrizac, J. and J. Jambor, *The synthesis of crystalline scorodite, FeAsO<sub>4</sub>·2H<sub>2</sub>O*. Hydrometallurgy, 1988. **19**(3): p. 377-384.
12. González-Contreras, P., J. Weijma, and C.J.N. Buisman, *Continuous bioscorodite crystallization in CSTRs for arsenic removal and disposal*. Water Research, 2012. **46**(18): p. 5883-5892.
13. Gonzalez-Contreras, P., J. Weijma, R.v.d. Weijden, and C.J.N. Buisman, *Biogenic Scorodite Crystallization by Acidianus sulfidivorans for Arsenic Removal*. Environmental Science & Technology, 2010. **44**(2): p. 675-680.
14. Okibe, N., M. Koga, S. Morishita, M. Tanaka, S. Heguri, S. Asano, K. Sasaki, and T. Hirajima, *Microbial formation of crystalline scorodite for treatment of As (III)-bearing copper refinery process solution using Acidianus brierleyi*. Hydrometallurgy, 2014. **143**: p. 34-41.
15. Bissen, M. and F.H. Frimmel, *Arsenic — a Review. Part I: Occurrence, Toxicity, Speciation, Mobility*. Acta hydrochimica et hydrobiologica, 2003. **31**(1): p. 9-18.
16. Higashidani, N., T. Kaneta, N. Takeyasu, S. Motomizu, N. Okibe, and K. Sasaki, *Speciation of*

- arsenic in a thermoacidophilic iron-oxidizing archaeon, *Acidianus brierleyi*, and its culture medium by inductively coupled plasma–optical emission spectroscopy combined with flow injection pretreatment using an anion-exchange mini-column. *Talanta*, 2014. **122**: p. 240-245.
17. Escobar, B., E. Huenupi, I. Godoy, and J.V. Wiertz, *Arsenic precipitation in the bioleaching of enargite by Sulfolobus BC at 70 °C*. *Biotechnology Letters*, 2000. **22**(3): p. 205-209.
  18. Lindström, E.B., Å. Sandström, and J.-E. Sundkvist, *A sequential two-step process using moderately and extremely thermophilic cultures for biooxidation of refractory gold concentrates*. *Hydrometallurgy*, 2003. **71**(1): p. 21-30.
  19. Ding, J., R. Zhang, Y. Yu, D. Jin, C. Liang, Y. Yi, W. Zhu, and J. Xia, *A novel acidophilic, thermophilic iron and sulfur-oxidizing archaeon isolated from a hot spring of tengchong, yunnan, China*. *Brazilian journal of microbiology* : [publication of the Brazilian Society for Microbiology], 2011. **42**(2): p. 514-525.
  20. Tanaka, M. and N. Okibe, *Factors to Enable Crystallization of Environmentally Stable Bioscorodite from Dilute As(III)-Contaminated Waters*. *Minerals*, 2018. **8**(1): p. 23.
  21. Debekaussen, R., Droppert, D., Demopoulos, and G. P., *Ambient pressure hydrometallurgical conversion of arsenic trioxide to crystalline scorodite*. *CIM bulletin*, 2001. **94**: p. 116-122.
  22. Choi, Y., A.G. Gharelar, and N. Ahern, *Method for arsenic oxidation and removal from process and waste solutions*. 2014, Google Patents.
  23. Choi, Y., A. Ghahremaninezhad, and N. Ahern. *Process for activated carbon-assisted oxidation of arsenic species in process solutions and waste waters*. in *COM 2014-Conference of Metallurgists*. 2014.
  24. EPA, U.S., in *Field Applications of In Situ Remediation Technologies: Chemical Oxidation*. 1998, Washington D.C.: EPA.
  25. van Vliet, D.M., S. Palakawong Na Ayudthaya, S. Diop, L. Villanueva, A.J.M. Stams, and I. Sánchez-Andrea, *Anaerobic Degradation of Sulfated Polysaccharides by Two Novel Kiritimatiellales Strains Isolated From Black Sea Sediment*. *Frontiers in Microbiology*, 2019. **10**(253).
  26. Edgar, R.C., *MUSCLE: a multiple sequence alignment method with reduced time and space complexity*. *BMC Bioinformatics*, 2004. **5**(1): p. 113.
  27. Price, M.N., P.S. Dehal, and A.P. Arkin, *FastTree: Computing Large Minimum Evolution Trees with Profiles instead of a Distance Matrix*. *Molecular Biology and Evolution*, 2009. **26**(7): p. 1641-1650.
  28. Letunic, I. and P. Bork, *Interactive tree of life (iTOL) v3: an online tool for the display and annotation of phylogenetic and other trees*. *Nucleic Acids Research*, 2016. **44**(W1): p. W242-W245.
  29. Sievers, F., *Fast,scalable generation of high-quality protein multiple sequence alignments using Clustal Omega*. *Mol.Syst.Biol.*, 2011. **7**: p. 539.
  30. Shannon, P., A. Markiel, O. Ozier, N.S. Baliga, J.T. Wang, D. Ramage, N. Amin, B. Schwikowski, and T. Ideker, *Cytoscape: A Software Environment for Integrated Models of Biomolecular Interaction Networks*. *Genome Research*, 2003. **13**(11): p. 2498-2504.
  31. Fujita, T., R. Taguchi, M. Abumiya, M. Matsumoto, E. Shibata, and T. Nakamura, *Effect of pH on atmospheric scorodite synthesis by oxidation of ferrous ions: Physical properties and stability of the scorodite*. *Hydrometallurgy*, 2009. **96**(3): p. 189-198.
  32. Paktunc, D., J. Dutrizac, and V. Gertsman, *Synthesis and phase transformations involving*

## CHAPTER 4

- scorodite, ferric arsenate and arsenical ferrihydrite: Implications for arsenic mobility.* *Geochimica et Cosmochimica Acta*, 2008. **72**(11): p. 2649-2672.
33. Singhania, S., Q. Wang, D. Filippou, and G.P. Demopoulos, *Acidity, valency and third-ion effects on the precipitation of scorodite from mixed sulfate solutions under atmospheric-pressure conditions.* *Metallurgical and Materials Transactions B*, 2006. **37**(2): p. 189-197.
  34. Lakerveld, R., J.J.H. van Krochten, and H.J.M. Kramer, *An Air-Lift Crystallizer Can Suppress Secondary Nucleation at a Higher Supersaturation Compared to a Stirred Crystallizer.* *Crystal Growth & Design*, 2014. **14**(7): p. 3264-3275.
  35. Frijters, C.T., M. Silvius, J. Fischer, R. Haarhuis, and R. Mulder, *Full-scale applications for both COD and nutrient removal in a CIRCOX airlift reactor.* *Water Sci Technol*, 2007. **55**(8-9): p. 107-14.
  36. van Houten, B.H.G.W., K. Roest, V.A. Tzeneva, H. Dijkman, H. Smidt, and A.J.M. Stams, *Occurrence of methanogenesis during start-up of a full-scale synthesis gas-fed reactor treating sulfate and metal-rich wastewater.* *Water Research*, 2006. **40**(3): p. 553-560.
  37. Vega-Hernandez, S., J. Weijma, and C.J.N. Buisman, *Immobilization of arsenic as scorodite by a thermoacidophilic mixed culture via As(III)-catalyzed oxidation with activated carbon.* *Journal of Hazardous Materials*, 2019. **368**: p. 221-227.
  38. Jia, Y., L. Xu, X. Wang, and G.P. Demopoulos, *Infrared spectroscopic and X-ray diffraction characterization of the nature of adsorbed arsenate on ferrihydrite.* *Geochimica et Cosmochimica Acta*, 2007. **71**(7): p. 1643-1654.
  39. Qazi, S.J.S., A.R. Rennie, J.K. Cockcroft, and M. Vickers, *Use of wide-angle X-ray diffraction to measure shape and size of dispersed colloidal particles.* *Journal of Colloid and Interface Science*, 2009. **338**(1): p. 105-110.
  40. Mullin, J.W., *Crystallisation, 4th Edition* Organic Process Research & Development, ed. B. Heinemann. Vol. 6. 2001, Oxford, UK. : American Chemical Society. 600 pp.
  41. Gomez, M.A., Assaoudi, H., Becze, L., Cutler, J. N. and Demopoulos, G. P., *Vibrational spectroscopy study of hydrothermally produced scorodite (FeAsO<sub>4</sub>·2H<sub>2</sub>O), ferric arsenate sub-hydrate (FAsH; FeAsO<sub>4</sub>·0.75H<sub>2</sub>O) and basic ferric arsenate sulfate (BFAS; Fe[(AsO<sub>4</sub>)<sub>1-x</sub>(SO<sub>4</sub>)<sub>x</sub>(OH)<sub>x</sub>·wH<sub>2</sub>O).* *Journal of Raman Spectroscopy*, 2010. **41**((2)): p. p. 212-221.
  42. Gonzalez-Contreras, P., J. Weijma, and C.J.N. Buisman, *Bioscorodite Crystallization in an Airlift Reactor for Arsenic Removal.* *Crystal Growth & Design*, 2012. **12**(5): p. 2699-2706.
  43. Sun, Y., Q. Yao, X. Zhang, H. Yang, N. Li, Z. Zhang, and Z. Hao, *Insight into mineralizer modified and tailored scorodite crystal characteristics and leachability for arsenic-rich smelter wastewater stabilization.* *RSC Advances*, 2018. **8**(35): p. 19560-19569.
  44. Fujita, T., R. Taguchi, M. Abumiya, M. Matsumoto, E. Shibata, and T. Nakamura, *Novel atmospheric scorodite synthesis by oxidation of ferrous sulfate solution. Part II. Effect of temperature and air.* *Hydrometallurgy*, 2008. **90**(2): p. 85-91.
  45. Gonzalez Contreras, P.A., *Bioscorodite: biological crystallization of scorodite for arsenic removal.* 2012, Wageningen university: [S.l.s.n.].
  46. Caetano, M.L., V.S.T. Ciminelli, S.D.F. Rocha, M.C. Spitale, and C.L. Caldeira, *Batch and*

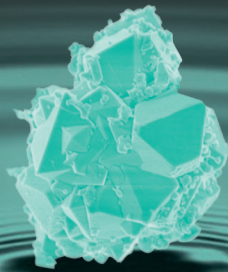
- continuous precipitation of scorodite from dilute industrial solutions*. Hydrometallurgy, 2009. **95**(1): p. 44-52.
47. Harvey, M.C., M.E. Schreiber, J.D. Rimstidt, and M.M. Griffith, *Scorodite Dissolution Kinetics: Implications for Arsenic Release*. Environmental Science & Technology, 2006. **40**(21): p. 6709-6714.
  48. Kish, A., J. Miot, C. Lombard, J.-M. Guigner, S. Bernard, S. Zirah, and F. Guyot, *Preservation of Archaeal Surface Layer Structure During Mineralization*. Scientific Reports, 2016. **6**(1): p. 26152.
  49. Zhang, R., T.R. Neu, V. Blanchard, M. Vera, and W. Sand, *Biofilm dynamics and EPS production of a thermoacidophilic bioleaching archaeon*. New Biotechnology, 2019. **51**: p. 21-30.
  50. Zhang, R., T.R. Neu, Y. Zhang, S. Bellenberg, U. Kuhlicke, Q. Li, W. Sand, and M. Vera, *Visualization and analysis of EPS glycoconjugates of the thermoacidophilic archaeon Sulfolobus metallicus*. Applied Microbiology and Biotechnology, 2015. **99**(17): p. 7343-7356.
  51. Liu, L.-Z., Z.-Y. Nie, Y. Yang, X. Pan, X. Xia, Y.-H. Zhou, J.-L. Xia, L.-J. Zhang, X.-J. Zhen, and H.-Y. Yang, *In situ characterization of change in superficial organic components of thermoacidophilic archaeon Acidianus manzaensis YN-25*. Research in Microbiology, 2018. **169**(10): p. 590-597.
  52. Orell, A., S. Schopf, L. Randau, and M. Vera, *Biofilm Lifestyle of Thermophile and Acidophile Archaea*, in *Biocommunication of Archaea*, G. Witzany, Editor. 2017, Springer International Publishing: Cham. p. 133-146.
  53. Hegler, F., C. Schmidt, H. Schwarz, and A. Kappler, *Does a low-pH microenvironment around phototrophic FeII-oxidizing bacteria prevent cell encrustation by FeIII minerals?* FEMS Microbiology Ecology, 2010. **74**(3): p. 592-600.
  54. Dopson, M. and E.B. Lindstrom, *Analysis of community composition during moderately thermophilic bioleaching of pyrite, arsenical pyrite, and chalcopyrite*. Microbial Ecology, 2004. **48**(1): p. 19-28.
  55. Rawlings, D.E. and D.B. Johnson, *The microbiology of biomining: development and optimization of mineral-oxidizing microbial consortia*. Microbiology (Reading, England), 2007. **153**(Pt 2): p. 315-324.
  56. Johnson, D.B., *Biodiversity and interactions of acidophiles: Key to understanding and optimizing microbial processing of ores and concentrates*. Transactions of Nonferrous Metals Society of China, 2008. **18**(6): p. 1367-1373.
  57. Okibe, N., S. Morishita, M. Tanaka, T. Hirajima, and K. Sasaki. *Effect of Cu (II) on Bio-Scorodite Crystallization Using Acidianus brierleyi*. in *Advanced Materials Research*. 2015. Trans Tech Publ.
  58. Gonzalez-Contreras, P., J. Weijma, and C.J. Buisman, *Kinetics of ferrous iron oxidation by batch and continuous cultures of thermoacidophilic Archaea at extremely low pH of 1.1–1.3*. Applied microbiology and biotechnology, 2012. **93**(3): p. 1295-1303.
  59. Zammit, C.M., N. Cook, J. Brugger, C.L. Ciobanu, and F. Reith, *The future of biotechnology for gold exploration and processing*. Minerals Engineering, 2012. **32**: p. 45-53.
  60. Battaglia-Brunet, F., M.C. Dictor, F. Garrido, C. Crouzet, D. Morin, K. Dekeyser, M. Clarens, and P. Baranger, *An arsenic(III)-oxidizing bacterial population: selection, characterization, and performance in reactors*. Journal of applied microbiology, 2002. **93**(4): p. 656-667.
  61. DeFlaun, M.F., J.K. Fredrickson, H. Dong, S.M. Pfiffner, T.C. Onstott, D.L. Balkwill, S.H. Streger, E. Stackebrandt, S. Knoessen, and E. van Heerden, *Isolation and characterization of*

## CHAPTER 4

- a Geobacillus thermoleovorans strain from an ultra-deep South African gold mine*. Systematic and Applied Microbiology, 2007. **30**(2): p. 152-164.
62. Menzel, P., S.R. Gudbergdóttir, A.G. Rike, L. Lin, Q. Zhang, P. Contursi, M. Moracci, J.K. Kristjansson, B. Bolduc, S. Gavrilov, N. Ravin, A. Mardanov, E. Bonch-Osmolovskaya, M. Young, A. Krogh, and X. Peng, *Comparative Metagenomics of Eight Geographically Remote Terrestrial Hot Springs*. Microbial Ecology, 2015. **70**(2): p. 411-424.
63. Liu, J., Q. Li, W. Sand, and R. Zhang, *Influence of Sulfobacillus thermosulfidooxidans on Initial Attachment and Pyrite Leaching by Thermoacidophilic Archaeon Acidianus sp. DSM 29099*. Minerals, 2016. **6**(3): p. 76.
64. Maulani, N., Q. Li, W. Sand, M. Vera, and Z. Ruiyong, *Interactions of the extremely acidophilic archaeon Ferroplasma acidiphilum with acidophilic bacteria during pyrite bioleaching*. Applied Environmental Biotechnology, 2016. **1**(2): p. 1-13.



## CHAPTER 5



# **EXPLORING ALTERNATIVE FE SOURCES FOR THE SCORODITE BIOMINERALIZATION IN THE GAC- CATALYZED AS(III)-OXIDATION.**

Authors: Silvia Vega-Hernandez, Jan weijma, Cees J.N. buisman

Manuscript submitted for publication

### ABSTRACT

Pyrite ( $\text{FeS}_2$ ) is one of the most common minerals found in hydrometallurgical streams, making it a potential alternative iron source in the biological scorodite formation ( $\text{FeAsO}_4 \cdot 2\text{H}_2\text{O}$ ) towards arsenic fixation from these streams. Here we present the results of the biologically-mediated oxidation of As(III) species, catalyzed by granular activated carbon, for the concomitant precipitation of scorodite targeting pyrite as iron source. We carried out this experiment batch bottles containing  $4 \text{ gL}^{-1}$  of granular activated carbon,  $5 \pm 0.5 \text{ gL}^{-1}$  of pyrite, and a mixed microbial culture previously enriched at pH of 1.3 and  $70 \text{ }^\circ\text{C}$  (same conditions here tested). Complete pyrite leaching was reached after nine days enabling the loading of  $2.25 \text{ gL}^{-1}$  As (III) in the biotic test as well the complete oxidation and removal. In contrast to chemical control where oxidation was at least 3.5 lower. Solids characterization confirmed the formation of scorodite precipitates ranging from  $50\text{--}90 \text{ }\mu\text{m}$  in size, with a Fe / As ratio up to 1.08, and a water content close to the theoretical scorodite value (2 moles). TCLP tests of these particles of 20 hours and during the long-term 208 days resulted in arsenic leached of  $0.52 \text{ mg.L}^{-1}$  As and  $1.8 \pm 0.22 \text{ mgL}^{-1}$  respectively.

A thin layer of high carbon content coating the crystals was observed by SEM-EDX, suggesting the initial nucleation and further crystal development within the biofilm compartment. The supply of pyrite also resulted in higher cell density. Thus, according to the obtained results, the supply of pyrite which is cheaper than chemical Fe reagents could be used as an alternative iron in the biological scorodite formation.

**Keywords:** Arsenic oxidation; Pyrite leaching; Biomineralization; Scorodite

## 1. INTRODUCTION

Mining has played an important role in the economic and social development of many countries but in turn, has resulted also in environmental challenges. Owing to the high demand for essential metals like copper and the depletion of high-grade minerals, the exploitation is currently directed to lower grade ores. However, these are considerably more complex to process, more energy intensive [1] and also have resulted in increased volumes of metallurgical waste [2]. These residues constitute a potential threat in the long term due to the increasing concentrations of impurities like penalty elements such as arsenic (As) [3, 4].

The current goal of hydrometallurgical processes is oriented towards reducing socio-economic and environmental footprint associated with mine waste. In this context, a proper waste management and reduction of environmental liabilities integrated to the recovery of metals is required. For the immobilisation of As into stable waste products for final disposal, it is still a challenge to keep the potential As leaching from these residues below permitted levels [5]. Therefore, the removal of arsenic from hydrometallurgical process wastewaters remains a prominent research topic [6].

Technological approaches to remove arsenic commonly involve co-precipitation, adsorption, or coagulation [7-14]. Several studies have suggested that crystalline ferric arsenate dihydrate ( $\text{FeAsO}_4 \cdot 2\text{H}_2\text{O}$ , scorodite) is the ideal medium for arsenic fixation due to the high stability, low Fe/As, which results in high arsenic removal and less waste [15-18].

The applied methods for scorodite precipitation depend on the type of solution; on one hand chemical treatment, developed at high temperature ( $<95^\circ\text{C}$ ) is usually used to concentrated As solutions (up to  $10 \text{ g}\cdot\text{L}^{-1}$ ) [19-24]. However, under milder temperature conditions, thermoacidophilic Fe(II)-oxidizing microbes mediate the oxidation and immobilization of arsenic in more dilute streams [25-28].

Most of the methods for scorodite precipitation are applicable for As in the pentavalent form, As(V). Nonetheless, since the trivalent form, As(III) is more prevalent in acid bleed streams, a preliminary oxidation step is required [29, 30]. At these conditions, the oxidation of As(III) by air or oxygen is inefficient [31, 32] and biological As(III) oxidation at  $70^\circ\text{C}$  is scarcely reported [28, 33]. In contrast, higher rates are achieved by advance oxidation process with ozone or hydrogen peroxide however, its application is expensive [29, 32].

## CHAPTER 5

Oxidation of As(III) is also possible by the application of activated carbon as catalyst in acidic solutions. The method works effectively with up to 99% oxidation of As(III) using only oxygen from air as reagent [34]. Oxidation is likely due to the generation of  $\text{H}_2\text{O}_2$  once the carbon catalyst makes contact in the oxygenated acid solution [35], which was also detected by semi-quantitative measurement using reagent strips (Quantofix) at higher concentrations of GAC ( $20 \text{ g}\cdot\text{L}^{-1}$ ) (Chapter 3). Meanwhile, also other methods for As(III) oxidation are in development in other laboratories [36].

The catalyzed oxidation of As(III) with activated carbon has been integrated into the removal of arsenic in biological precipitation systems containing Fe(II) [37] and to the chemical treatment of arsenic-containing minerals in Fe(III) solutions [34, 38]. The bioscorodite concept requires the addition of Fe(II) from a chemical source, for which in our previous work we used ferrous sulfate reagent ( $\text{FeSO}_4\cdot 7\text{H}_2\text{O}$ ) as the iron source. However, this substantially adds cost to the process, with current market prices of US\$25 per kmol Fe(II).

Hereby, we aim to use pyrite mineral as the main iron source for the development of the thermoacidophilic mixed culture in the biomineralization of scorodite. Use of pyrite instead of the reagent  $\text{FeSO}_4$  would reduce the cost for Fe chemical by about half. Pyrite was used as growth substrate for a mixed thermoacidophilic iron oxidizing culture in the presence of As(III) and GAC, aiming to produce scorodite.

## 2. MATERIALS AND METHODS

### 2.1. CULTURE CONDITIONS AND INOCULUM

The defined growth medium used in the experiments contained  $3.0 \text{ mM } (\text{NH}_4)_2\text{SO}_4$ ,  $2 \text{ mM } \text{MgSO}_4\cdot 7\text{H}_2\text{O}$  and  $1.5 \text{ mM } \text{KH}_2\text{PO}_4$  and  $1.3 \text{ mM } \text{KCl}$ , as described by Norris (1985) [39]. Micronutrients and  $0.2\% \text{ w/v}$  yeast extract and were supplemented according to DSM88 growth medium for *Sulfolobales*. The medium was prepared without addition of Fe(II) or As(III) and the solution pH was adjusted to 1.3 with  $50 \text{ mM } \text{H}_2\text{SO}_4$ . At the start of experiments, reagent-grade sodium arsenite ( $\text{NaAsO}_2$ ,  $0.05 \text{ M}$ , Fluka Sigma-Aldrich, USA) was added to the basal medium. All chemicals used were analytical-reagent grade.

The thermoacidophilic iron oxidizing mixed culture used in this study was previously adapted to As(III)-containing solutions and enriched in a continuous reactor during 100 days for the removal of arsenic by precipitation as scorodite (Chapter 4). Furthermore,

the analysis of the microbial community in the bioreactor revealed the dominance of archaeal *Acidianus* species.

## 2.1. PYRITE MINERAL

Pyrite ( $\text{FeS}_2$ ) was used as sole Fe source in the experiments. The ore concentrate was kindly provided by Prof. Sandström of Luleå University (Sweden) and obtained from the Boliden Mineral AB from Aitik plant, Sweden. Elemental composition of the mineral is shown in Table 1, adapted from Gahan, Sundkvist [40]. The concentrate sample was pre-washed with sulphuric acid (pH 1) in order to remove acid consuming gangue minerals prior to its use in the experiments.

**Table 1.** Elemental composition of pyrite concentrate used in this study, adapted from Gahan, Sundkvist [40].

Fe (%)	S (%)	Si (%)	Al (%)	K (%)	Ca (%)	Mg (%)	Mn (%)	Ba (mg/kg)	Cu (mg/kg)	As (mg/kg)	Cr (mg/kg)	Zn (mg/kg)
36.4	39.6	7.4	2.1	1.3	0.8	0.3	0.1	4.06	446	36	26	76

## 2.2. GAC

Granular activated carbon NORIT GAC 830W was used as catalyst in this study. The characteristics of the used GAC were previously reported in Chapter 2. Before its addition to the experimental flasks, the fresh GAC was washed with sulphuric acid (1 M) followed by rinsing with deionized water in order to remove impurities. The samples of GAC withdrawn from the continuous bioreactor (Chapter 4) were washed with the acid culture medium.

## 2.3. EXPERIMENTAL PROCEDURE

A series of batch tests were performed in order to assess the oxidation of As(III) and Fe(II) from pyrite used as the main iron source for microbial growth in addition to the biological formation of scorodite.

The flasks were initially inoculated with As(III) ( $0.6 \text{ gL}^{-1}$ ), GAC ( $4 \text{ gL}^{-1}$ ), and pyrite ( $5 \pm 0.5 \text{ gL}^{-1}$ ). Biotic experiments were conducted in triplicate and were inoculated with 10% v/v of the enriched mixed culture at a cell density of approximately  $5.4 \cdot 10^7$

## CHAPTER 5

cell·ml<sup>-1</sup> and 4 g·L<sup>-1</sup> of GAC collected from the continuous bioreactor used previously for scorodite precipitation (Chapter 4). Abiotic controls were performed in duplicate at similar conditions but contained 10% v/v of acid sterile water and fresh GAC. An additional biotic control experiment (positive control) was prepared only with the enriched inoculum and pyrite in order to determine the extent of biological Fe(II) oxidation from pyrite in absence of As(III) and the catalyst.

The batch experiments were carried out in 250 ml serum flasks containing 125 ml working volume. Bottles were closed with a butyl rubber stopper, crimped aluminum seal, and placed in a thermostat shaker incubator at 150 rpm and 70 °C. The gas in the headspace was replenished with air supplemented with 1% CO<sub>2</sub> after each As(III) spike.

Liquid samples were taken regularly for analysis of pH, Eh, Fe(II), Fe(III), As(III) and As(V). These samples were previously filtered through a 0.2 μm polyethersulfone (PES) syringe filter (Whatman). Furthermore, at the end of the experiment, the precipitates from the bottles were collected by centrifugation, washed with a solution containing 50 mM sulphuric acid, followed by washing with deionized water and dried in a vacuum oven at 60°C temperature before solids characterization.

### 2.4. ANALYTICAL METHODS

Aqueous samples for analysis of dissolved Fe and As species were filtered over a 0.45 μm cellulose acetate membrane filter. The pH and redox potential (ORP) of the samples were measured with glass electrodes QP181X and QR480X-Pt, respectively (Prosense, Netherlands). Fe(II) and Fe(III) concentrations were measured using Dr. Lange Cuvette experiment LCK 320 and a Xion 500 spectrophotometer (Hach-Lange, Germany).

Dissolved As(III) and As(V) concentrations were measured with an HPLC connected to a UV photospectrometer. The HPLC was an ultimate VWD 3000 RS (Dionex, Netherlands) equipped with an ion exclusion column using sulfuric acid 10 mM as the mobile phase, according to Gonzalez-Contreras, Gerrits-Benneheij [41].

### 2.5. PHYSICOCHEMICAL SOLID CHARACTERIZATION

The methods employed for the physicochemical characterization of the generated precipitates included XRD, FTIR, TGA and SEM. Furthermore, the analyses were carried out as described previously (Chapter 3 and 4)

Additionally, the quantitative estimation of major elements on the precipitates was performed by energy dispersive X-ray fluorescence (ED-XRF) using an Epsilon 4 Spectrometer manufactured by Malvern Panalytical.

## 2.6. TOXICITY CHARACTERISTIC LEACHING PROCEDURE

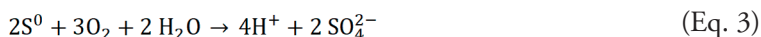
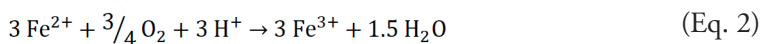
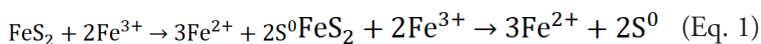
The Leaching of As from the produced solids was assessed following the standard Toxicity Characteristic Leaching Procedure (TCLP) of USEPA [42]. The bottles containing acetate buffer at pH 4.95 as extraction fluid and the scorodite precipitates (20%w/w), were maintained in a shaker at 20°C with a stirring speed of 100 rpm during the test. The concentration of arsenic was measured on the filtered liquid after 20 hours according to the method. Furthermore, the procedure was repeated in a long-term experiment during 208 days as well as the renewal of the extraction solvent after each sampling.

All the results are shown as the mean of the experimental replicates and the error bars show the mean ( $\pm$ ) standard deviation.

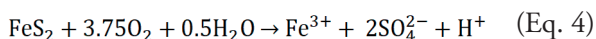
## 3. RESULTS AND DISCUSSION

### 3.1. PYRITE OXIDATION

Pyrite oxidation involves a series of chemical reactions aided by lixivants such as Fe(III) or  $H_2O_2$  and is mediated by microbiological activity [43, 44] according to the following equations [45, 46]:



Overall, pyrite oxidation consumes 3.75 mol  $O_2$  per mol  $FeS_2$



Pyrite oxidation in biotic and abiotic experiments with GAC was evaluated, through

the estimation of total Fe released from pyrite (Figure 1), considering the dissolved Fe(II) and Fe(III) in solution, and the Fe(III) precipitated as scorodite. The latter was calculated from the precipitated As, assuming a molar ratio Fe/As in the precipitate of 1, as in mineral scorodite. It is worthy to note that indeed, scorodite was the only solid phase in the residue of biotic experiment as detected in the x-ray powder diffractogram as shown in (Figure S4), The estimated Fe leached from pyrite increased linearly until day 9, after which it stabilized around 1600-1900 mg·L<sup>-1</sup> from day 9-17. This range is fairly close to the added amount of Fe (about 1.97 g·L<sup>-1</sup>) as pyrite (36.4% Fe of 5.4 g·L<sup>-1</sup> pyrite, Table 1). Thus, it appears that the mixed culture promoted the complete leaching of pyrite already on day 9, at a rate, which was approximately 3.5 times higher than in the control without the culture.

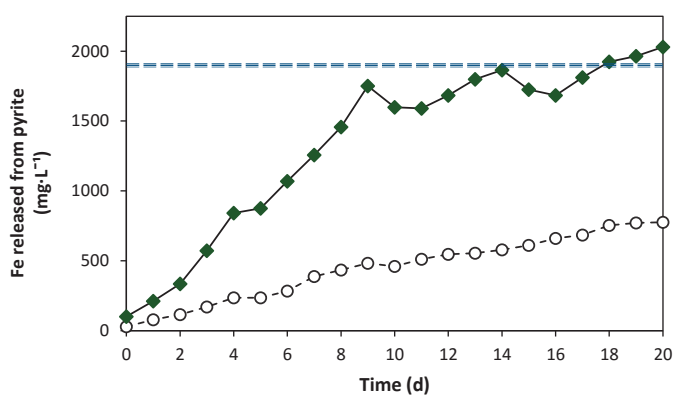


**Figure 1.** Estimation of the total Fe concentration released during the leaching of 5 g·L<sup>-1</sup> pyrite in the catalyzed As(III) oxidation with 4 g·L<sup>-1</sup> GAC at 70°C with the thermophilic mixed culture (solid lines) and abiotic control (dashed lines). The horizontal line on the graph is used to indicate the baseline concentration of Fe in the supplemented pyrite.

Ferric iron is one of the main oxidants for pyrite dissolution [47, 48]. Being also an important source for scorodite precipitation, Fe(III) ions derived from the oxidation processes ought to increase in solution. In all the tested conditions the dissolved iron concentration was measured as a result of the pyrite oxidation (Figure 2), however, the initial concentration of Fe(III) measured at the start of the biotic tests (likely from the biological sample), suggested that mineral dissolution could be thereby initiated according reaction 3.3. The complete leaching of pyrite in the biotic experiment on day 9 can explain the drop of the Fe(II) concentration from that day onwards (Figure 2A), as it implies that only Fe(II) oxidation took place, while Fe(II) was not further generated through pyrite leaching. The Fe(III) concentration fluctuated between approximately 200 and 400 mg·L<sup>-1</sup> which can be explained by Fe(III) generation through Fe(II)

oxidation on one hand, and Fe(III) removal through scorodite precipitation on the other hand. In biotic controls without As(III) and catalyst, high amount of Fe(III) and total Fe at the end of the experiment were the extent of dissolution of pyrite (Figure 3). Despite That Fe(II) in solution followed an increasing linear trend, suggesting the constant leaching in abiotic test, the kinetic was slow; furthermore, the poor concentration of dissolved Fe(III) in solution, which fluctuated with negligible increase and depletion throughout the experiment resulted in the low redox potential ( $\leq 410$  mV) (Figure 2A and B respectively). Hence, these observations suggested that the indirect dissolution of the mineral [49] by Fe(III) ions might be the main mechanism in abiotic test, taking also into account that the low arsenic removal at this condition was due to deposition on the GAC surface.

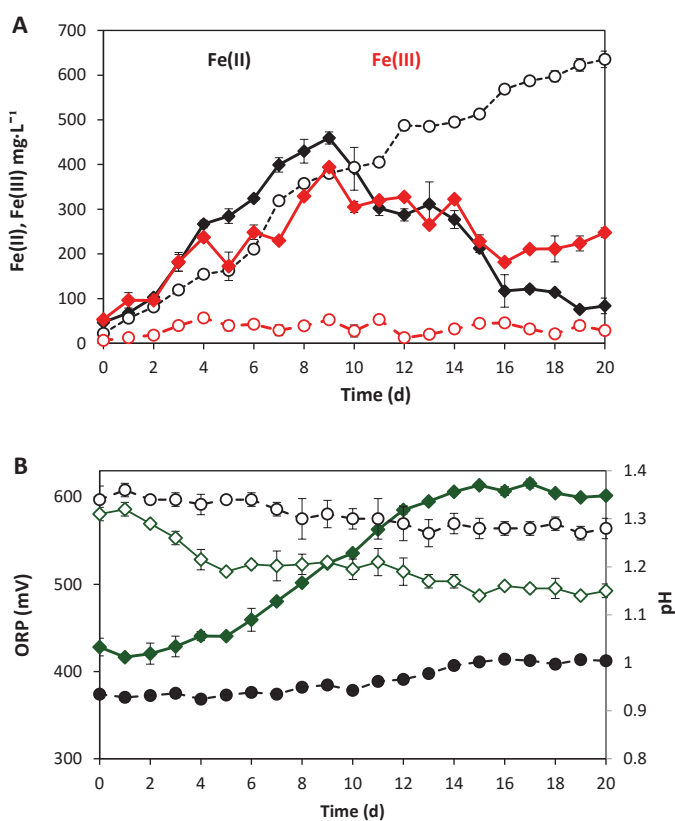
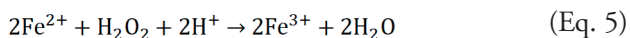


**Figure 2.** Dissolved iron species (A) and redox potential (right axis) and pH (left axis) (B) during the oxidation/leaching of 5 gL<sup>-1</sup> pyrite in the catalyzed As(III) oxidation with 4 gL<sup>-1</sup> GAC at 70°C with the thermophilic mixed culture (solid lines) and abiotic control (dashed lines).

The assisted leaching of sulfide minerals by activated carbon is an additional application

reporting the significant influence of the catalyst under acidic conditions [50-52]. The mechanism founded on the electrical surface conductivity of activated carbon that favors the galvanic interaction with the mineral, which acts as anode in the acid electrolyte. Previous studies on the treatment of copper sulfide minerals showed that the performance of activated carbon in the leaching kinetics is enhanced in chemical in excess of Fe(III) as the initial solution lixiviant [38, 50, 53, 54] but also in bioleaching systems [55-57]. Additionally, more recent studies on the assisted leaching of pyrite by carbon catalysts in Fe(III) solutions [58, 59] not only support the previous finding but also provided insight about the significant impact of carbon-based catalyst as a sulfur sink in the process. Furthermore, the above-mentioned studies showed the pronounced effect of temperature in the dissolution kinetics and suggested that Fe(III) regeneration might be also aided by the catalyst according to equation (Eq. 5) [60]. Our previous observations (Chapter 2 and 3) have also demonstrated the influence of carbon in the chemical oxidation of Fe(II). Nevertheless, the conversion proceeded at a lower rate, depending on the concentration of GAC in solution.



In any case, the abiotic leaching was not comparable to bio-oxidation experiments indicating the important contribution of biological Fe(III) regeneration under these acidic conditions where the chemical oxidation of Fe(III) is negligible [61]. One of the main benefits of activated carbon application in the mineral leaching at high Fe(III) concentration, is the formation of elemental sulfur rather than sulfate [58], which is likely the result of surface complexes promoting the adsorption of the molecule [38, 58, 59]. This is important in operational terms because a proper control of acidity can avoid or reduce the neutralization step in the downstream process. Although the impact of the carbon catalyst on the yield of sulfur species was not addressed in this study, the analysis of the mineral phases and elemental composition of the residue by XRD (Figure S1) and XRF (Table 2) suggested that sulfate rather than sulfur must have formed during the oxidative reactions.

The solution of biotic experiments turned to a dark green suspension after day 5, which became more turbid at the end of the experiments (Figure 3B). These differed from the abiotic experiment, that remained clear during the experiment (Figure 3D) and from the positive control without GAC and As(III), which resembled in color a ferric sulfate aqueous solution (Figure 3C). The solids collected at the end of the biotic tests with As(III), pyrite, and GAC had the characteristic green color of scorodite mineral and consisted of flakes and powder that could easily be separated from the granules; furthermore, pyrite remnants were not observed in the collected samples.

## PYRITE AS NATURAL IRON SOURCE FOR THE BIOSCORODITE CRYSTALLIZATION

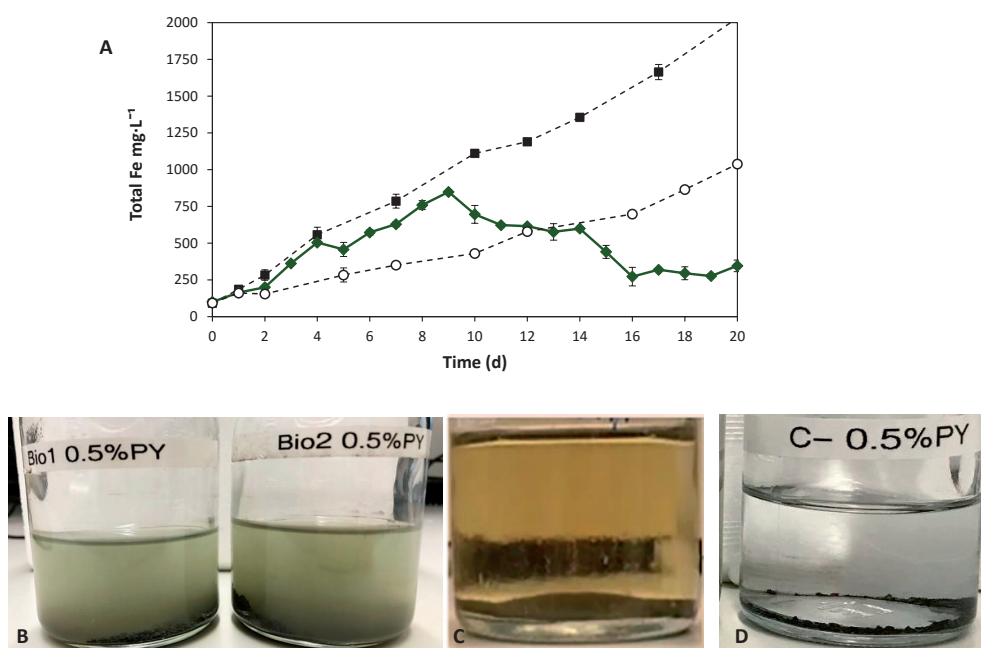


**Figure 3.** Total dissolved Fe concentration (A), batch bottles of biotic and abiotic experiments during the oxidation of 5 g L<sup>-1</sup> pyrite and the catalyzed As(III) oxidation with 4 g L<sup>-1</sup> GAC (B and D respectively) and the biotic control with 5 g L<sup>-1</sup> pyrite in absence of GAC and As(III) (C) at day 20. In (A), total Fe: ○ abiotic, ◆ biotic, tests with As(III), pyrite and GAC; ■ biotic control only with pyrite

Taking into account the total arsenic removal (2.25 g L<sup>-1</sup> As) (Figure 4), digestion of the precipitates and granules and the final dissolved concentrations of iron (Figure 3A), the abovementioned estimation implied that least 99% of the Fe(II) from pyrite was oxidized in biotic experiments. Therefore, the absence of pyrite and additional minerals phases besides scorodite from the solid characterization analysis indicated that likely all the removed Fe(III) was used in the crystallization. In contrast, the absence of precipitates in abiotic tests and the relatively constant concentration of dissolved arsenic (Figure 4) suggested, on one hand, that part of the generated Fe(III) was mainly used in pyrite leaching which accounted for 28% according to the dissolved Fe(II). Whereas, on the other hand, an additional fraction might have precipitated or adsorbed on the GAC surface accordingly the measured Fe form granule digestion.

### 3.2. GAC-CATALYZED ARSENITE OXIDATION AND ARSENIC PRECIPITATION IN THE PRESENCE OF PYRITE

In the treatments with GAC, pyrite, and the microbial culture, arsenite ( $600 \text{ mg}\cdot\text{L}^{-1} \text{ As(III)}$ ) was oxidized to below the analytical detection limit ( $0.5 \text{ mg}\cdot\text{L}^{-1} \text{ As}$ ) within 4 days (Figure 4A). Furthermore, after spiking about  $550 \text{ mg}\cdot\text{L}^{-1} \text{ As(III)}$  on days 5, 10, and 15, the complete arsenic conversion took place during the same period. As(III) oxidation followed pseudo-zero-order kinetics after the 2<sup>nd</sup>, 3<sup>rd</sup> and, 4<sup>th</sup> spike (Figure 4A); thus, As(III) concentration linearly decreased with time at a rate of  $140\text{-}160 \text{ mg}\cdot\text{L}^{-1} \cdot \text{d}^{-1}$ , corresponding to an overall specific oxidation rate of  $35\text{-}40 \text{ mgAs(III)}\cdot\text{gGAC}^{-1} \cdot \text{day}^{-1}$ . Comparable rates were determined in batch experiments with the same GAC concentration during the initial 0-2 days (Chapter 3). Thereby, suggesting that the presence of carbon initiated the As(III)-oxidation reaction; nonetheless, it might also be influenced by pyrite which, has been further reported as an As(III)-catalyst [62, 63]. Furthermore, it is also of significance noting the mechanical strength of GAC, which supported the oxidative reactions in the current biotic experiments even 100 days post-reaction in the continuous airlift reactor (Chapter 4).

In the chemical experiments, As(III) oxidation followed a similar rate as compared to biotic experiments; however, it deviated and slowed down after 24 hours, reaching the full oxidation on day 15 rather than 4 days, as observed in the latter (Figure 4A). These results contrasted with the previous reaction kinetics, determined at similar experimental conditions (Chapter 3), nonetheless, ferrous sulfate instead of pyrite as the iron source to the media. In the process GAC is used as catalyst for the dissolution of pyrite, as well as for As(III), and Fe(II) oxidation. In the same way, pyrite has been also pointed as catalyst for As(III) oxidation. Previous studies on the chemically assisting-leaching as well as pyrite-catalyzed As(III) oxidation have shown the significant effect of higher temperature ( $90^\circ\text{C}$ ), and dissolved iron species (especially Fe(III)) on the performance of carbon catalysts [60, 64]. Thus, being the latter a crucial element to initiate both reactions, its deficiency in solution suggested that it was a rate-limiting factor in abiotic reactions. Furthermore, the differed Fe(III) concentrations between the biotic and abiotic experiments ( $<100 \text{ mg}\cdot\text{L}^{-1}$ ), indicated that pyrite oxidation could have taken place through the microbial regeneration of Fe(III), allowing the simultaneous catalytic oxidation of As(III). While, in abiotic conditions, the oxidation capacity of GAC ( $\text{H}_2\text{O}_2$ ) seemed to be mainly directed to assist pyrite oxidation.

The total arsenic concentration in abiotic tests remained above  $400 \text{ mg}\cdot\text{L}^{-1} \text{ As}$  (Figure 5), with about  $170 \text{ mg}\cdot\text{L}^{-1} \text{ As}$  depleted at the end of the experiment (day 20). However, the absence of other solids phase in the final solid residue from the clear solution besides

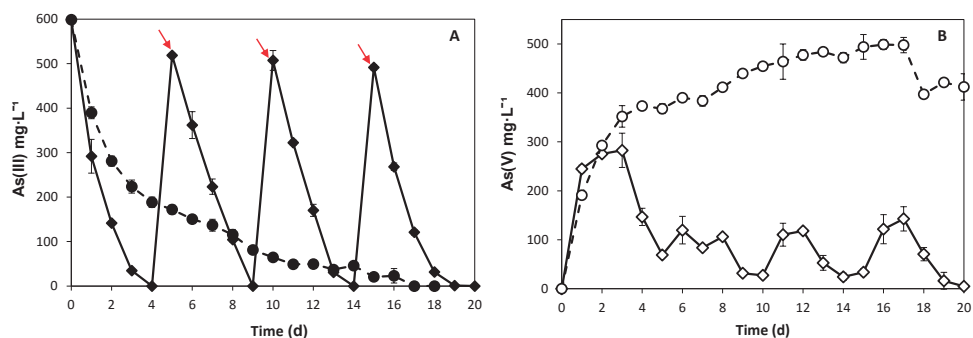


**Figure 4.** Dissolved As species during the As(III) oxidation catalyzed by 4 g L<sup>-1</sup> GAC in addition of 5 g L<sup>-1</sup> pyrite in biotic and abiotic experiments (solid and dashed line respectively).

the GAC suggested that arsenic removal might have occurred through precipitation on the bottle walls and the GAC surface, albeit visible solids were not detected either. In contrast, approximately 98% (2.21 g L<sup>-1</sup> As) of the oxidized As(III), successively spiked to the biotic tests was removed from solution in 20 days (Figure 4 and 5). The obtained results in abiotic experiments agreed with previous observations, irrespective of the supplied iron source, and the solution saturation (Chapter 2 and 3). As(V) did not precipitate in the abiotic tests although the concentration was higher after day 4 (Figure 4B), as well as the Fe(III) concentrations and the pH fluctuation (1.29-1.36) (Figure 2) that in the abiotic experiment. Thus, despite the crucial role of the supersaturation in the solid phase transition, at times may not be enough to initiate the crystallization, thereby suggesting in line with previous results, that arsenic precipitation was microbially mediated using pyrite as Fe source. In this indirect process, it is presumed that scorodite is biologically induced through the rate of Fe(II) bio-oxidation and the excretion of extracellular organic substances, which generate the appropriate micro-environment for complexation of Fe(III) and As(V), thus, leading to the formation of first scorodite precursors. The development of total dissolved arsenic species from solution is shown in more detail in Figure 5. Arsenic was readily precipitated from the start of the biotic experiment, with 47% of the arsenic removed in 3 days.

Furthermore, arsenic precipitation was continuous in the remainder of the experiment, with concentrations of As(V) remaining below 150 mg L<sup>-1</sup>. After the final spike on day 15, the concentration of total dissolved As dropped to 5 mg L<sup>-1</sup> on day 20 with an average Fe(III) concentration of 330 mg L<sup>-1</sup>.

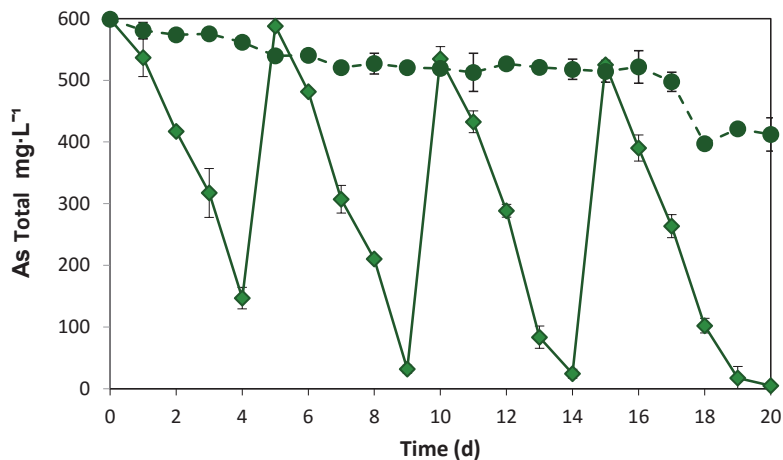


**Figure 5.** Removal of dissolved total arsenic (sum of As(III) and As(V) in biotic and biotic experiments (solid and dashed line respectively) with 4 gL<sup>-1</sup> GAC and 5 gL<sup>-1</sup> pyrite.

### 3.3. CHARACTERIZATION OF THE BIOLOGICAL SCORODITE PRECIPITATES

The solids collected at the end of the biotic experiment were identified as scorodite by X-ray diffraction. The chemical composition and concentration (% dry weight) of the obtained solid residue by X-ray fluorescence (Table 2) confirmed that scorodite was the predominant phase of the sample while other components such as ferric oxide, phosphate and silica oxide were only present in trace amounts.

**Table 2.** Chemical analysis of minerals present in the biotic precipitates by XRF

Chemical composition	Weight (%)
SiO <sub>2</sub>	2.75
P <sub>2</sub> O <sub>5</sub>	3.29
SO <sub>3</sub>	3.04
K <sub>2</sub> O	0.17
CaO	0.03
TiO <sub>2</sub>	0.05
Fe <sub>2</sub> O <sub>3</sub>	2.04
FeAsO <sub>4</sub> ·2H <sub>2</sub> O	88.61
BaO	0.02

The residues from biotic experiments observed by SEM (Figure 6 and 7) consisted predominantly of crystals with an overall average size between 50–90 μm (Figure 6A).

Precipitates of similar morphology were also obtained during continuous removal of arsenic in the bioreactor system (Chapter 4). However, due to the longer incubation time, the crystalline structures tripled in size. The ratio Fe/As of the precipitates measured by ICP ranged between 1.04-1.08, slightly higher than the value for scorodite (1.0), which can be explained by the presence of 2% of  $\text{Fe}_2\text{O}_3$  as determined by XRF (Table 2).

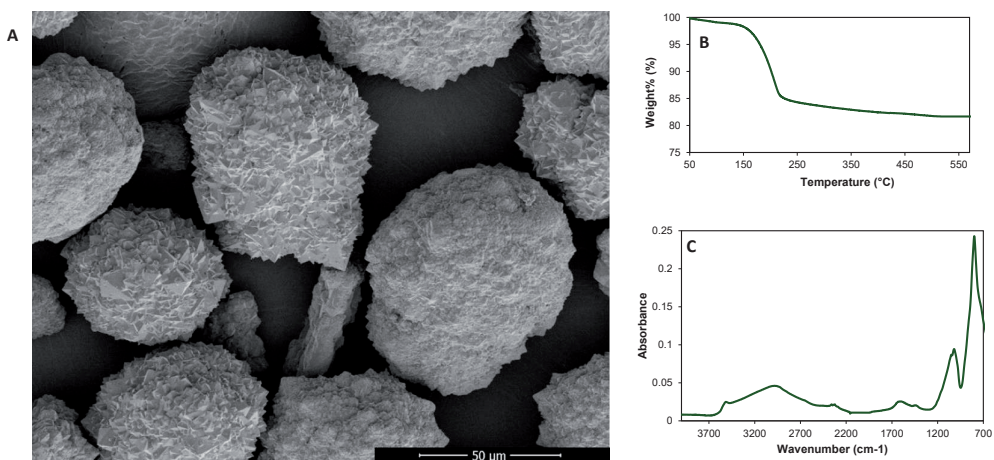


**Figure 6.** Structural characterization of the synthesized scorodite in biotic experiments. Morphology of the precipitates obtained by SEM image at 1200X magnification (A), structural water content determined by TGA analysis and FTIR spectrum of the collected precipitates (C).

Additionally, the estimated structural water loss of the precipitates (Figure 6B), determined by thermogravimetric analysis (TGA) was 15.3%, corresponding to approximately 1.95 molecules of structural water, slightly lower than the theoretical value of 2 mol  $\text{H}_2\text{O}$  per mol of scorodite (15.6%). The weight loss determined between 170°C and 235°C was assigned to the crystallization waters of scorodite [65]. However, water evaporation took place before 170°C and was attributed to the presence of poorly crystalline material according to previous observations [54, 66] and the data obtained by XRF analysis (Table 2). Afterwards, the weight loss increased to 17.3% (between 235-500 C), probably owing to the decomposition of organic matter on the precipitates. Analysis of vibration bands from arsenic showed an intense band at 795  $\text{cm}^{-1}$ , within the region, attributed to stretching vibration of arsenate in scorodite [67, 68]. A broader and a sharper band developed between 2978 and 3525  $\text{cm}^{-1}$  respectively and corresponded to the O-H stretching vibration of scorodite  $\text{H}_2\text{O}$  molecules [28, 67]. Other peaks were observed at 1010, 1025 and 1541  $\text{cm}^{-1}$  and have been related to the phosphate contamination but also to the presence of cell proteins and organic material [69, 70].

## CHAPTER 5

The presence of irregular lobed cells were found in solution and randomly attached to the scorodite crystals and pyrite mineral accordingly to SEM (Figure 7), suggesting that pyrite dissolution could have taken place through contact and non-contact mechanisms. Moreover, the mixed culture grew optimally using pyrite as a substrate, which resulted in a higher density of planktonic cells compared to the concentrations observed in the continuous system (Figure S2). The microbial composition analysis of the mixed culture, previously performed (Chapter 4) showed the predominance of archaeal species of the genus *Acidianus* and *Sulfolobus*. Similarly, the growth of the aforementioned species through the bioleaching of pyrite has been widely reported [62, 71, 72]. Hence, by the oxidation of Fe(II) reduced inorganic sulfur compounds (RISCs) can generate Fe(III) and/or protons to support the mineral oxidation [73].

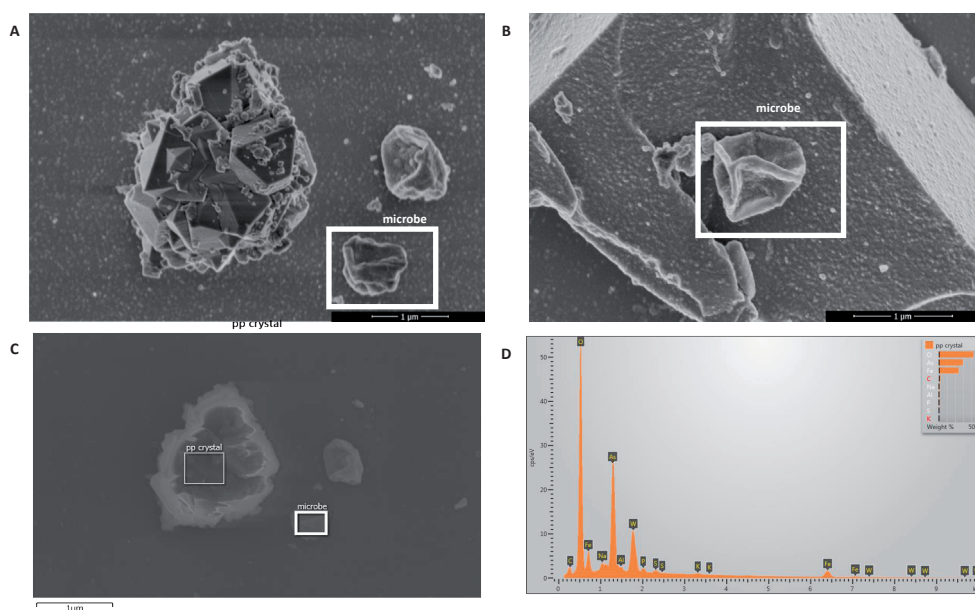


**Figure 7.** SEM photograph of planktonic and attached microbes observed with the crystals at (A) and the pyrite mineral (B) at 50000X and 60000X magnification respectively. EDX-spectrum of the bioscorodite crystals(C and D).

Along with the increase of biomass, the crystallization with pyrite as Fe source also led to the formation of aggregates with a well-defined crystal structure at the end of the experiment as observed by SEM (day 20) (Figure 7 and 8). Moreover, The SEM-EDX analysis of the precipitates collected earlier (day 14) indicated the presence of dipyramidal crystallites (2-3 μm) as well as less defined structures (Figure 7A and 8B), Interestingly, the analysis revealed the presence of a sticky-like material binding the

precipitates (Figure 8). The content of C (13%wt.) and N (3%wt.) of the material designated as “crystal-bridge”, coating the precipitates indicated the biofilm formation. Additionally, the high concentration of Fe (50%wt.) and to a lesser extent As (12%wt.) determined in the organic matrix suggesting the possible complexation of these ions. A lower concentration of organic material (3%wt.C) was also observed in the crystals collected at day 20 together, which also contained 29.98%wt.As and 23.16%wt.Fe, these values closely resemble the value of mineral scorodite (32%wt.As and 24%wt.Fe) [70]. Based on the detection of the organic material on the precipitates collected at day 14 and day 20, it is suggested that the nucleation starts on the organic compartments, resulting in the growth and solids clustering as a mix of amorphous and crystalline material that develop within the biofilm.

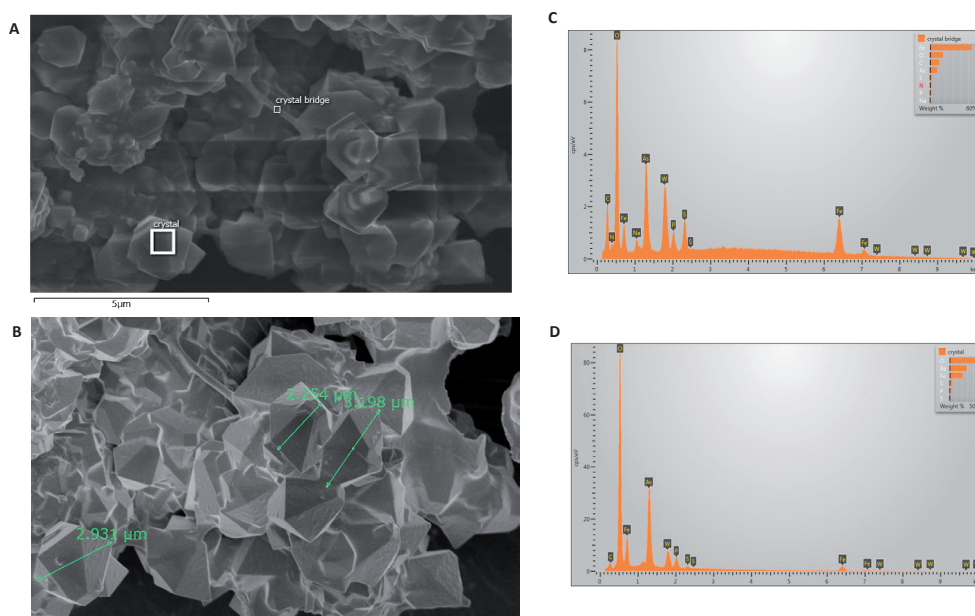


**Figure 8.** SEM-EDX of the precipitates collected on day 14 from biotic experiments. Magnification of the SEM was 15000X.

The dissolution of arsenic from the obtained crystals was tested as reported by the standard toxicity characteristic leaching procedure (TCLP) (Figure S3). The amount of arsenic leached from the solids after 20 hours (as stated in the method) was  $0.52 \text{ mg L}^{-1}$  As. This concentration remained relatively low until day 30, where sharply increased to  $1.44 \text{ mg L}^{-1}$  As at day 60. After this period, the leaching stabilized reaching a  $1.8 \pm 0.22 \text{ mg L}^{-1}$  until day 208.

## CHAPTER 5

According to the standard leaching test, the produced scorodite classified as a safe material for arsenic fixation. Still, the obtained arsenic rates were below the permissible limit ( $5 \text{ mg}\cdot\text{L}^{-1}$ ) which might suggest that the generated precipitates can be a good option for safe disposal. Nonetheless, further studies should be carried in order to determine for instance the physical and chemical changes as result of longer periods of storage. According to the development of well-defined crystal structure of the precipitates obtained in this study, we expected to have comparable leaching rates with the solids produced in continuous systems (Chapter 4). However, until day 60 of leaching test, the scorodite produced in this study doubled the concentration of arsenic released compared to the former solids. Besides the long-term leaching time tested, the main difference between the produced solids in this study and the continuous reactor system was regarded to the aging time of the crystals, thus, indicating the significance of the aging process on the crystal maturation and also the stability of the precipitates. Yet other factors, such as the extraction media and temperature conditions must be addressed to have an overview of the precipitates stability.

### 3. CONCLUSIONS AND OUTLOOK

The obtained results showed that the inoculated thermophilic mixed culture and the reused GAC from a continuous reactor were effective on the oxidation and the fixation of trivalent arsenic in acid solutions containing iron minerals. Thus, pyrite, which is an abundant mineral in the environment furthermore, predominant in metallurgical processes could be used as a cheaper Fe source for the scorodite process and growth substrate for the thermoacidophilic culture. The biological influence on the dissolution and oxidation of pyrite played a key role for the continuous supply of Fe(III) in the bioleaching and the precipitation process, which allowed the complete removal of arsenic and the complete bioleaching of pyrite turning into a dense green solid scorodite phase. In the same way, the biologically induced mineralization led to the formation of relatively low-leaching crystals over long-term. Therefore suggesting the high potential of the biological scorodite crystallization (bioscorodite) as a low-cost alternative for the efficient removal of As(V) and safe disposal. Additionally the performance of the recycled activated carbon in biotic experiments after the continuous process reactor (Chapter 4) was still better over the fresh carbon (abiotic controls). The latter might be of benefit for cost-reduction related to the catalyst, whereby, it would be interesting to address how active can be in the long-term. At the end of the experiments, scorodite was the dominant solid phase in biological experiments, which were easily separated from the liquid and the GAC granules. The precipitation of biogenic scorodite of low solubility and good stability in the long term as observed in this study was determined

by the control of biological reactions, and, still combined with the use of GAC, which is a cheap and stable catalyst.

## SUPPORTING INFORMATION OF CHAPTER 5

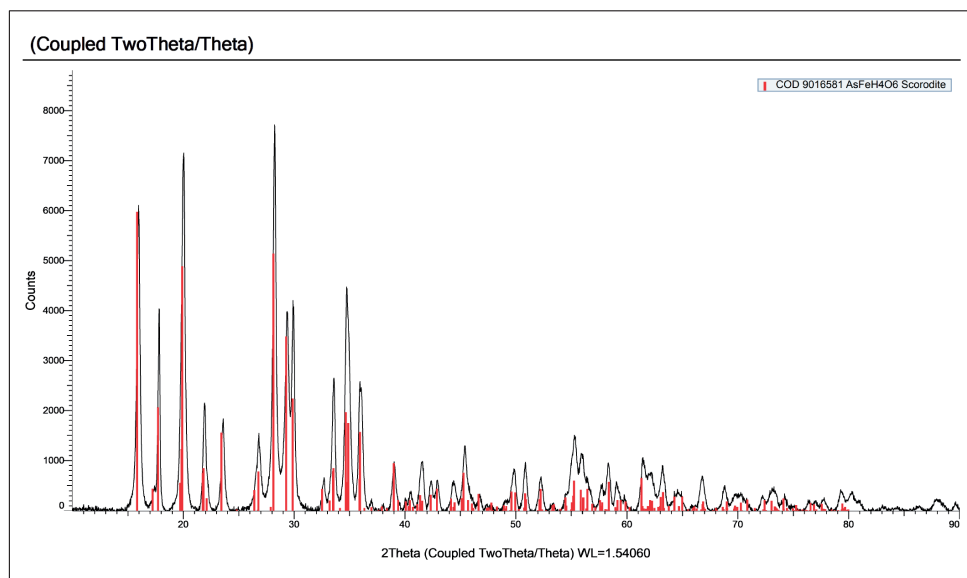


**Figure S1.** X-ray diffractogram (XRD) of the scorodite precipitates collected at day 20 from batch experiments containing  $4 \text{ g L}^{-1}$  GAC with  $2.25 \text{ g L}^{-1}$  As(III) and  $5 \text{ g L}^{-1}$  pyrite.

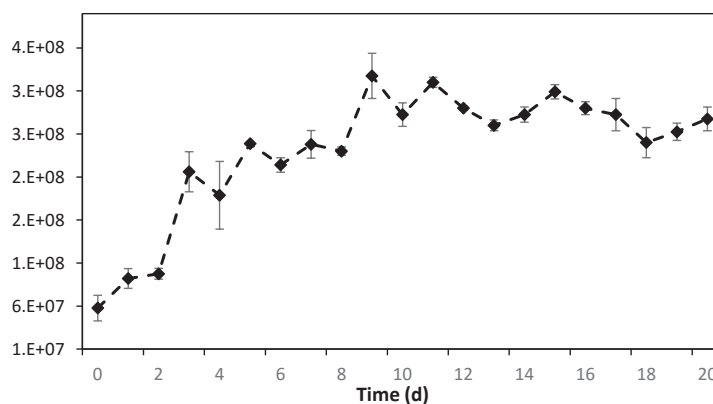


**Figure S2.** Cell density of planktonic cells from biotic experiments containing  $4 \text{ g L}^{-1}$  GAC with  $2.25 \text{ g L}^{-1}$  As(III) and  $5 \text{ g L}^{-1}$  pyrite.

## CHAPTER 5

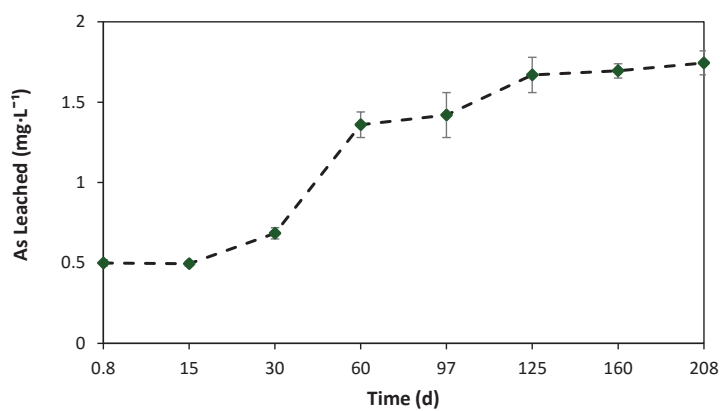


**Figure S3.** Long-term leaching of the produced scorodite in biotic experiments containing 4 g L<sup>-1</sup> GAC with 2.25 g L<sup>-1</sup> As(III) and 5 g L<sup>-1</sup> pyrite.

## REFERENCES

1. Mason, L., et al., *Availability, addiction and alternatives: three criteria for assessing the impact of peak minerals on society*. Journal of Cleaner Production, 2011. **19**(9): p. 958-966.
2. Johnson, D.B. and K.B. Hallberg, *Acid mine drainage remediation options: a review*. Science of The Total Environment, 2005. **338**(1): p. 3-14.
3. EU, *Proposal for a DIRECTIVE OF THE EUROPEAN PARLIAMENT AND OF THE COUNCIL amending Directive 2004/37/EC on the protection of workers from the risks related to exposure to carcinogens or mutagens at work COM/2018/0171 final - 2018/081 (COD)*, E. parliament, Editor. 2018: Brussels, 5.4.2018.
4. USEPA., *Water-related environmental fate of 129 priority pollutants*. EPA 440/4 ;79-029 a-b. 1980, Washington, D.C.: Office of Water Planning and Standards, Office of Water and Waste Management, U.S. Environmental Protection Agency. 2 v.
5. Cortina, J., Litter, M., Gibert, O., Valderrama, C., Sancha, A., Garrido, S., Ciminelli, V., *Latin American experiences in arsenic removal from drinking water and mining effluents*. CRC Press Taylor, 2016: p. p. 391-416.
6. Dunne, R.C., S.K. Kawatra, and C.A. Young, *SME Mineral Processing and Extractive Metallurgy Handbook*. 2019: Society for Mining, Metallurgy & Exploration, Incorporated.
7. Mohan, D. and C.U. Pittman, *Arsenic removal from water/wastewater using adsorbents—A critical review*. Journal of Hazardous Materials, 2007. **142**(1): p. 1-53.
8. Jia, Y. and G.P. Demopoulos, *Coprecipitation of arsenate with iron(III) in aqueous sulfate media: Effect of time, lime as base and co-ions on arsenic retention*. Water Research, 2008. **42**(3): p. 661-668.
9. De Klerk, R.J., et al., *Continuous circuit coprecipitation of arsenic(V) with ferric iron by lime neutralization: Process parameter effects on arsenic removal and precipitate quality*. Hydrometallurgy, 2012. **111-112**: p. 65-72.
10. Eguez, E.H. and E.H. Cho, *Adsorption of arsenic on activated charcoal*. JOM Journal of the Minerals, Metals and Materials Society, 1987. **39**(7): p. 38-41.
11. Demopoulos, G.P., D.J. Droppert, and G. Van Weert, *Precipitation of crystalline scorodite (FeAsO<sub>4</sub> · 2H<sub>2</sub>O) from chloride solutions*. Hydrometallurgy, 1995. **38**(3): p. 245-261.
12. Park, J.H., Y.-S. Han, and J.S. Ahn, *Comparison of arsenic co-precipitation and adsorption by iron minerals and the mechanism of arsenic natural attenuation in a mine stream*. Water Research, 2016. **106**: p. 295-303.
13. Le Berre, J.F., R. Gauvin, and G.P. Demopoulos, *Characterization of Poorly-Crystalline Ferric Arsenate Precipitated from Equimolar Fe(III)-As(V) Solutions in the pH Range 2 to 8*. Metallurgical and Materials Transactions B, 2007. **38**(5): p. 751-762.
14. Ahoranta, S.H., et al., *Arsenic removal from acidic solutions with biogenic ferric precipitates*. Journal of hazardous materials, 2016. **306**: p. 124-132.
15. Dutrizac, J. and J. Jambor, *The synthesis of crystalline scorodite, FeAsO<sub>4</sub> · 2H<sub>2</sub>O*. Hydrometallurgy, 1988. **19**(3): p. 377-384.

## CHAPTER 5

16. Demopoulos, G.P., *On the preparation and stability of Scorodite*. R.G. Reddy, V. Ramachandran (Eds.), *Arsenic Metallurgy*, TMS, Warrendale, PA (2005), , 2005: p. 25-50.
17. Fujita, T., et al., *Environmental leaching characteristics of scorodite synthesized with Fe(II) ions*. Hydrometallurgy, 2012. **111-112**: p. 87-102.
18. Swash, P. and A. Monhemius, *The scorodite process: A technology for the disposal of arsenic in the 21st century In Effluent Treatment in the Mining Industry*. Sánchez, M.A.; Vergara, F; Castro, S.H., Eds., *Universidad de Concepción: Concepción, Chile*. 1998.
19. Swash, P. and A. Monhemius, *Hydrothermal precipitation from aqueous solutions containing iron (III), arsenate and sulphate*, in *Hydrometallurgy'94*. 1994, Springer. p. 177-190.
20. Monhemius, A.J. and P.M. Swash, *Removing and stabilizing as from copper refining circuits by hydrothermal processing*. JOM, 1999. **51**(9): p. 30-33.
21. Gomez, M.A., et al., *The effect of copper on the precipitation of scorodite (FeAsO<sub>4</sub>·2H<sub>2</sub>O) under hydrothermal conditions: Evidence for a hydrated copper containing ferric arsenate sulfate-short lived intermediate*. Journal of Colloid and Interface Science, 2011. **360**(2): p. 508-518.
22. Filippou, D. and G.P. Demopoulos, *Arsenic immobilization by controlled scorodite precipitation*. JOM, 1997. **49**(12): p. 52-55.
23. Demopoulos, G., et al. *The atmospheric scorodite process*. in *Copper*. 2003.
24. Fujita, T., et al., *Effect of pH on atmospheric scorodite synthesis by oxidation of ferrous ions: Physical properties and stability of the scorodite*. Hydrometallurgy, 2009. **96**(3): p. 189-198.
25. González Contreras, P., J. Weijma, and C. Buisman. *Arsenic immobilization by biological scorodite crystallization: effect of high ferric concentration and foreign seeds*. in *Advanced Materials Research*. 2009. Trans Tech Publ.
26. González-Contreras, P., J. Weijma, and C.J.N. Buisman, *Continuous bioscorodite crystallization in CSTRs for arsenic removal and disposal*. Water Research, 2012. **46**(18): p. 5883-5892.
27. Okibe, N., et al., *Simultaneous oxidation and immobilization of arsenite from refinery waste water by thermoacidophilic iron-oxidizing archaeon, Acidianus brierleyi*. Minerals Engineering, 2013. **48**: p. 126-134.
28. Tanaka, M. and N. Okibe, *Factors to Enable Crystallization of Environmentally Stable Bioscorodite from Dilute As(III)-Contaminated Waters*. Minerals, 2018. **8**(1): p. 23.
29. Nazari, A.M., R. Radzinski, and A. Ghahreman, *Review of arsenic metallurgy: Treatment of arsenical minerals and the immobilization of arsenic*. Hydrometallurgy, 2016.
30. Twidwell, L.G. and J.W. McCloskey, *Removing arsenic from aqueous solution and long-term product storage*. JOM, 2011. **63**(8): p. 94.
31. Molnár, L.u., E. Virčíkova, and P. Lech, *Experimental study of As(III) oxidation by hydrogen peroxide*. Hydrometallurgy, 1994. **35**(1): p. 1-9.
32. Bissen, M. and F.H. Frimmel, *Arsenic — a Review. Part II: Oxidation of Arsenic and its Removal in Water Treatment*. Acta hydrochimica et hydrobiologica, 2003. **31**(2): p. 97-107.
33. Okibe, N., et al., *Microbial formation of crystalline scorodite for treatment of As (III)-bearing copper refinery process solution using Acidianus brierleyi*. Hydrometallurgy, 2014. **143**: p. 34-41.
34. Choi, Y., A. Ghahremaninezhad, and N. Ahern. *Process for activated carbon-assisted oxidation of*

- arsenic species in process solutions and waste waters. in *COM 2014-Conference of Metallurgists*. 2014.
35. Radzinski, R.L., *An investigation into the activated carbon-catalyzed arsenic oxidation process*. 2017, Queen's University (Canada).
  36. Okibe, N. and Y. Fukano, *Bioremediation of highly toxic arsenic via carbon-fiber-assisted indirect As(III) oxidation by moderately-thermophilic, acidophilic Fe-oxidizing bacteria*. *Biotechnology Letters*, 2019. **41**(12): p. 1403-1413.
  37. Vega-Hernandez, S., J. Weijma, and C.J.N. Buisman, *Immobilization of arsenic as scorodite by a thermoacidophilic mixed culture via As(III)-catalyzed oxidation with activated carbon*. *Journal of Hazardous Materials*, 2019. **368**: p. 221-227.
  38. Jahromi, F.G., D.H. Cowan, and A. Ghahreman, *Lanxess Lewatit® AF 5 and activated carbon catalysis of enargite leaching in chloride media; a parameters study*. *Hydrometallurgy*, 2017. **174**: p. 184-194.
  39. Norris, P.R. and D.W. Barr, *Growth and iron oxidation by acidophilic moderate thermophiles*. *FEMS Microbiology Letters*, 1985. **28**(3): p. 221-224.
  40. Gahan, C.S., J.-E. Sundkvist, and Å. Sandström, *A study on the toxic effects of chloride on the biooxidation efficiency of pyrite*. *Journal of Hazardous Materials*, 2009. **172**(2): p. 1273-1281.
  41. Gonzalez-Contreras, P., et al., *HPLC inorganic arsenic speciation analysis of samples containing high sulfuric acid and iron levels*. *Toxicological & Environ Chemistry*, 2011. **93**(3): p. 415-423.
  42. EPA, U.S., in *Field Applications of In Situ Remediation Technologies: Chemical Oxidation*. 1998, Washington D.C.: EPA.
  43. Boon, M., J.J. Heijnen, and G.S. Hansford, *The Mechanism and Kinetics of Bioleaching Sulphide Minerals*. *Mineral Processing and Extractive Metallurgy Review*, 1998. **19**(1): p. 107-115.
  44. Rohwerder, T., et al., *Bioleaching review part A*. *Applied Microbiology and Biotechnology*, 2003. **63**(3): p. 239-248.
  45. Dold, B., *Evolution of acid mine drainage formation in sulphidic mine tailings*. *Minerals*, 2014. **4**(3): p. 621-641.
  46. Barrett, J. and M. Hughes, *The mechanism of the bacterial oxidation of arsenopyrite-pyrite mixtures: The identification of plant control parameters*. *Minerals Engineering*, 1993. **6**(8): p. 969-975.
  47. Moses, C.O., et al., *Aqueous pyrite oxidation by dissolved oxygen and by ferric iron*. *Geochimica Cosmochimica Acta*, 1987. **51**.
  48. Holmes, P.R. and F.K. Crundwell, *The kinetics of the oxidation of pyrite by ferric ions and dissolved oxygen: an electrochemical study*. *Geochimica et Cosmochimica Acta*, 2000. **64**(2): p. 263-274.
  49. Crundwell, F.K., *How do bacteria interact with minerals?* *Hydrometallurgy*, 2003. **71**(1): p. 75-81.
  50. Wan, R.Y., et al. *Electrochemical features of the ferric sulfate leaching of CuFeS<sub>2</sub>/C aggregates*. in *Proceedings - The Electrochemical Society*. 1984.
  51. Zhang, W.-m. and S.-f. Gu, *Catalytic effect of activated carbon on bioleaching of low-grade primary copper sulfide ores*. *Transactions of Nonferrous Metals Society of China*, 2007. **17**(5): p. 1123-1127.
  52. Nakazawa, H., et al., *Effect of carbon black to facilitate galvanic leaching of copper from chalcopyrite in the presence of manganese(IV) oxide*. *Hydrometallurgy*, 2016. **163**: p. 69-76.
  53. Dixon, D. and B. Rivera-Vasquez, *Leaching process for copper concentrates with a carbon catalyst*. WO

## CHAPTER 5

- patent, 2011(2011/047477A1).
54. Jahromi, F.G. and A. Ghahreman, *In-situ oxidative arsenic precipitation as scorodite during carbon catalyzed enargite leaching process*. Journal of Hazardous Materials, 2018. **360**: p. 631-638.
  55. Liang, C.-L., et al., *Effect of activated carbon on chalcopyrite bioleaching with extreme thermophile Acidianus manzaensis*. Hydrometallurgy, 2010. **105**(1): p. 179-185.
  56. Nakazawa, H., H. Fujisawa, and H. Sato, *Effect of activated carbon on the bioleaching of chalcopyrite concentrate*. International Journal of Mineral Processing, 1998. **55**(2): p. 87-94.
  57. Ahmadi, A., *Effect of Activated Carbon Addition on the Conventional and Electrochemical Bioleaching of Chalcopyrite Concentrates*. Geomicrobiology journal, 2013. **v. 30**(no. 3): p. pp. 237-244-2013 v.30 no.3.
  58. Cowan, D.H., F.G. Jahromi, and A. Ghahreman, *Atmospheric oxidation of pyrite with a novel catalyst and ultra-high elemental sulphur yield*. Hydrometallurgy, 2017. **173**: p. 156-169.
  59. Cowan, D.H., F.G. Jahromi, and A. Ghahreman, *A parameters study of the novel atmospheric pyrite oxidation process with Lewatit® AF 5 catalyst*. Hydrometallurgy, 2019. **183**: p. 87-97.
  60. Ahumada, E., et al., *Catalytic oxidation of Fe(II) by activated carbon in the presence of oxygen.: Effect of the surface oxidation degree on the catalytic activity*. Carbon, 2002. **40**(15): p. 2827-2834.
  61. Plumb, J.J., R. Muddle, and P.D. Franzmann, *Effect of pH on rates of iron and sulfur oxidation by bioleaching organisms*. Minerals Engineering, 2008. **21**(1): p. 76-82.
  62. Wiertz, J.V., M. Mateo, and B. Escobar, *Mechanism of pyrite catalysis of As (III) oxidation in bioleaching solutions at 30 C and 70 C*. Hydrometallurgy, 2006. **83**(1): p. 35-39.
  63. Escobar, B., et al., *Arsenic precipitation in the bioleaching of enargite by Sulfolobus BC at 70 °C*. Biotechnology Letters, 2000. **22**(3): p. 205-209.
  64. Jahromi, F.G. and A. Ghahreman, *Effect of Surface Modification with Different Acids on the Functional Groups of AF 5 Catalyst and Its Catalytic Effect on the Atmospheric Leaching of Enargite*. Colloids and Interfaces, 2019. **3**(2).
  65. Bluteau, M.-C. and G.P. Demopoulos, *The incongruent dissolution of scorodite — Solubility, kinetics and mechanism*. Hydrometallurgy, 2007. **87**(3): p. 163-177.
  66. Le Berre, J.F., R. Gauvin, and G.P. Demopoulos, *A study of the crystallization kinetics of scorodite via the transformation of poorly crystalline ferric arsenate in weakly acidic solution*. Colloids and Surfaces A: Physicochemical and Engineering Aspects, 2008. **315**(1): p. 117-129.
  67. Yuan, Z., et al., *Effect of hydroquinone-induced iron reduction on the stability of scorodite and arsenic mobilization*. Hydrometallurgy, 2016. **164**: p. 228-237.
  68. Ondruš, P., et al., *Parascorodite, FeAsO<sub>4</sub>·2H<sub>2</sub>O—a new mineral from Kaňk near Kutná Hora, Czech Republic*, in *American Mineralogist*. 1999. p. 1439.
  69. Legal, J.M., M. Manfait, and T. Theophanides, *Applications of FTIR spectroscopy in structural studies of cells and bacteria*. Journal of Molecular Structure, 1991. **242**: p. 397-407.
  70. Gonzalez-Contreras, P., et al., *Biogenic Scorodite Crystallization by Acidianus sulfidivorans for Arsenic Removal*. Environmental Science & Technology, 2010. **44**(2): p. 675-680.
  71. Clark, D.A. and P.R. Norris, *Oxidation of mineral sulphides by thermophilic microorganisms*. Minerals Engineering, 1996. **9**(11): p. 1119-1125.

## PYRITE AS NATURAL IRON SOURCE FOR THE BIOSCORODITE CRYSTALLIZATION

72. Zhang, R., et al., *Biofilm dynamics and EPS production of a thermoacidophilic bioleaching archaeon*. New Biotechnology, 2019. **51**: p. 21-30.
73. Shiers, D., et al., *Substrate utilisation by Acidianus brierleyi, Metallosphaera hakonensis and Sulfolobus metallicus in mixed ferrous ion and tetrathionate growth media*. Minerals Engineering, 2013. **48**: p. 86-93.

## CHAPTER 6



# GENERAL DISCUSSION

### GENERAL DISCUSSION

Arsenic is a toxic element for all life domains. In the non-ferrous extractive metallurgy, it is a well-known penalty element in the ore concentrates and one of the unwanted toxic constituents of the obtained process effluent, and therefore subject to strict regulations. Due to the reduced market of arsenic, its banning and toxicity, the manufacturing and recycling of arsenic-containing products is currently not of economic interest. Hence, the primary aim of arsenic management in the final stage of metallurgical processing is its stabilization and subsequent disposal (Chapter 1).

The general approach for the removal of arsenic in metallurgical wastewater streams from relative dilute arsenic concentration ( $< 3\text{g/L As}$ ) is co-precipitation. Arsenic is co-precipitated through the formation of amorphous ferric arsenate compounds and As-bearing ferrihydrite [1]. Although the stability is adequate at Fe/As molar higher than 4, the arsenic co-precipitation process has an elevated iron consumption. The prior, in addition to the use of neutralization chemicals (pH 4-9) to achieve optimal arsenate removal, leads to the formation of a voluminous sludge with poor dewatering characteristics [2, 3].

Crystalline ferric arsenate, scorodite ( $\text{FeAsO}_4 \cdot 2\text{H}_2\text{O}$ ), is the preferred carrier for arsenic fixation. The precipitation of scorodite is a suitable option for arsenic-rich and iron-deficient solutions such as acid process/bleed effluents and offers advantages such as the low solubility of arsenic, the high arsenic content (25-30 wt.%) and good dewatering properties of the mineral [4-7].

The chemical precipitation of scorodite (mainly from As(V) solutions) under pressurized (hydrothermally at  $T > 150\text{ }^\circ\text{C}$ ) [8, 9], and atmospheric conditions ( $T < 95\text{ }^\circ\text{C}$ ) [10, 11], introduced the 1990s has been well-documented. The latter was based on controlling the arsenic and iron saturation in solution, exercised mainly by the pH control and the addition of crystal seeds [12, 13]. On the other hand, the biological crystallization of scorodite was previously demonstrated [14] through the bio-oxidation of ferrous iron in As(V) solutions at  $70\text{ }^\circ\text{C}$ . The obtained precipitates resembled in characteristics of the mineral scorodite and showed a low solubility over long-term leaching tests. Thus indicating the high potential of the biological scorodite crystallization (bioscorodite) as a low-cost alternative for the efficient removal of As(V) and safe disposal. Most of the developed methods have focused on the scorodite precipitation starting from As in its pentavalent state. Nonetheless, arsenite, As(III), is the predominant inorganic arsenic species reported in metallurgical process effluents and as  $\text{As}_2\text{O}_3$  in flue-dust [15, 16]. Thus, a primary step of oxidation to its pentavalent form is a requisite regardless the

chosen method for arsenic removal.

The research described in this thesis aimed to incorporate the range of applications of the bioscorodite concept for the treatment of As(III)-bearing solutions. Through this work and the promising outcomes, we combined in a single process unit the chemical oxidation of As(III), catalyzed by granular activated carbon (GAC), and the biological oxidation of Fe(II) for the concomitant precipitation of ferric arsenate, scorodite.

## 1. GAC-CATALYZED AS(III) OXIDATION

The simultaneous biological oxidation of Fe(II) and As(III) is pivotal to enable bioscorodite precipitation. Initially, we tested the ability of a Fe-oxidizing thermoacidophilic mixed culture to oxidize As(III) at pH 1.3, and 70°C. No detectable concentration of As(V) was present in the absence of Fe(II) (Chapter 2); however, we observed a negligible amount of arsenic (about 20-30 mg/L) adsorb on cells. Although arsenic has no biological function for the development of thermoacidophilic microbes, its uptake is not suppressed by the positive membrane potential and it occurs due to the chemical analogy to other molecules. Some examples include the substitution of As(V) by phosphate or uptake of As(III) via aquaglyceroporins transporters [17]. Conversely, in the presence of Fe<sup>2+</sup>, the conversion of As(III) took place in solution, at an average rate of 0.03 g L<sup>-1</sup> d<sup>-1</sup> (Chapter 3) which might be attributed to the presence *A. brierleyi* in the mixed culture based on the comparable reported rates for this strain at similar experimental conditions [18]. The latter provided an indication of the microbial contribution to the As(III) oxidation when Fe<sup>2+</sup> is simultaneously oxidized as an energy substrate. Furthermore, the oxidized species were readily removed from the solution, and just over 50% of As was removed by precipitation at an estimated molar Fe/ As ratio between 1-1.4.

The use of granular activated carbon (GAC) was introduced as a catalyst in combination with biological treatment following the first objective of achieving the complete oxidation of As(III). Initial experiments conducted with 9 and 20 g L<sup>-1</sup> GAC resulted in the complete oxidation of both As(III) and Fe(II) and a high removal of arsenic (>90%). The high ratio of activated carbon governed the oxidative reactions. Interestingly, biologically induced crystallization, and not chemical, was the primary mechanism for the precipitation of scorodite in these experiments (Chapter 2).

Owing to its catalytic role, the oxidative support of GAC was directly correlated to its concentration in solution. Higher concentration also influenced the chemical oxidation rate of Fe(II), thereby affecting the solution saturation state and leading to the rapid

precipitation in the presence of an iron-oxidizing culture. However, the control over the saturation is a crucial parameter for scorodite crystallization, and in the bioscorodite formation process, this is achieved through the biological oxidation of ferrous iron in solution. With the former in mind and to determine the catalytic role of GAC, not only in the oxidation of Fe(II) but also the impact in the arsenic precipitation, the GAC concentration was reduced to 4 g.L<sup>-1</sup>.

By lowering the GAC concentration to 4 g.L<sup>-1</sup>, the volumetric oxidation rate decreased with a factor of 2 and 4 when compared to the experiments with 9 and 20 g GAC.L<sup>-1</sup> respectively. Furthermore, it was observed that at lower catalyst concentrations the As(III) oxidation slightly differed in biotic and abiotic tests. The difference in abiotic and biotic rate can be likely explained by the contribution of microbially induced As(III) oxidation initially observed in the absence of a catalyst (Chapter 3). The primary mechanism behind the conversion of As(III) by activated carbon lies in the in-situ formation of hydrogen peroxide (H<sub>2</sub>O<sub>2</sub>) [19]. Hydrogen peroxide is the main oxidant and by-product of GAC-catalyzed oxidation processes, and, we were able to determine it, especially at higher concentrations of GAC.

With the aim of developing a continuous process for As(III) oxidation and removal as scorodite, we started-up a gas-lift reactor containing 4 g.L<sup>-1</sup> of GAC fed with influent concentrations of As(III) and Fe(II) based on preliminary batch tests (Chapter 4). During the initial stage of continuous reactor operation, the oxidation of arsenic fluctuated between 50-60%, which also influenced the rate of precipitation. To enhance the As(III) oxidation in continuous experiments for the gas-lift reactor, we increased the dissolved oxygen concentration (from 3.1 to 4.1 mg O<sub>2</sub> L<sup>-1</sup>) and the recycle flow (from 60-100 L h<sup>-1</sup>). The increase in the recirculation flow provided the additional advantage of effectively suspending the particle lifting and better distribution of the activated carbon granules GAC along the reactor. These modifications in operation helped to increase further the oxidation of arsenite, where at steady-state conditions (reached at day 58), the efficiency of arsenite oxidation and removal was over 90% (99% oxidation and 93% removal).

Besides oxidation, the adsorption of As and Fe onto GAC also occurred. This phenomenon was initially quicker, especially for arsenic, and eventually slowed down when approaching the adsorption equilibrium. This is relevant, especially in abiotic experiments. Both processes are surface-mediated, As(III) has a lower tendency to adsorb on the carbon surface than its oxidized form As(V) [20]. Possibly, after the oxidation takes place on or near the surface sites of the carbon, As(V) is adsorbed. Although the measured adsorption (1.5 ± 0.5 mg arsenic per gram of GAC) could be negligible at lower

GAC concentrations and high arsenic concentration, it becomes more substantial with increasing concentration of the catalyst and lower concentrations of arsenic. Similarly, it is also significant for abiotic conditions where the surface-dependent processes (oxidative or adsorptive) are hindered. This is most likely ascribed to the blockage of these active sites and pores on the activated carbon.

## 2. THE BIOLOGICAL OXIDATION OF Fe(II) IS THE KEY TO THE FORMATION OF CRYSTALLINE SCORODITE

The lower dosage of GAC not only resulted in lower As(III)-oxidation rates but also affected the chemical oxidation of Fe(II) (in abiotic tests), as merely 25% of Fe(II) conversion was observed during the experiments. Conversely, in the presence of microorganisms, 96% of Fe(II) was oxidized under the same conditions.

The thermoacidophilic mixed culture carried out the oxidation of Fe(II) in As(III)-solutions; however, the obtained rates of oxidation (0.03 g. Fe(II).L-1d-1) are still low for industrial application. Certainly, the conditions needed for bioscorodite crystallization are challenging for the microbial growth due to the low pH (1.1-1.3) and the presence of arsenic.

The gas-lift reactor was operated with 4g.L-1 of GAC and inoculated with the mixed culture, based on the prior batch results (chapter 4). The reactor was operated in three stages: an initial batch mode stage (12 days), and the second and third stages consisted of continuous operation of the reactor with an HRT of 3.1 and 2.2 days, respectively for 98 days. During Stage I, close to 80% of the Fe(II) oxidation was achieved in the solution initially containing 1 g. L-1 of Fe(II) and 1 g. L-1 of As(III) and concomitant Fe precipitation was also observed. During stage II, the reactor was switched to continuous operation where Fe(II) oxidation rate gradually increased in comparison to the oxidation of As(III) (80% of Fe over 60% of As conversion). At the end of the batch operation (after day 8) and the start of continuous operation, the formation of a gelatinous ferric phase took place in the reactor.

Since the formation of a secondary amorphous iron phase was observed together with scorodite, two adjustments were made to avoid the formation of amorphous iron: 1) stricter pH control, and 2) the reduction of Fe(II) concentrations in the feed. In the first adjustment, the pH was maintained at  $\leq 1.25$ , since the precipitation was observed to occur over the initial pH of 1.3 and increased to 1.4. In the second adjustment, the reduction of Fe(II) concentrations in the feed to  $0.63 \pm 0.02$  g. L-1, kept the same

## CHAPTER 6

Fe/As molar ratio ( $1.29 \pm 0.01$ ) in the influent. The initial concentration in the feed resulted in a molar ratio of Fe/As precipitated of 4, during stage I, and 2.3 at the start of stage II. However, after adjustment of the influent concentration, the precipitation ratio stabilized to an average value Fe/As of 1.2. The rate of Fe(II) bio-oxidation was not markedly influenced by the operational modifications of the reactor (that also included the improved mixing of the granules in the system) nor by the reduction of the HRT on stage III. Therefore, it seemed not to be the limiting step for the precipitation during the reactor operation. Nevertheless, the obtained rates ( $0.3 \pm 0.01$  g.Fe(II).L<sup>-1</sup>d<sup>-1</sup>) remain as a restriction to expand the range of application of this process beyond the current state.

Since the presence of As(III) can also negatively impact the iron oxidation activity of the mixed culture, optimizing the operational parameters for a stable simultaneous As(III) oxidation is critical for the development of a more robust biological process and would allow the treatment of higher concentration of As(III) and Fe(II) in the influent solution. Still, some strategies can be further considered for the process optimization and enhancement of the biological Fe(II) oxidation rate in the system such as:

- a) The HRT optimization: the hydraulic retention time is one of the most critical parameters of a continuous operation that might result in a lower capital-cost of the unit process. To enhance the oxidation rates, a follow-up study should assess the minimum HRT where near complete oxidation of the influent ferrous iron can be sustained avoiding microbial washout from the system. Based on the obtained results throughout the continuous bioreactor operation (especially in stage III, where the maximum conversion was achieved after 45 days), it seems feasible to project that increasing the iron volumetric loading rate to at least  $0.6$  g.Fe(II).L<sup>-1</sup>d<sup>-1</sup> (HRT of 1 day) might result in a similar oxidation efficiency (Chapter 4).
- b) The selection of a favorable mixed culture: since the extent of scorodite precipitation is also dependent on the concentration of Fe(III) in solution and the presence of biomass, improving the Fe(II) bio-oxidation performance at elevated concentrations is crucial if we aim to increase the initial concentration of arsenic in the system. Acidophiles obtain electrons from the oxidation of Fe(II) used to reduce oxygen (Ilbert and Bonnefoy, 2013). As only one electron can be obtained with relatively low Gibbs free energy change, dissimilatory Fe(II)-oxidizing microbes needs to oxidize large quantities of Fe(II) in order to gain enough energy for maintenance and growth (Gonzalez-Contreras et al., 2012). Although at the start of the experiments, the negative effect of As(III) was significant in the biological oxidation of Fe(II), the prolonged exposure might have resulted in the adaptation of the microbes as observed in the increased cell density. Determining the supply of other carbon sources might also contribute to the microbial growth of thermoacidophilic microbes

at the studied conditions. Members of Sulfolobales can grow autotrophically by CO<sub>2</sub> fixation or heterotrophically by the growth on yeast extract (Bertoldo et al., 2004). We added 0.01% of yeast as a supplement to the growth media reported in the experimental chapters as we found out in preliminary tests no difference after increasing concentration to 0.03 and 0.05% yeast extract in the media (unpublished data). It is uncertain if the carbon source could be a limiting factor in our system despite the addition of organic sources or if the addition of inorganic carbon sources such as CO<sub>2</sub> could have been more effective boosting microbial growth. To elucidate the latter, it would be worthwhile also to evaluate the enrichment of CO<sub>2</sub> in the inlet gas and the impact on microbial growth.

- c) Exploring other iron sources in continuous reactor systems: we have seen that the addition of other iron substrates such as pyrite greatly contributed to the activity of the microbes. Mixed culture obtained from the reactor promoted almost the complete leaching of the mineral. Over 90% of Fe(II) oxidized was oxidized from the mineral (2.4 gFe(II)·L<sup>-1</sup>), allowing the removal of 2.25 gAs(III)·L<sup>-1</sup> (Chapter 5). Compared with preliminary batch tests, these results indicated an improved activity of the iron-oxidizing microbes as a result of a better adaptation to As(III) in the media or the influence of a secondary energy substrate such as sulfur from the mineral. In any event, the main outcome was the boost in microbial growth, reflected in the higher cell density of planktonic cells and attached to the mineral surface, according to the bioleaching mechanisms mentioned earlier (Mikkelsen et al., 2007; Tributsch, 1999).

### 3. BIOSCORODITE PERFORMERS

In general, a common feature of thermoacidophilic systems is the relatively low microbial diversity, as observed in the bioleaching process were no more than three species of thermoacidophilic iron and sulfur oxidizing microorganisms dominate continuous operations [26, 27]. Synthesis of bioscorodite, under thermophilic conditions (>60°C), is mainly performed by archaea. Furthermore, only a smaller number of other bacterial species are present [28].

The scale-up of crystallization to the gas-lift reactor resulted in the enrichment of archaeal species in the reactor system (Chapter 4). 16S rRNA gene survey analysis of planktonic and bioscorodite-associated biomass showed that phylogenetically the thermoacidophilic culture clustered very close to *Acidianus* and *Sulfolobus* spp., accordingly, with the addition of *A. brierleyi* and *S. metallicus* to the mixed culture. Nonetheless, the former was the most abundant archaeon detected in solution (43%) and the solids (92%).

## CHAPTER 6

The visualization of the first scorodite precipitates produced in batch tests by SEM confirmed the attachment of rod-shaped microorganisms (Chapter 2). The cell morphology of the trapped cells was associated with the presence of *Sulfobacillus* spp. in the mixed culture. Although the reported optimal growth for these iron- and sulfur-oxidizing species ranged between 40-60 °C [29], the presence of *Sulfobacillus* spp. can be only explained by their keen ability to adapt in extreme conditions as observed by other authors [28, 30]. Nonetheless, after several sub-cultures, only a small fraction (1-2%) was identified through 16S rRNA clone library (Chapter 4).

The crystallization of scorodite is an indirect process driven by the presence of microbes, regardless of the heterogeneity (size, morphology, crystallinity) of the obtained precipitates in batch and reactor tests. Therefore, indirect biomineralization can take place at or near the cell wall via two mechanisms: 1) biologically induced mineralization, or 2) biologically influenced mineralization [31]. Despite the fact that both mechanisms are dependent on the presence of biological surfaces (i.e., cell walls or extracellular material), they differ. The first mechanism relies on the biological oxidation of Fe(II) to reach the solution saturation with respect to the mineral phase. In contrast, the second is regarded as a passive mineralization mechanism. Thereby, chemical conditions may favor the precipitation on the organic surface [32].

Our first results (Chapter 2) indicated that the scorodite precipitation was biologically influenced as it did not take place in abiotic controls despite the high solution saturation achieved with 9 g.L<sup>-1</sup> and, similarly with 20 g.L<sup>-1</sup> GAC (Chapter 3). Based on the initial findings (Chapter 2), and according to the SEM observations of the microorganisms firmly attached to the smaller precipitates, we postulated that microbial cells served as a surface for heterogeneous nucleation. In the passive influenced mineralization, microbial metabolism is negatively affected since the microorganisms do not gain energy from the oxidation reactions [32]. Hence, the Fe(II)-oxidizing microbes mainly perform as a binding and nucleation surface that in most cases leads to their encrustation in the precipitates. This certainly is a metabolic constraint because the microbial mixed culture only derives their energy from Fe(II)-oxidation under the studied conditions, and overall, it seems that Fe(II)-oxidizing microorganisms have to compete with the rapid abiotic Fe(II) oxidation catalyzed by higher GAC concentrations.

On the contrary, when the media was supplemented with a lower GAC concentration (4 g.L<sup>-1</sup>) (Chapter 3, 4 and 5), Fe(II) bio-oxidation induced the concomitant crystallization of scorodite. Therefore, the rate of precipitation, determined by the bio-oxidation reaction, resulted in the formation of bigger particles in the bulk solution rather than in GAC surface (Chapter 3). Through the biologically induced mechanism, the mineral

formation is impacted in several ways by the microbial activity. Firstly, by the influence on the low supersaturation level, maintained during the bio-oxidation reaction (Chapter 2). Despite the crucial role of supersaturation in the solid phase transition, at times may not be enough to initiate the crystallization as observed in abiotic experiments of this thesis (Chapter 2, 3 and 5), thereby the significance of the second means: the production of microbial extracellular polymers. Archaeal cell envelope of Sulfolobales is surrounded by an S-layer mainly composed of proteins as indicated in earlier reports [33]. Thus, by the growth of thermoacidophilic microbes on Fe(II), the secretion of these extracellular proteins and polysaccharides (EPS) is promoted [34] allowing them to generate microenvironments where the energy barrier for critical crystal-nucleus formation is reduced. Accordingly, the formation of an EPS-like matrix observed during the initial stages of continuous precipitation suggested that precursors of the bioscorodite crystals primarily are formed on the cell surface (Chapter 4).

EPS formation by thermoacidophilic archaea has been scarcely researched and the available studies mostly focused on the beneficial effect on bioleaching of sulfide minerals. Pyrite and sulfur have been also suggested as effective growth substrates [35], and the apparent production of EPS is stimulated by contact of cells with the mineral. The crystallization with pyrite as substrate resulted in a higher density of planktonic and also cells attached to the mineral. Therefore, the obtained precipitates consisted of aggregates with a well-defined crystalline structure that contained traces of organic compounds on the surface. Furthermore, a thin layer of high carbon content coating the aggregates of heterogeneous precipitates (with more or less defined crystal morphology) confirmed the biofilm formation.

Fe detection in the organic matrix indicated the complexation of these ions, which at thermoacidophilic conditions, might facilitate the bioleaching or bio-oxidation of pyrite and the complexation of arsenic. This could also explain the organic residues found in the precipitates.

Based on the detection of the organic material on the precipitates it is suggested that the nucleation starts on the organic compartments, resulting in the growth and solids clustering as a mix of amorphous and crystal material that develop within the EPS matrix and biofilm (Chapter 4).

**4. PROOF OF PRINCIPLE: FEASIBILITY OF BIOLOGICAL SCORODITE CRYSTALLIZATION FROM AS(III)-SOLUTIONS**

To the best of the author's knowledge, the continuous and simultaneous chemical oxidation of arsenite and biological oxidation of ferrous iron to produce scorodite is demonstrated for the first time in this thesis. Furthermore, the results obtained here introduced indicate that crystalline scorodite could be continuously precipitated, which extends the operational window of the bioscorodite process for the treatment of larger volumes of diluted As(III)-solution.

The formation of biogenic scorodite is determined, in one hand, by the regulation of the saturation level through the oxidation of ferrous iron and As(III), and on the other hand, by cell surface and (or) the organic components [36]. With 4 g.L<sup>-1</sup> GAC, the Fe and As predominantly precipitated in solution while at a high concentration (20.g L<sup>-1</sup> GAC), the clear majority of precipitates deposited on the GAC surface. The biocrystallization of scorodite in As(III) solutions with 4 g.L<sup>-1</sup> of GAC was directed through the biological oxidation Fe(II), which was the predominant reaction at these conditions, and it reflected in the control of the solution saturation with respect to scorodite. As a result, crystal growth overcame the primary nucleation, and a dense solution that turned to light green color (resembling the mineral) was observed due to the formation of settleable scorodite particles that accumulated in the bottom of the flasks and could be visually differentiated from the granules (Chapter 3).

In this study, scorodite precipitation was achieved only in biotic tests and without the addition of crystal seeds. Furthermore, the presence of the microorganisms firmly attached to the scorodite precipitates was also observed (Chapter 3). From these results, we proposed the indirect biomineralization of scorodite as the primary mechanism towards the formation of particles in the bulk solution. In the biomineralization mechanism, biological surfaces plays an important role in the induction stage owing that nucleation occurs on the cell wall or by the formation of organic substances (i.e., exopolymers) produced as a result of microbial metabolic activity [37, 38]. Accordingly, it was also determined that intact cells are needed for the precipitation instead of cell debris which is linked likely to physical adsorption (Chapter 2).

Still, being the process biologically mediated, the lack of saturation control in solutions influenced by the high concentration of catalyst induced the formation of smaller particles as well as more amorphous material (Chapter 2). Although most of the Fe and As precipitated as fine particles that visually covered the carbon granules in biotic tests, a fraction was associated with the GAC, as observed in the abiotic controls. Considering

an adsorption of As(V) of 1.5 mg gGAC<sup>-1</sup>, the average amount of arsenic removed was 9.5 mg gGAC<sup>-1</sup> (Chapter 2 and 3). This suggested that in addition to the adsorptive and oxidative capacity GAC also might serve as a surface for heterogeneous nucleation. Since the oxidation readily took place at the start of abiotic tests and the saturation index was even higher than in biotic tests it is hypothesized that the oxidized As(V) and Fe(III) adsorbed to GAC were prone to precipitate as small particles on the surface pores (used as nucleation sites) either as scorodite or As-containing Fe(III) hydroxides. Hence, the latter might have led to the solid deposition and coating of the outer surface, which further interrupted the activity of the granules. Furthermore, this also would explain why the solution remained clear, with more than 70% of ions dissolved.

The control of pH below 1.3 was crucial to prevent the formation of amorphous materials. The gelatinous fraction was a short-lived amorphous phase, as its occurrence stopped after the control of the pH under 1.25 and adjustment of influent Fe(II) concentration prior described.

## 5. PARTICLE SIZE AND THE STABILITY OF THE PRODUCED PRECIPITATES

We focused on a single step precipitation method to produce scorodite without the addition of chemical reagents. The main difficulty was to balance the oxidation reactions with the formation of particles that meet the main criteria: low arsenic leaching and good settling properties of the solids.

The resultant product from the initial experiments performed in addition of 9 g.L<sup>-1</sup> GAC consisted of colloidal particles of whitish color (<1 μm). Although the precipitates looked crystalline, one of the main drawbacks was the poor solid settling properties, which in practice can result in a less efficient and costly solid-separation process. In addition, the yield of smaller particles negatively affected the mobilization of arsenic. This occurred most likely due to the formation of phases of differing crystallinity or amorphous material, which were identified by the broader hump pattern in the solids X-ray diffractogram (XRD) (chapter 3, Figure 6). Conversely, the controlled Fe(II) bio-oxidation achieved at lower catalyst concentration resulted in the precipitation of scorodite, observed as single particles and aggregates (visually like flakes) that exceeded 10 μm in size. Despite that produced samples were identified as scorodite by XRD, both precipitates significantly differed in size and solubility. The scorodite particles produced with the lowest GAC concentration (4 g.L<sup>-1</sup>) produced a more stable particulate compared to those with a higher GAC concentration. In a leaching test of 24 hours

## CHAPTER 6

and 30 days, the scorodite particles produced with the lowest GAC concentration leached  $0.8 \pm 0.2$  mg L<sup>-1</sup> As. In contrast, the leachate of finer scorodite particles, the product of the highest GAC concentration experiments, leached  $5.1 \pm 0.2$  mg L<sup>-1</sup> As. This improved leaching characteristic was attributed to lower Fe/As molar ratio of the scorodite precipitates produced with the low GAC concentration (<1.2:1 compared to  $\geq 1.35:1$  of the finer particles) and also to the development of more crystalline phase in the particles of bigger size.

The initial Fe/ As concentration in solution of the test and pH was set at 1.29 and 1.3 respectively. Owing to the higher solution saturation (4.4) the precipitation at higher concentration of GAC, arsenic was readily removed. During this period, the solution pH increased from the initial and maintained at values close to 1.4. In contrast, at lower catalyst concentration, the pH dropped as cause of scorodite precipitation and ranged between of 1.22-1.24 while the solution saturation remained closed to 1. the difference in pH is probably related to the adsorption of iron and possibly formation of iron hydroxides complexes on the GAC surface at high concentrations [39]. Additionally, the low structural development of crystalline scorodite was also inferred by the significant content of interstitial water of the fine particles.

Therefore, the settleable particles obtained after reducing the GAC concentration were observed as 2 different types of precipitates by scanning electron microscopy (SEM) bigger crystals with orthorhombic shape and aggregates with less conserved crystalline structure and irregular size that might be defined as crystal's habit I and II according to previous observations [14].

The crystallization process was evaluated in the bioreactor experiments through the characterization of the evolving precipitates in addition to the elemental (Fe and As) composition analysis (Chapter 4). This led to the formation of particles of heterogeneous morphologies that finally ended up in the growth of defined crystalline structures at the end of the process. Hence, differing from the characteristics of the obtained solids produced in the previous batch experiments with the same GAC concentration (Chapter 3).

The produced precipitates at the end of batch and beginning of continuous operation (stage I and stage II) where characterized by the formation of a secondary phase in the reactor caused by the over precipitation ferric iron. Hence, a higher Fe/As molar ratio of removal in solution (1.8) and also in the digested precipitates was measured at the start of stage II (1.65) which further decreased to a stable value maintained during stage III. The higher ratio yielded amorphous precursors that likely evolved into more

crystalline structures observed as layers, deposited on the surface of some of these irregular precipitates. This phenomenon suggests that the initial formation of a less stable ferric arsenate (and even ferric oxyhydroxides) phases followed dissolution and recrystallization towards the transformation more defined structures [40, 41]. Thereby, the formation of the poor crystalline (or amorphous) phases observed in the reactor, as well as a higher concentration of GAC in batch bottles, were linked to the increase on pH implying the innate tolerance to pH fluctuation [42]

We identified the precipitates produced at the end of the continuous operation as: (1) a fraction that remained in suspension, presumably facilitating the precipitation of scorodite on the existing particles instead of the reactor walls; and, (2) the solids settled to the bottom of the reactor, which was beneficial for the collection of the solids from the solution. During stage III of continuous operation, the precipitation of scorodite led to the growth of crystals aggregates of a size ranging between 15 and 300  $\mu\text{m}$ . The surface analysis through SEM-EDX revealed that these precipitates comprised well-ordered planes of dipyramidal form with an estimated size of 1-2  $\mu\text{m}$  and Fe/As of 1.04. The stability analysis showed the correlation between the quality of the precipitates (i.e., size and crystal development) and the reduced release of arsenic. Theoretically, all the samples produced during the bioreactor tests were classified as non-hazardous waste according to the employed USEPA's toxicity characteristic leaching procedure (TCLP) in the short term (20 hours) and after 60 days performed. The highest arsenic leaching measured was 2  $\text{mg}\cdot\text{L}^{-1}$  As from the samples collected in stage I, while the permissible maximum concentration of arsenic in the extraction solvent (acetate buffer, pH 4.95) is 5  $\text{mg}\cdot\text{L}^{-1}$  As [43].

The obtained precipitates obtained when pyrite was used as Fe source showed a particle ranging between size between 50 and 90  $\mu\text{m}$ . Clusters of dipyramidal crystals of 3  $\mu\text{m}$  were identified. These precipitates had well-defined and crystalline structures and showed a leaching of 0.52  $\text{mg}\cdot\text{L}^{-1}$  As after 20 hours of test which amounted to 1.44  $\text{mg}\cdot\text{L}^{-1}$  As after 60 days and stabilized to  $1.86\pm 0.22$   $\text{mg}\cdot\text{L}^{-1}$  As until the end of the long-term repeated leaching (208 days) (Chapter 5).

## 6. PROCESS VALORIZATION AND FUTURE PERSPECTIVE

The oxidation of As(III) is essential in the process of arsenic immobilization. However, this alone does not ensure the effective removal of arsenic from solution. It must be followed either by adsorption or precipitation. The traditional fixation takes place by co-precipitation of the oxidized As(V) with Fe(III). Nonetheless, the resultant product

## CHAPTER 6

is a mixture of amorphous precipitate as in the case of arsenical ferrihydrite with a high molar Fe/As ratio of 3 to 5 which results in substantial volumes of sludge.

One of the benefits of the proposed biological process in this thesis is the lower Fe/As molar ratio of the compact precipitate (close to 1), translating into a significant lower Fe consumption and a lower mass of the solid waste residue. Since scorodite is the main product obtained at a relatively low crystallization temperature (70°C) and constant pH (1-1.2), the process does not require the addition of external seeds (i.e., gypsum or chemical scorodite) or stepwise neutralization. This reduces operational costs related to waste management and disposal.

The work presented in this thesis demonstrated that the biological scorodite precipitation takes place simultaneously to the catalyzed As(III) by activated carbon oxidation, thereby providing a novel alternative for arsenic immobilization and safe disposal of As from acidic wastewater streams (i.e., metallurgical effluents). To evaluate the perspective of the biological process, based on the obtained results with the continuous bioreactor (Chapter 4), we analyzed the potential of scorodite crystallization in a single step, considering some operational parameters related to the catalyzed arsenic oxidation (i.e., costs for GAC) and precipitation (Fe chemical costs). In table 1 we present a comparison with a 2-stage chemical process. In this process As(III) is continuously oxidized in a column reactor, thus, the effluent of this process is the influent of a second unit where the atmospheric precipitation of scorodite takes place [44, 45]. This process uses ferrous iron (chemical reagent) as the iron source for the analysis of biological and chemical systems.

Other aspects are described more qualitatively:

- a) The type of reactor: the process used for comparison consisted of a column upflow reactor used for the oxidation step and a mechanical stirred reactor for the separate scorodite precipitation.
- b) Operational units: The single-stage As(III) oxidation and precipitation in the gas-lift reactor at 70°C offers more advantages compared to separate units than only the avoided investment cost for a separate As(III) oxidation reactor. For example, the use of gas-lift reactor as single unit is effective for mass transfer of oxygen, by recycling the effluent gas, providing sufficient oxygen for both arsenite and ferrous iron oxidation. In contrast, the two-unit process requires a second gas-pumping system for the precipitation of scorodite, increasing the capital costs associated with oxygen supply (notably if only pure oxygen is used) for arsenic oxidation and separately for the chemical oxidation of Fe(II). Furthermore, the single process in the gas-lift offers a well-mixed system which, compared to a stirred reactor, is more suitable to

- keep both scorodite crystals and GAC particles in suspension, minimizing attrition.
- c) GAC addition: In both processes, the oxidation efficiency was similar (96 and 99%). The activated carbon used in both studies is a commercially available product of relatively low-cost,. Although the calculated cost associated with the use of GAC in both systems seems to be negligible compared to the cost of Fe, The addition of a higher concentration of GAC as compared to the chemical process for arsenic precipitation can be only of benefit in a 2-stage operation. This allowed a higher arsenic loading rate of  $6.67 \text{ g.L}^{-1}.\text{d}^{-1}$ , in comparison with our process ( $0.3 \text{ g.L}^{-1}.\text{d}^{-1}$ ), which in industrial terms (i.e. for the metallurgical industry), is interesting for the oxidation process. However, such catalyst concentrations could have a negative impact on the bioscorodite system, if the precipitation of settleable crystalline scorodite is aimed, as observed previously in chapter 3 and as mentioned above in Section 6.3.
- d) Cost of iron supply: in the compared processes the supplied iron source was considered a reagent chemical. If no neutralization is needed in both processes, one of the main differences between the biological process and the 2-stage chemical process lies in the extra input of oxygen that implies the oxidation of Fe(II) (besides the As(III) oxidation used in the first unit) and the type of oxygen added. One of the advantages of the bioscorodite production is the lower iron consumption. We considered the supply of chemical iron for the analysis which in economic terms is not of difference. However, one benefit of the biological scorodite process is the possible use of alternate iron sources such as pyrite. This sulfide mineral is predominant in the environment and in metallurgical processes. Thermoacidophilic microbes can oxidize the pyrite, resulting in dissolution of iron. We presume that this oxidation is indirect, viz. through chemical oxidation of pyrite by ferric iron, followed by microbial (re)oxidation of the formed ferrous iron oxygen to ferric iron. With the use of pyrite, which is cheaper than chemical Fe sources, the costs of the process could be reduced. Preliminary batch-tests showed the efficacy of using pyrite as an alternative Fe source. Performing tests with pyrite in the continuous system would validate this option and provide the guidelines for a potential industrial application.

## CHAPTER 6

**Table 1.** Comparative cost of Fe and GAC for the treatment of As(III)-rich streams in the GAC catalyzed oxidation process

	Bioscorodite crystallization (Chapter 4)	GAC-catalyzed As(III) oxidation coupled to atmospheric precipitation [44, 45]
Operational stages	1	2
Type of reactor	Gas-lift	Column (oxidation), stirred reactor (precipitation)
Temperature (°C)	70	25(oxidation), 70 (precipitation)
GAC (g·L <sup>-1</sup> )	4	480
HRT (h)	52.8	3.6(oxidation) 7(precipitation)
Ratio GAC:As (g·g <sup>-1</sup> )	0.13	0.72
Arsenic concentration (g·L <sup>-1</sup> )	0.65	1
Iron source	Fe(II)	Fe(II)
Arsenic oxidation efficiency (%)	≥99	≥96
Fe/as molar ratio precipitates	1.2	1.5
Seeds (g·L <sup>-1</sup> )	-	-
Oxidizing reagent	Oxygen-enriched air	Oxygen
Arsenic loading rate (g·L <sup>-1</sup> ·d <sup>-1</sup> )	0.295	6.667
Iron loading rate (g·L <sup>-1</sup> ·d <sup>-1</sup> )	0.273	7.333
As removal efficiency (%)	93	98
Concentration of arsenic precipitated (g·L <sup>-1</sup> )	26.7	170
Cost GAC in oxidation process (\$·g As <sup>-1</sup> )	0.0001	0.0005
Cost Fe for arsenic precipitation (\$·g As <sup>-1</sup> )	0.0002	0.0002

## REFERENCES

1. Twidwell, L., R.G. Robins, and J. Hohn, *The Removal of Arsenic from Aqueous Solution by Coprecipitation with Iron (III)*. 2005.
2. De Klerk, R.J., Y. Jia, R. Daenzer, M.A. Gomez, and G.P. Demopoulos, *Continuous circuit coprecipitation of arsenic(V) with ferric iron by lime neutralization: Process parameter effects on arsenic removal and precipitate quality*. Hydrometallurgy, 2012. **111-112**: p. 65-72.
3. Jia, Y. and G.P. Demopoulos, *Coprecipitation of arsenate with iron(III) in aqueous sulfate media: Effect of time, lime as base and co-ions on arsenic retention*. Water Research, 2008. **42**(3): p. 661-668.
4. Lagno, F., S.D.F. Rocha, S. Chryssoulis, and G.P. Demopoulos, *Scorodite encapsulation by controlled deposition of aluminum phosphate coatings*. Journal of Hazardous Materials, 2010. **181**(1): p. 526-534.
5. Demopoulos, G.P., *Arsenic Immobilization Research Advances: Past, Present and Future*. Canadian Institute of Mining, Metallurgy and Petroleum, 2014.
6. Langmuir D., M.J.a.R.J., *Solubility products of amorphous ferric arsenate and crystalline scorodite (FeAsO<sub>4</sub>·2H<sub>2</sub>O) and their application to arsenic behavior in buried mine tailings*. Geochimica et Cosmochimica Acta, 2006. **70**(12): p. 2942 - 2956.
7. Robins, R.G., P.M. Dove, J.D. Rimstidt, D.K. Nordstrom, and G.A. Parks, *Solubility and stability of scorodite, FeAsO<sub>4</sub>·2H<sub>2</sub>O; discussions and replies*. American Mineralogist, 1987. **72**(7-8): p. 842-855.
8. Swash, P. and A. Monhemius, *Hydrothermal precipitation from aqueous solutions containing iron (III), arsenate and sulphate*, in *Hydrometallurgy'94*. 1994, Springer. p. 177-190.
9. Monhemius, A.J. and P.M. Swash, *Removing and stabilizing as from copper refining circuits by hydrothermal processing*. JOM, 1999. **51**(9): p. 30-33.
10. Demopoulos, G.P., D.J. Droppert, and G. Van Weert, *Precipitation of crystalline scorodite (FeAsO<sub>4</sub> · 2H<sub>2</sub>O) from chloride solutions*. Hydrometallurgy, 1995. **38**(3): p. 245-261.
11. Droppert, D.J., *"The Ambient Pressure Precipitation of Crystalline Scorodite (FeAsO<sub>4</sub>·2H<sub>2</sub>O) from Sulphate Solutions,"* in *Department of Mining and Metallurgical Engineering*. 1996, McGill University: Montreal.
12. Demopoulos, G., F. Lagno, Q. Wang, and S. Singhania. *The atmospheric scorodite process*. in *Copper*. 2003.
13. Singhania, S., Q. Wang, D. Filippou, and G.P. Demopoulos, *Temperature and seeding effects on the precipitation of scorodite from sulfate solutions under atmospheric-pressure conditions*. Metallurgical and Materials Transactions B, 2005. **36**(3): p. 327-333.
14. Gonzalez-Contreras, P., J. Weijma, R.v.d. Weijden, and C.J.N. Buisman, *Biogenic Scorodite Crystallization by Acidianus sulfidivorans for Arsenic Removal*. Environmental Science & Technology, 2010. **44**(2): p. 675-680.
15. Riveros, P., J. Dutrizac, and P. Spencer, *Arsenic disposal practices in the metallurgical industry*. Canadian Metallurgical Quarterly, 2001. **40**(4): p. 395-420.

## CHAPTER 6

16. Chai, L.-Y., Q.-Z. Li, Q.-W. Wang, Y.-Y. Wang, W.-C. Yang, and H.-Y. Wang, *Arsenic Behaviors and Pollution Control Technologies in Aqueous Solution*, in *Arsenic Pollution Control in Nonferrous Metallurgy*, L.-Y. Chai, Editor. 2019, Springer Singapore: Singapore. p. 29-120.
17. Dopson, M. and D.S. Holmes, *Metal resistance in acidophilic microorganisms and its significance for biotechnologies*. Applied Microbiology and Biotechnology, 2014. **98**(19): p. 8133-8144.
18. Okibe, N., M. Koga, K. Sasaki, T. Hirajima, S. Heguri, and S. Asano, *Simultaneous oxidation and immobilization of arsenite from refinery waste water by thermoacidophilic iron-oxidizing archaeon, Acidianus brierleyi*. Minerals Engineering, 2013. **48**: p. 126-134.
19. Choi, Y., A. Ghahremaninezhad, and N. Ahern. *Process for activated carbon-assisted oxidation of arsenic species in process solutions and waste waters*. in *COM 2014-Conference of Metallurgists*. 2014.
20. Gupta, S.K. and K.Y. Chen, *Arsenic Removal by Adsorption*. Journal (Water Pollution Control Federation), 1978. **50**(3): p. 493-506.
21. Ilbert, M. and V. Bonnefoy, *Insight into the evolution of the iron oxidation pathways*. Biochimica et Biophysica Acta (BBA) - Bioenergetics, 2013. **1827**(2): p. 161-175.
22. Gonzalez-Contreras, P., J. Weijma, and C.J. Buisman, *Kinetics of ferrous iron oxidation by batch and continuous cultures of thermoacidophilic Archaea at extremely low pH of 1.1–1.3*. Applied microbiology and biotechnology, 2012. **93**(3): p. 1295-1303.
23. Bertoldo, C., C. Dock, and G. Antranikian, *Thermoacidophilic Microorganisms and their Novel Biocatalysts*. Engineering in Life Sciences, 2004. **4**(6): p. 521-532.
24. Tributsch, H., *Direct versus indirect bioleaching*. Process Metallurgy, 1999. **9**: p. 51-60.
25. Mikkelsen, D., U. Kappler, R.I. Webb, R. Rasch, A.G. McEwan, and L.I. Sly, *Visualisation of pyrite leaching by selected thermophilic archaea: Nature of microorganism–ore interactions during bioleaching*. Hydrometallurgy, 2007. **88**(1): p. 143-153.
26. Rawlings, D.E. and D.B. Johnson, *The microbiology of biomining: development and optimization of mineral-oxidizing microbial consortia*. Microbiology (Reading, England), 2007. **153**(Pt 2): p. 315-324.
27. Dinkla, I.J.T., M. Gericke, B.K. Geurkink, and K.B. Hallberg, *Acidianus Brierleyi is the Dominant Thermoacidophile in a Bioleaching Community Processing Chalcopyrite Containing Concentrates at 70°C*. Advanced Materials Research, 2009. **71-73**: p. 67-70.
28. Johnson, D.B., *Biodiversity and interactions of acidophiles: Key to understanding and optimizing microbial processing of ores and concentrates*. Transactions of Nonferrous Metals Society of China, 2008. **18**(6): p. 1367-1373.
29. Watling, H.R., F.A. Perrot, and D.W. Shiers, *Comparison of selected characteristics of Sulfolobus species and review of their occurrence in acidic and bioleaching environments*. Hydrometallurgy, 2008. **93**(1): p. 57-65.
30. Kinnunen, P.-M., W. Robertson, J. Plumb, J. Gibson, P. Nichols, P. Franzmann, and J. Puhakka, *The isolation and use of iron-oxidizing, moderately thermophilic acidophiles from the Collie coal mine for the generation of ferric iron leaching solution*. Applied microbiology and biotechnology, 2003. **60**(6): p. 748-753.
31. Frankel, R.B. and D.A. Bazylinski, *Biologically Induced Mineralization by Bacteria*. Reviews in

- Mineralogy and Geochemistry, 2003. **54**(1): p. 95-114.
32. Fortin, D. and S. Langley, *Formation and occurrence of biogenic iron-rich minerals*. Earth-Science Reviews, 2005. **72**(1): p. 1-19.
  33. Albers, S.-V. and B.H. Meyer, *The archaeal cell envelope*. Nature Reviews Microbiology, 2011. **9**(6): p. 414-426.
  34. Zhang, R., T.R. Neu, Q. Li, V. Blanchard, Y. Zhang, A. Schippers, and W. Sand, *Insight Into Interactions of Thermoacidophilic Archaea With Elemental Sulfur: Biofilm Dynamics and EPS Analysis*. Frontiers in microbiology, 2019. **10**: p. 896-896.
  35. Xia, J.-l., Y. Yang, H. He, X.-j. Zhao, C.-l. Liang, L. Zheng, C.-y. Ma, Y.-d. Zhao, Z.-y. Nie, and G.-z. Qiu, *Surface analysis of sulfur speciation on pyrite bioleached by extreme thermophile Acidianus manzaensis using Raman and XANES spectroscopy*. Hydrometallurgy, 2010. **100**(3): p. 129-135.
  36. Gonzalez Contreras, P.A., *Bioscorodite: biological crystallization of scorodite for arsenic removal*. 2012, Wageningen university: [S.l.s.n.].
  37. Lowenstam, H.A., *Minerals formed by organisms*. Science, 1981. **211**(4487): p. 1126.
  38. Weiner, S. and P.M. Dove, *An Overview of Biomineralization Processes and the Problem of the Vital Effect*. Reviews in Mineralogy and Geochemistry, 2003. **54**(1): p. 1-29.
  39. Huang, C.P. and L.M. Vane, *Enhancing As<sup>5+</sup> Removal by a Fe<sup>2+</sup> Treated Activated Carbon* Research Journal of the Water Pollution Control Federation, 1989. **61**(9/10): p. 1596-1603.
  40. Paktunc, D., J. Dutrizac, and V. Gertsman, *Synthesis and phase transformations involving scorodite, ferric arsenate and arsenical ferrihydrite: Implications for arsenic mobility*. Geochimica et Cosmochimica Acta, 2008. **72**(11): p. 2649-2672.
  41. Tanaka, M., K. Sasaki, and N. Okibe, *Behavior of sulfate ions during biogenic scorodite crystallization from dilute As(III)-bearing acidic waters*. Hydrometallurgy, 2018. **180**: p. 144-152.
  42. Singhanian, S., Q. Wang, D. Filippou, and G.P. Demopoulos, *Acidity, valency and third-ion effects on the precipitation of scorodite from mixed sulfate solutions under atmospheric-pressure conditions*. Metallurgical and Materials Transactions B, 2006. **37**(2): p. 189-197.
  43. USEPA, *Toxicity characteristic leaching procedure (TCLP) method 1311*. 1992, EPA Publication SW-846.
  44. Fujita, T., R. Taguchi, M. Abumiya, M. Matsumoto, E. Shibata, and T. Nakamura, *Novel atmospheric scorodite synthesis by oxidation of ferrous sulfate solution. Part II. Effect of temperature and air*. Hydrometallurgy, 2008. **90**(2): p. 85-91.
  45. Wu, C., H. Mahandra, and A. Ghahreman, *Novel Continuous Column Process for As(III) Oxidation from Concentrated Acidic Solutions with Activated Carbon Catalysis*. Industrial & Engineering Chemistry Research, 2020. **59**(21): p. 9882-9889.

## SUMMARY



# SUMMARY

## SUMMARY

Arsenic (As), is the 20th most abundant natural element in the earth's crust. Furthermore, an important source of drinking water contamination and undesirable element overproduced during the extraction of valuable metals from low-grade ores. To date, scorodite is the most appropriate carrier for long-term arsenic fixation in metallurgical processes. Furthermore, Biological scorodite crystallization (bioscorodite) from diluted As(V) streams demonstrated being cost-efficient and sustainable solution for the treatment of diluted As(V) solutions. Since As(III) is predominant in acid effluents and scorodite needs the As to be in the As(V) an oxidation previous oxidation step is required (**Chapter 1**).

This thesis **Expanding the bioscorodite process for As(III) wastewater remediation**, explored at laboratory scale, the possibilities of arsenic immobilization from the treatment acid As(III)-bearing solutions through the biological oxidation and precipitation in a single unit process aiming to broad the range of application of the bioscorodite concept. In this thesis, the proof of principle, reactor selection and operational conditions of bioscorodite crystallization were studied.

**Chapter 2** describes the possibilities of biological and chemical As(III) oxidation ( $0.5 \text{ g L}^{-1}$ ) at low pH ( $\leq 1.3$ ) and high temperature ( $70^\circ$ ) using a thermoacidophilic iron-oxidizing mixed culture and, chemically, by the addition granular activated carbon catalyst (GAC). Biotic experiments showed that only negligible amount removal of arsenic ( $20\text{-}30 \text{ mg L}^{-1}$ ), ascribed to biological adsorption. Conversely in the addition of  $9 \text{ g L}^{-1}$  GAC resulted in the complete As(III) oxidation.

Bearing this in mind the addition of  $0.5 \text{ g L}^{-1}$  Fe(II) at a molar ratio Fe/As of 1.4 to biotic and abiotic experiments showed that crystalline scorodite can only be precipitated in the presence of the ferrous iron-oxidizing mixed culture. Thus, proving the proof of principle that scorodite precipitation under the studied condition is a biologically mediated process. Nevertheless, the obtained crystalline precipitates consisted of colloidal aggregates ( $< 1 \mu\text{m}$ ) meaning a drawback due to the poor solid settling properties, which in practice can result in a less efficient and costly solid-separation process. Despite that biomineralization was the main mechanism behind the removal of arsenic, GAC also influenced the chemical oxidation rate of Fe(II), consequently, affecting the solution saturation level.

**Chapter 3** focuses on the optimization of the biological scorodite precipitation. The approach in this study involved the control of the solution saturation. Hereby, we studied the effect of GAC, on the biological scorodite precipitation at thermoacidophilic conditions in batch experiments. The obtained results showed that a reduced concentration

of GAC to  $4 \text{ g}\cdot\text{L}^{-1}$  allowed a control of the saturation through the biological oxidation of ferrous iron, which, was the predominant reaction at these conditions and a higher As removal. As a result, crystal growth overcame the primary nucleation and scorodite precipitates with a bigger particle size were produced without the addition of crystal seeds.

Furthermore, the scorodite particles produced with the lowest GAC concentration ( $4 \text{ g}\cdot\text{L}^{-1}$ ) produced a more stable particulate compared to those with a higher GAC concentration.

In order to get and insight into the possible applicability of the process to higher volumes, to simulated streams and the long term stability of the crystals, **Chapter 4** evaluates the feasibility of scaling up the biocrystallization process using a bench-scale airlift reactor. The As(III) oxidation catalyzed by granular activated carbon (GAC), biological Fe(II) oxidation and scorodite crystallization took place simultaneously in the reactor during 98 days, enabling the treatment of influent solution containing  $0.65 \text{ g}\cdot\text{L}^{-1}$  As(III). At a hydraulic retention time of 2.2 days. During continuous operation, the precipitation of scorodite led to the growth of larger size crystals ( $250 \mu\text{m}$ ) that settled to the bottom facilitating the collection of the solids from the solution. Additionally, the development of the crystal structure (comparable to mineral scorodite) correlated to the lower arsenic leaching in the short term (20 hours) and after 60 days ( $0.4 \text{ mg}\cdot\text{L}^{-1}\text{As}$ ) indicating the good solid stability. Under this conditions mainly archaeal population were enriched in the reactor. Furthermore, the predominance of thermoacidophilic archaea of the genus *Acidianus* and *sulfolobus*, obtained by the molecular analysis and, the visualized EPS like-structures indicated that scorodite formation is mediated by the microbial surface or by the exopolymeric organic components.

**Chapter 5** addresses the supply of alternative iron sources in for the bioscorodite precipitation. Pyrite ( $\text{FeS}_2$ ), and abundant mineral in hydrometallurgical process was used as a potential iron source in the biological scorodite crystallization. The experiment we performed in batch bottles containing  $4 \text{ g}\cdot\text{L}^{-1}$  of granular activated carbon and  $5 \pm 0.5 \text{ g}\cdot\text{L}^{-1}$  of pyrite. The mixed culture inoculated in the biotic experiments as well as the GAC were collected from the previous continuous reactor tests. Complete pyrite leaching was reached after nine days enabling the loading of  $2.25 \text{ g}\cdot\text{L}^{-1}$  As (III) in the biotic test along with the complete oxidation and removal. In contrast to chemical control were oxidation was at least 3.5 lower and no removal was observed. Scorodite precipitates of crystalline structure with a Fe / As ratio between 1.04-1.08 were the main mineral phase produced in biotic test. The long-term leaching of the precipitates resulted in the released of  $1.8 \pm 0.22 \text{ mg}\cdot\text{L}^{-1}$  As. A thin layer of high carbon content coating the

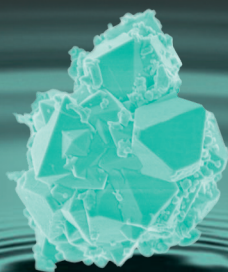
## SUMMARY

crystals was observed by SEM-EDX, suggesting the initial nucleation and further crystal development within the biofilm compartment. The supply of pyrite also resulted in higher cell density. Thus, according to the obtained results, the use of pyrite which is cheaper than chemical Fe reagents could be used as a potential iron source reducing the cost of the process.

Lastly in **Chapter 6**, a novel alternative for arsenic immobilization and safe disposal of As from acidic wastewater streams (i.e., metallurgical effluents) was provided. The overall evaluation of the results presented in this thesis are discussed, as well as some required parameters that might result in the further development of the process are addressed. To the best of the author's knowledge, the continuous and simultaneous chemical oxidation of arsenite and biological oxidation of ferrous iron to produce scorodite is demonstrated for the first time. Thus, Based on the obtained results, the future perspective of biological scorodite crystallization in a single step was evaluated, considering some operational parameters related to the catalyzed arsenic oxidation (i.e., costs for GAC) and precipitation (Fe chemical costs). One of the benefits of the proposed biological process in this thesis is the lower Fe/As molar ratio of the compact precipitate (close to 1), translating into a significant lower Fe consumption and a lower mass of the solid waste residue. Moreover, taking into account that the process does not require the addition of external seeds (i.e., gypsum or chemical scorodite) or stepwise neutralization operational costs related to waste management and disposal. are also reduced. Other aspects related to the operational cost of a single for As(III) oxidation and precipitation, the reusability of the GAC as well as the use of cheaper alternative Fe sources such as pyrite greatly contribute to reduce the cost of the process. The work presented in this thesis demonstrated that the biological scorodite precipitation takes place simultaneously to the catalyzed As(III) by activated carbon oxidation, thereby providing a novel alternative for arsenic immobilization and safe disposal of As from acidic wastewater streams (i.e., metallurgical effluents).



## ACKNOWLEDGEMENTS



# ACKNOWLEDGEMENTS

## ACKNOWLEDGEMENTS

My journey has ended and I must say that I am incredibly happy to be writing this section. It has been a long journey and made me reflect several times on whether I was following the right path. It was not always easy; however, this was a great experience that I do not regret having lived, which taught me many things, especially at a professional level but also personally.

I'm deeply grateful with the program of the Chilean government's CONICYT for awarding me the PhD scholarship that allowed me to live, study and perform my research during these last years in the Netherlands. In the same way, I want to thank my promoters/supervisors Jan and Cees. Jan thanks to give me the opportunity of doing my PhD research in your group. Many thanks Jan for your support during the course of my PhD, your compromise and critical supervision helped me to grow and learn much during the past years.

I would also like to thank the thesis reading committee for taking the time to read and evaluate my thesis

Life as PhD was not always easy but it had also a high ratio of funny moments. Thanks to ETE colleagues for the nice atmosphere created in the department's Togetherness and We day. My gratitude also to my office mates, Ilse, Dandan and Jess for the chill chats and especially thanks to Carlos, Thomas, Ivonne, Laura, Noe and Azie for all the funny moments, the input every time I needed it and your friendship. I am also deeply grateful to the members of ETE lab who supported me during my experiments and helped me every time with great disposition with "toxic arsenic girl".

A special appreciation goes to my dear paranymphs Andrea and Adrian who accepted the duty of being next to me the day of my PhD defence. You both have taken an important place in my life, many thanks for sharing the feeling of brotherhood that I needed, and that is even more valuable living in a foreign country.

The hardest part when I embarked on the PhD adventure was leaving behind friends and family. I can now remember when I came to the Netherlands with heavy luggage from one of the driest zone of the earth to one of the rainy and at that time snowy places. I just asked myself what do I do here and what do I do now? At that moment, I could just remember my father telling me I was his brave heart. Those were the words he told when we first embarked from Venezuela to Chile being 9 years old and up to today is a sort of motto that always reminds me where I come from and give me the energy to move forward.

Juan, papo, me faltaría vida para agradecerte, por tanto, has estado en cada paso que he dado, tenemos una conexión tan especial que no pongo en duda que el sentimiento ese día será el de “nos estamos graduando”. Marlen y Silvia las madres genética y prestada que la vida puso en mi camino. Muchas gracias por todas las enseñanzas, y por ser el nido en el que pude desarrollar con firmes valores de igual manera le agradezco a mi tía Chani y susy por su cariño y por haber formado parte de ese nido materno (muchas veces de alcahuetas). Una mención especial para la mamita Iris, Benilde, Tata niño, Reynaldito y Cristóbal, este libro está dedicado especialmente a ustedes.

Quiero darle las gracias extendidamente al resto del batallón que conforma mi familia, los que me conocen saben que tengo más hermanos, tíos y primos que “el circo de los Montini” (algo muy típico de Chile) pero cada uno ha formado parte especial en diferentes etapas. Quiero dar especial Gracias a la tía Tibi, a mis hermanos Eli, Juanes, Braulio, Cesar y particularmente, a Fer y Hyorman, quienes han estado desde tengo memoria (¡uf! Son tantas las historias por contar) aun así en muchos momentos de mi doctorado a la distancia, y quienes me recuerdan hasta el día de hoy lo que es ser una niña, ¡los adoro! Jimmy y Dafne, para mí, ambos son muy especiales no solo por los recuerdos cosechados desde que era la compañerita a los 9 años, sino porque han sido para mí ejemplo de muchos valores, una suma de constancia y amor que aun hoy siento de ti como mi hermano cuando me recibes en tu hogar con mi familia. Mimi, te incluyo en esta sección porque te convertiste para mí en una hermanita más grande (aunque solo de edad). Fue muy curiosa la forma de conocernos, pero aún más hermoso el lazo que han mantenido tu familia y la que ahora yo he formado en este lado del mundo.

Quiero agradecer enormemente a mis amigas de secundaria, Nycole, Sofia, Romy, ¿cómo pasa el tiempo no? ¡Alrededor de 16 años de amistad! La distancia muchas veces es la mejor excusa que tenemos para no cultivar relaciones, pero si hay algo de lo que puedo hablar con orgullo es de mis “amigas del cole”, las que han estado ahí para mí sin importar la diferencia de hora, para recargarnos de energía de risas y de aquellos recuerdos que nos permitirán escribir memorias en un futuro. Gracias porque a pesar de estar en este lado del Atlántico, nos hemos permitido seguir creciendo juntas y porque es un lazo tan especial, que solo se va extendiendo con la adición de nuevos integrantes, a las familias que cada una hemos formado durante los últimos años.

Despite the most difficult part of embarking on this adventure was leaving the Chilean Family and friends I must say I was very fortunate to meet those who currently are part of my Spanish and Dutch family.

## ACKNOWLEDGEMENTS

Una mención especial a mi familia malagueña, porque así los considero, a aquellos que me enseñaron no solo el inmenso valor al aceite de oliva sobretodo porque es del arroyo Carrión pero que también me acogieron como una más, Gracias Isabel, Diegos y Dani por hacerme sentir siempre en casa.

Asimismo, me gustaría expresar mi sincero agradecimiento A la familia Anton, que siempre nos hicieron sentir en su hogar, así como en Holanda en familia y en especial a Iván quien sabe es uno más de nuestro clan.

Jos and Mylene you both have been very special to me and to the family I have formed with Vic. You have supported me in different but complementary ways during my Ph.D. many thanks for that and the nice memories; hopefully, we will collect more in any warm coastal country. I want to extend my gratitude to Jos because your input, words, and energy were crucial in the last stretch.

I cannot forget to mention those international friends that Still from Chile or here in the Netherlands made also the PhD life happier. Many thanks to Ori, Ctaerina Giannina, Parrita, Livio y sannesita Magdalena (“The lovers”) who brought very special moments during this journey and memories that I still keep with me. Claudia B. you became a friend but I want to give you a special thanks because your guidance and dedication as my former supervisor during the bachelor and specialization influenced my decision of pursuing a scientific career.

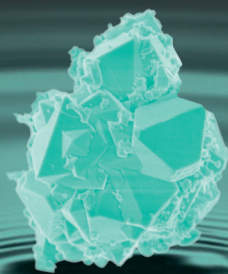
I was very fortunate to meet the Chilean community of Wageningen, people that not only reminded me what was being a real Chilean during every conversation and noisy laughs but also welcomed me as one of their family. Thanks to Catita, Panchi, Lucia, Marcia Chumbis, Yelica and Daniel. I miss you guys but I can only thank you all for those nice weekends, barbeques and the famous Chilean wine tasting events.

I would also like to thanks the IBL team who allowed me to get a space to finish the writing of my PhD thesis when I just moved to Leiden.

Finally, yet importantly, I would like to dedicate some special words to my beloved compañero, Victor. I can only thank life to put you right on my way. We have learned so much together in the short path we have been walking through, although I think now you might know more about arsenic than I know about plants. This thesis is partly yours and honestly, I would never have made all of this without your infinite support. I don't need to say much because you know it all but I can only be grateful to you. The kindest, the good love, the one that awakens my soul.

## ACKNOWLEDGEMENTS

## ABOUT THE AUTHOR



# ABOUT THE AUTHOR

## **ABOUT THE AUTHOR**



Silvia Patricia Vega Hernandez was born on 14th of November 1988 in Ciudad Bolívar, Venezuela, place where she lived for few years before moving with her family to the city of Antofagasta, capital of Antofagasta region in northern Chile. In 2012, she concluded her undergraduate studies in Biotechnology and the specialization in Environmental Biotechnology at the University of Antofagasta. Being the northern region a major mining and arid area of Chile, during her specialization degree she studied the biological application of indigenous microorganisms from of Atacama Desert for copper recovery using natural seawater. She worked for 2 years as research assistant in the laboratory of Algal biotechnol-

ogy and sustainability (BIOAL) of the abovementioned university. During this period, she was involved in the European project Miracles, focused on the screening of new microalgae strains from extreme climates for potential use in biotechnological processes. Her work consisted of the cultivation of microalgae strains from Atacama Salt flat with the potential for the synthesis of bioactive compounds (i.e. pigments, polyunsaturated fatty acids) of industrial interest and their characterization. In 2014 Silvia was awarded with a PhD fellowship from the Chilean Commission for Scientific and Technological Research which gave her the opportunity to study abroad. Thus, at the end of the same year, she relocated to the Netherlands to start her doctoral research at the department of environmental technology of Wageningen University. Her PhD research focused on the development of a biological process for the removal of the most toxic arsenic species (As(III)) from acidic effluents.

The findings of her research project are described in this thesis. After her PhD Silvia would like to continue in a similar line of research, digging into the potential and application of microbes for the development of cleaner process for water treatment.

**ABOUT THE AUTHOR**



*Netherlands Research School for the  
Socio-Economic and Natural Sciences of the Environment*

**D I P L O M A**

*for specialised PhD training*

The Netherlands research school for the  
Socio-Economic and Natural Sciences of the Environment  
(SENSE) declares that

***Silvia Patricia  
Vega Hernandez***

born on 14 November 1988 in Bolivar, Venezuela

has successfully fulfilled all requirements of the  
educational PhD programme of SENSE.

Wageningen, 1 September 2020

Chair of the SENSE board

Prof. dr. Martin Wassen

The SENSE Director

Prof. Philipp Pattberg

*The SENSE Research School has been accredited by the Royal Netherlands Academy of Arts and Sciences (KNAW)*



**K O N I N K L I J K E N E D E R L A N D S E  
A K A D E M I E V A N W E T E N S C H A P P E N**



The SENSE Research School declares that **Silvia Patricia Vega Hernandez** has successfully fulfilled all requirements of the educational PhD programme of SENSE with a work load of 48.3 EC, including the following activities:

**SENSE PhD Courses**

- o Environmental research in context (2015)
- o Research in context activity: 'Initiating and organizing team building activities to strengthen ETE-MIB PhD cluster community' (2018)
- o SENSE Writing Week (2017)

**Selection of Other PhD and Advanced MSc Courses**

- o Biological processes for resource recovery, Wageningen University (2015)
- o Renewable Energy: Sources, Technology & Applications, Wageningen University (2015)
- o Techniques for Writing and Presenting a Scientific Paper, Wageningen Graduate Schools (2016)
- o Scientific Writing, Wageningen Graduate Schools (2017)
- o Information Literacy, Wageningen Graduate Schools (2017)
- o Project and Time Management, Wageningen Graduate Schools (2017)
- o Data management planning, Wageningen Graduate Schools (2016)
- o Brain training, Wageningen Graduate Schools (2017)
- o Mobilising your - scientific – network, Wageningen Graduate Schools (2018)

**External training at a foreign research institute**

- o X-Ray diffractometry training, PANalytica, Wageningen, The Netherlands (2015)

**Management and Didactic Skills Training**

- o Organization of Biocrystallization meeting for Biorecovery group of Wageningen University and Wetsus (2016)
- o Supervising three MSc students with thesis (2016-2019)
- o Teaching in the BSc course 'Introduction Environmental Technology' (2015-2017)
- o Teaching in the MSc course 'Biological processes for resource recovery' (2017)

**Oral Presentations**

- o *Immobilisation of Arsenic as Bioscorodite for safe disposal.* Symposium Jiaotong University, 4-16 June 2016, Xi'an, China
- o *Arsenic removal by controlling biological iron oxidation reactions.* International Mineral Processing Congress, 11-15 September 2016, Quebec, Canada
- o *Immobilization of Arsenic by a Thermoacidophilic mixed culture with Pyrite as energy source.* Goldschmidt2017, 13-18 August 2017, Paris, France

SENSE coordinator PhD education

Dr. ir. Peter Vermeulen

The research described in this thesis was financed by Dutch ministry of Economic Affairs through the Top consortium for Knowledge and Innovation (TKI) programme and Paques B.V (Balk, The Netherlands).

Silvia Vega was financially supported by CONICYT Becas Chile doctoral scholarship programme.

Cover design and Lay-out: HerikMedia | [www.herikmedia.nl](http://www.herikmedia.nl)

Printed by ProefschriftMaken | [www.proefschriftmaken.nl](http://www.proefschriftmaken.nl) on FSC-certified paper